A Comparative Study of Particulate and Gaseous Emissions, of a Diesel Engine Fuelled Conventionally and with Dimethyl Ether.

Byron Ajax Alexander Leonsins

A research report submitted to the Faculty of Engineering and the Built Environment, University of the Witwatersrand, Johannesburg, in partial fulfilment of the requirements for the degree of Master of Science in Engineering.

Johannesburg 2014

Declaration

I, Byron Ajax Alexander Leonsins of Johannesburg South Africa, hereby declare that the content of this report is my own unless otherwise referenced as such. This report is being submitted for the partial fulfilment of the degree Master of Science in Engineering, MSc (Eng), in mechanical, for the University of the Witwatersrand in Johannesburg. This report has not been submitted before for any other degree or examination in any other university.

Signed by:

(B A A Leonsins)

On the:

--------day of--------------------year-----------

(Date)

Abstract

A comparative study of the particulate and gaseous emissions of a 2 cylinder Lister-Petter compression ignition engine when fuelled with diesel and dimethyl ether was undertaken. The investigation involved the commissioning of a Cambustion DMS500 Fast particulate Spectrometer, allowing the spectral densities and cumulative concentrations of particulates in the exhaust stream to be sampled. The investigation was performed for changing engine speeds at various engine loads, namely: 1300rpm to 1800rpm at 25Nm to 45Nm. Along with particulates, THC, NOx, CO_2 and CO were measured using various Signal Gas Analysers. Various engine performance measures were also recorded, including maximum cylinder pressure and temperature, air/fuel ratio, exhaust temperature, shaft speed, torque and fuel conversion efficiency. The most notable finding was that particulate sizes were in the range of 150nm to 170nm under diesel fuelling whereas for dimethyl ether fuelling they were 5,5nm to 7nm. It was also found that increasing engine speed with dimethyl ether fuelling causes an increase in the particulate size, whereas with diesel fuelling increasing engine load resulted in an increase in size. The concentration of particulates was seen to increase with increasing engine speed. It was also found that under both fuelling methods there exists an indirectly proportional relationship between NOx and particulates.

Acknowledgements

Table of Contents

List of Figures

List of Tables

Nomenclature

DME   Dimethyl Ether

CO   Carbon Monoxide

HC   Hydrocarbons

THC   Total Hydrocarbons

NOx   Nitrous Oxides (di, tri, etc.)

CO_2 Carbon Dioxide

PM   Particulate Matter

PN   Particulate Number

A/F   Air/Fuel Ratio

ϕ Air/Fuel Equivalence Ratio

λ Relative Air/Fuel Ratio

EGR   Exhaust Gas Recirculation

DAC   Digital To Analogue Converter

Nm   Newton Meter

rpm   Revolutions Per Minute

BSPT   British Standard Pipe Thread

ATC   After Top Dead Centre

BTC   Before Top Dead Centre

isfc   Indicated Specific Fuel Consumption   g/(kWh)

$isNO_2$ Indicated Specific NO_2 Production   g/(kWh)

1. Introduction

Historically the need for an understanding of emissions from internal combustion engines was motivated by a desire for a performance improvement. Accurate engine emission analysis gives insight into the air-fuel ratio (AFR) the engine is operating under. Understanding the AFR allowed engineers to assess how efficiently the engine was converting the energy of the fuel into mechanical work. This translated into numerous design changes that improved fuel energy conversion efficiency. With the clear need for the conservation of scarce fossil fuel resources; improvements in fuel energy conversion efficiency are certainly of importance.

It must be understood that a clear trade off exists between the optimal fuel efficiency, optimum engine performance and lowest emissions. Of late the desired operating point has been for lower emissions, gaseous and particulate.

2. Motivation for research

In recent years the study of emission has been motivated by society's increasing awareness and sensitivity to air pollution and air quality. It is commonly believed that the internal combustion engine is a major source of urban air pollution. As a result of this perception, coupled with numerous studies that corroborate the belief, governments have responded with the introduction of numerous infringement standards. These standards serve to reduce outputs of emissions of new vehicles sold within the particular country referred to. The standards have reduced emissions to a mere fraction of what they were half a century ago. However, with the increase in vehicles on roads worldwide, the gross impact on the environment is still unacceptably high.

Having even an empirical understanding of what factors, such as engine loading and fuel used, result in higher or lower emissions outputs puts a designer in a better position to make informed choices that will result in an overall reduction in the emission output of the engine. In order to produce engines, that are relevant in today's times of increased sensitivity, it is increasingly necessary to experiment with the internal combustion engine in order to understand these operating limits.

The need for an understanding of what affects an engine's output of particulates is no different and is under the same type of infringement standards as the gaseous emissions are. The study to follow will give some insight into the effect that fuel type, engine loading and speed with the inferred performance measures, have on particulate and gaseous emissions. Any link between particulate output and gaseous emissions will also be considered.

2.1. Current Standards

In Table 1, below, is presented the European Emission Standards for passenger vehicles, in category M1. Although, countless standards for various countries and regions exist for all manner of internal combustion engines only one is presented

below. The important feature is the trend of reduction in emissions, gaseous and particulate, over the years. Extrapolation of this obvious trend gives insight as to where emission levels will need to be in years to come. If one looks, in particular, at the NOx emission limits it can be seen that the limit has reduced from 0.5 to 0.08 g/km from 2000 to 2014 for a compression ignition engine, thus a downward trend is evident. It is this leapfrog effect of technological progress and bureaucratic need that is a major driving force for emission studies.

Table 1: European Union Chronology of Emissions Standards [1]

EU Emission Standards for Passenger Cars (Category M_1*)							
Stage	**Date**	**CO**	**HC**	**HC+NOx**	**NOx**	**PM**	**PN**
		g/km					*#/km*
Compression Ignition (Diesel)							
Euro 1†	1992.07	2.72 (3.16)	-	0.97 (1.13)	-	0.14 (0.18)	-
Euro 2, IDI	1996.01	1.0	-	0.7	-	0.08	-
Euro 2, DI	1996.01[a]	1.0	-	0.9	-	0.10	-
Euro 3	2000.01	0.64	-	0.56	0.50	0.05	-
Euro 4	2005.01	0.50	-	0.30	0.25	0.025	-
Euro 5a	2009.09[b]	0.50	-	0.23	0.18	0.005[f]	-
Euro 5b	2011.09[c]	0.50	-	0.23	0.18	0.005[f]	6.0×10^{11}
Euro 6	2014.09	0.50	-	0.17	0.08	0.005[f]	6.0×10^{11}
Positive Ignition (Gasoline)							
Euro 1†	1992.07	2.72 (3.16)	-	0.97 (1.13)	-	-	-
Euro 2	1996.01	2.2	-	0.5	-	-	-
Euro 3	2000.01	2.30	0.20	-	0.15	-	-
Euro 4	2005.01	1.0	0.10	-	0.08	-	-
Euro 5	2009.09[b]	1.0	0.10[d]	-	0.06	0.005[e,f]	-
Euro 6	2014.09	1.0	0.10[d]	-	0.06	0.005[e,f]	6.0×10^{12} [e,g]

* At the Euro 1..4 stages, passenger vehicles > 2,500 kg were type approved as Category N_1 vehicles
† Values in brackets are conformity of production (COP) limits
a. until 1999.09.30 (after that date DI engines must meet the IDI limits)
b. 2011.01 for all models
c. 2013.01 for all models
d. and NMHC = 0.068 g/km
e. applicable only to vehicles using DI engines
f. 0.0045 g/km using the PMP measurement procedure
g. proposed; to be lowered to 6.0×10^{11} 1/km within three years from Euro 6 effective dates

3. Objectives and Aim

3.1. Investigation Aim

To determine what fuel and setting, with regard to speed and applied load, a compression ignition engine should be operated at to produce the lowest particulate emission possible.

3.2. Project Objectives

It is required that:

- The compression ignition engine assigned for use be serviced and returned into working order for the study.
- The high pressure Dimethyl Ether fuelling system for the test engine be commissioned back into service.
- The Signal Gas Analyser systems be serviced and fully tested and rigged for sampling the exhaust stream of the test engine.
- The new Cambustion DMS500 Fast Particulate Spectrometer be set up, commissioned in the engine test cell assigned and rigged for sampling the exhaust stream of the test engine

3.3. Experimental Objectives

This investigation will determine:

- The effect that differing engine speeds, at a fixed load, have on the output of particulates. This is with reference to the concentration of different sized particulates emitted.
- The effect that differing engine loads, at a fixed speed, have on the output of particulates. This is with reference to the concentration of different sized particulates emitted.
- The differences in particulate output when the engine is fuelled on diesel and dimethyl ether, for the above two tests. This is with reference to the concentration of different sized particulates emitted.
- If any link between the amount of particulates emitted and the engine's output of gaseous emissions exists. This will be done for the carbon dioxide, carbon monoxide, NOx and total hydrocarbons emissions of the engine. This is with reference to the concentration of the most abundant particulate.
- If any link between the amount of particulates emitted and various engine performance measures exists.
- The distinguishing factors that arise when dimethyl ether fuel is used for the above objectives, as compared to diesel.

4. Literature Survey

4.1. Historical Gas Measurements

The approach to gas measurement involved chemical processes whereby gases were reacted with various chemical solutions and conclusions about concentration were then made. An instrument called the Orsat Apparatus, shown in figure 1 below, was used to detect various gases including carbon dioxide, carbon monoxide and oxygen. Very simply the method involves the admittance of 100 units of the exhaust gas at atmospheric pressure followed by the absorption of the various constituent gases via different various chemical substances. After each absorption process is completed the volume is measured and thus the change represents the volume of each constituent gas. Volumes are determined by returning the pressure of the sample to atmospheric; and then inferring a height change in the sample bottle. The chemical substances used for absorption are usually potassium hydroxide for carbon dioxide, pyrogallic acid for oxygen and cuprous chloride for carbon monoxide [2].

Many other methods existed for measuring the volumes of constituent gases of a sample. However, most have been superseded by the advent of electronically controlled measurement devices using various principles and phenomena borrowed from the field of physics.
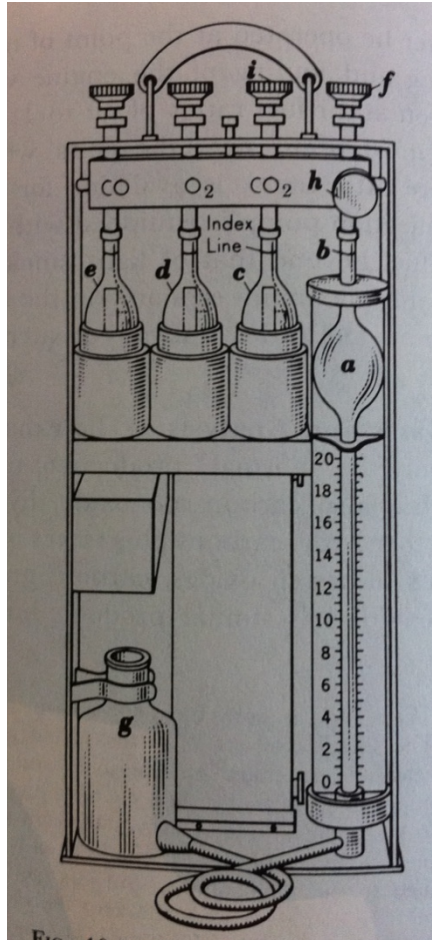
Figure 1: Orsat Apparatus [2]

4.2. Current Gas Analysis

4.2.1 Particulate Measurement

Particulates are seen to the observer as smoke, this smoke can be from various sources; its colour is often characteristic of the source and thus its primary constituents. Black smoke is usually comprised of carbon arising from an organic source. The primary source of black smoke is partially oxidised fuel, like what would be found during fuel rich operation. Blue smoke is characteristic of a high hydrocarbon content usually arising from the burning of lubricating oil and its presence could be attributed to a physical fault in the engine like a worn piston ring. White smoke is representative of water vapour; it can either be as a result of high

humidity in the surrounding air, which is drawn into the engine, or of complete oxidation of the fuel hydrogen constituent. Brown smoke is representative of nitrogen dioxide and is usually observed from large engines fuelled on heavy unrefined fuel, which is typical of marine engines [3].

The measurement of particulates can be achieved using various methods. A problem arises as these differing methods do not provide independent results. They are merely representative of a consequence of the presence of the smoke and do not provide any real insight into the constituents and their respective concentrations.

4.2.1.1. Opacimeters

This method involves determining a percentage that represents the degree that an undiluted smoke sample obscures a light beam. Zero percent is representative of clean air, usually nitrogen, and one hundred percent is representative of heavy dark black smoke, usually found with large diesel engines. This output may also include what is referred to as the absorption factor, having units: m^{-1}, this allows for a comparison of readings from different manufacture's machines [3].

4.2.1.2. Smoke Meters

The smoke meter provides a reading that is representative of the particulate content of an undiluted sample. The method involves passing the sample though filter paper and comparing the consequent 'blacking' of the paper to a scale. The scale will specify a smoke number; however, this is usually specific to the manufacturer. Thus the smoke meter is a good tool for a localised comparative study but as yet is not standardised for universal comparison and grading. This method is good for estimating smoke concentration but is useless for any insight into the smoke composition [3].

4.2.1.3.Particulate Samplers

The particulate sampler is similar to the smoke meter in that it passes a sample of smoke through filter paper, except in this instance the sample is diluted and the actual mass of the particulates trapped is measured. This would yield a result of mass at a mass flow rate of sample, thus: [(Kg particulates) / (Kg/s sample)]. The fact that the sample is diluted is more representative of the actual concentration that particulates would be in the surrounding atmosphere as a consequence of an engine's operation [3].

4.2.1.4.Microsoot Detectors

In response to the increasingly stringent levels of emissions it became necessary to detect soot particles in the range of 5μg / m^3 of exhaust gas. This is achieved via the use of laser scanners that exploit the photo-acoustic principal [3].

4.2.2 Gaseous Measurement

4.2.2.1.Non-Dispersive Infrared Analyser

This detector makes use of the fact that certain gases absorb different parts of the polychromatic light spectrum. The detector is called non-dispersive as all the light from the source passes through the gas sample and is subsequently filtered out for the wavelength of interest. The intensity of this wavelength is then measured and correlated to its original intensity thus providing a measurement that is indicative of the concentration of the gas. This detection method is used for carbon dioxide, which will absorb a band of the infrared spectrum at 4.26μm. The detector can also be tuned to detect carbon monoxide, which will absorb light at around 3.4μm; this would simply be achieved by changing the filter for one that admits light at this wavelength.

It must be noted that any sample passing into one of these analysers must be dried first as water vapour will behave in a similar fashion to carbon dioxide giving inaccurate results [3].

4.2.2.2.Chemiluminescence Detector

This detector exploits the phenomena whereby certain chemical reactions give off light as a by-product. These detectors are used for the detection of NO_x. It must firstly be explained that an engine will exhaust nitrogen monoxide, NO, and nitrogen dioxide, NO_2. Together these are described as NO_x. The reaction that is exploited is as follows:

$$NO + O_3 \rightarrow NO_2 + O_2 + Photon$$
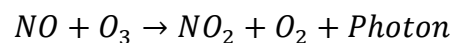
Thus the resulting photons can be detected by a photomultiplier and will give an indication of the concentration of nitrogen monoxide in the reactants. The reaction requires ozone, which is produced in the analyser using an ozoniser. An ozoniser produces ozone by generating an electrical discharge though oxygen in a vacuum chamber. As the engine produces both NO and NO_2, it is first necessary to catalytically convert the NO_2 into NO for the reaction to proceed. Thus the reaction is really a detection of both, hence NO_x [3].

4.2.2.3.Flame Ionization Detector

This type of detector is used in the detection of carbon atoms, thus it is indicative of the total hydrocarbons present in the sample. The phenomena at play involve an electric current flow from anode to cathode, within an electric field. The amount of free carbon atoms that are present are directly proportional to the electric current flow. The carbon atoms are extracted from the sample gas by burning the gas with a mixture of hydrogen and helium in a reaction chamber, which is heated to prevent

condensation of water vapour in the sample that would interfere with the current flow [3].

4.2.2.4. Paramagnetic Detection

These detectors are primarily used for the detection of oxygen. The detection method exploits the fact that oxygen molecules have a high paramagnetic susceptibility. Simply put they will gather in the region of highest magnetic flux when exposed to a magnetic field. In the detector the region of highest magnetic flux is a simple balance arm whose displacement is directly indicative of the concentration of oxygen molecules. Others gases such as carbon dioxide and nitrous oxides also exhibit this paramagnetic phenomenon thus the sample must be scrubbed of these before detection [3].

All the above methods of detection make use of a secondary response mechanism to the gas species presence and must thus be calibrated against gas samples of known concentration. This is achieved by the use of span gases with posses a mixture of the gas species under consideration and nitrogen, an inert carrier, at a known concentration. The detectors are also calibrated to a zero point with pure nitrogen. Thus two known points are provided, which is enough for the construction of a linearized response pattern.

4.3 Species Formation and Trends

4.3.1. Nitrogen Oxides (NOx)

4.3.1.1. NOx in Spark Ignition Engine

The formation of NO in spark ignition engines is well understood and is quite complex. It was found that the concentration of NO in the combustion chamber of an

engine can be accurately linked to the cylinder pressure and consequent temperature. The temperature and pressure of the cylinder will naturally experience a sharp increase after ignition by the spark. The concentration of NO, as seen in figure 2 below, is strongly linked to this increase in temperature and consequent pressure increase. The peaks of the NO concentration and the temperature and pressure peaks are seen to correspond well [4].
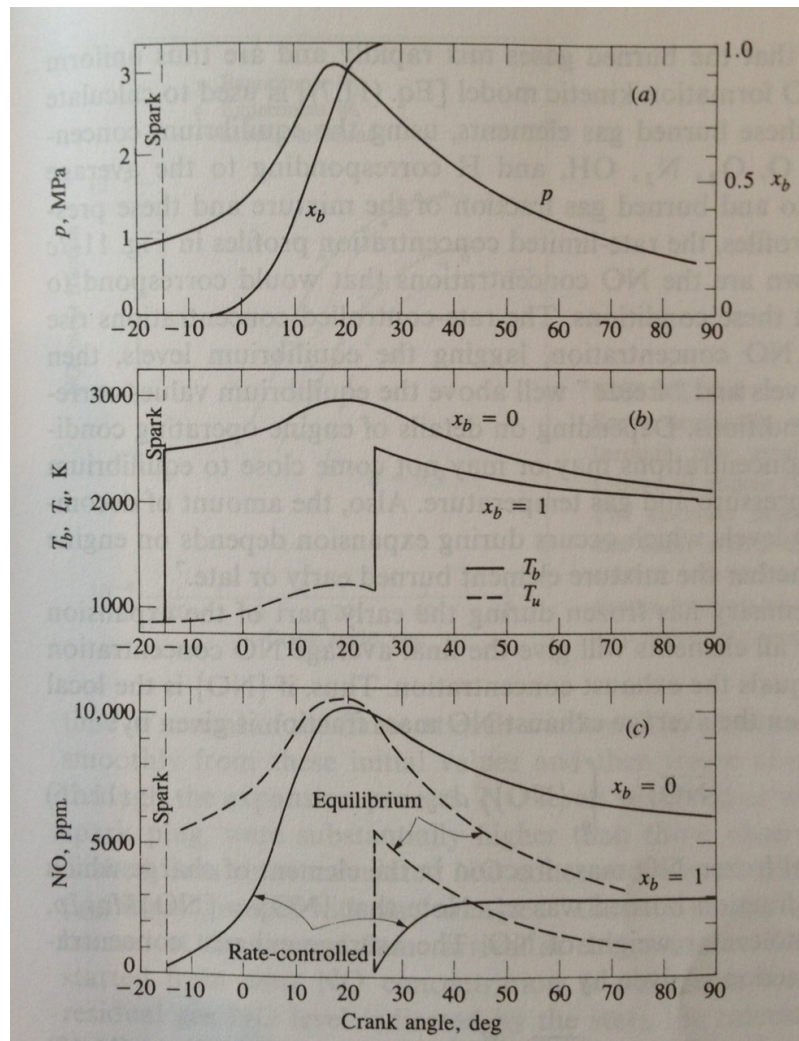
Figure 2: No formation as a function of cylinder pressure and temperature [7]

The formation of NO is well understood with regard to its changing trends with changing fuel/air equivalence ratio. From figure 3 below it is seen that NO concentration peaks at a fuel/air equivalence ratio of about 0.9. The maximum cylinder temperatures are achieved at a fuel/air equivalence ratio of about 1.1.
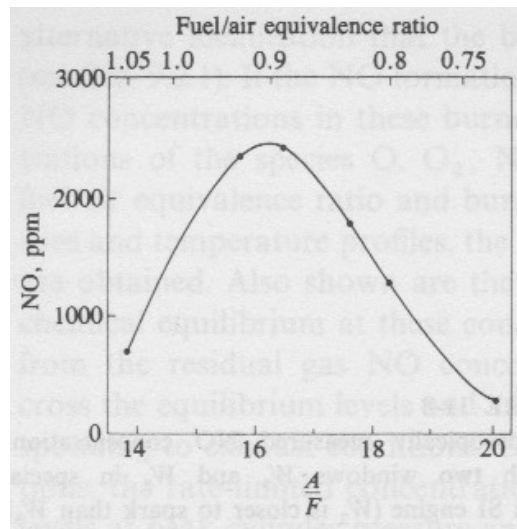
Figure 3: NO concentration versus air fuel ratio [5]

The failed expected correlation between cylinder temperature and NO formation can be explained by understanding the following probable reactions with regard to NO formation.

$$O + N_2 = NO + N$$

Equation 1

$$N + O_2 = NO + O$$

Equation 2

$$N + OH = NO + H$$
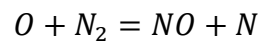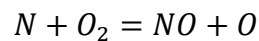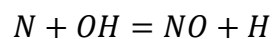
Equation 3

The above set of reactions is referred to as the extended Zeldovich mechanism. From equations 1 and 2 the importance of free oxygen for the formation of NO can be seen. Thus at the maximum cylinder temperature the system is operating slightly fuel rich thus the free oxygen concentration will be low preventing the formation of NO [6] [7].

A technique used for the control of the formation of nitrogen oxides in the internal combustion engine involves the recirculation of exhaust gases. This is where part of the engine's exhaust is actually mixed with the intake air. The effect it has on the

reduction of NO formation can be seen in figure 4 below. The effect of changing air fuel ratio is also seen [8].
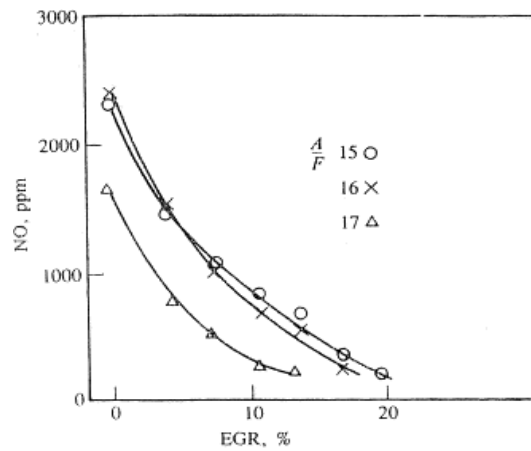
Figure 4: Effect of exhaust gas recirculation (EGR) on NO formation [5]

The effect of the actual ignition point of the charge in the combustion chamber greatly affects the concentration of NO in the exhaust stream. In a spark ignition engine, unlike a compression ignition engine where ignition is an automatic response to the cylinder pressure and consequent temperature, there is a certain degree of latitude that one has with regard to the desired point of ignition. This is simply achieved by altering the point at which the spark is actuated. For obvious reasons the point of spark actuation must still be before top dead centre otherwise insufficient time is given for the smooth expansion of the cylinder charge gases and engine knock might result. From figure 5 below the effect of spark timing at various air fuel ratios is shown. The best results are seen to occur with fuel lean operation and moderate spark advance BTDC [8].
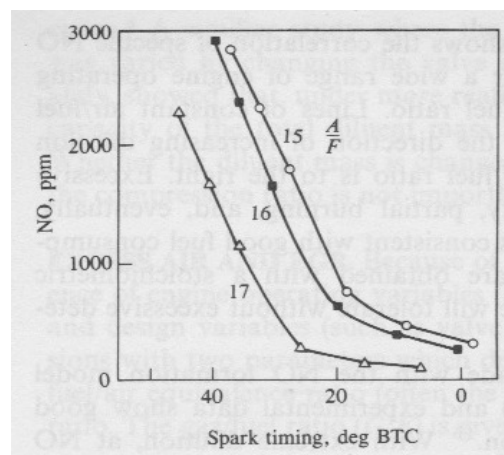
Figure 5: Effect of NO formation with regard to spark timing [5]

4.3.1.2.NOx in Compression Ignition Engine

The major difference between the compression ignition engine and the spark ignition engine is that the compression ignition engine always runs lean as throttling is accomplished by variation of fuel injection quantities. Ignition of the charge results from an automatic response to the cylinder pressure and consequent temperature, thus the point of ignition is not under control.

The same trends with regard to cylinder pressure and temperature are seen in the compression ignition engine as was in the spark ignition engine. Thus most of the NO produced by the engine is done so when cylinder temperatures and pressures are at their highest in the cycle. A distinguishing factor is that as the peak temperatures fall faster in a compression ignition engine the production of NO freezes faster than in a spark ignition engine. Thus as the cooler burnt gases mix with the hotter expanding gases NO decomposition is halted. [8]

As in the spark ignition engine the behaviour of NO production can be plotted against the fuel air equivalence ratio. By dropping the equivalence ratio it can be seen that the overall production of NO decreases. Thus by decreasing the amount of fuel the production of NO will also decrease; this can be attributed to the fact that the peak combustion temperature will be lower when less fuel is injected. The equivalence ratio for a diesel engine is also indicative of the throttling of the engine, as more fuel means the engine is throttled higher. The trends described above can be seen in figure 6 below [8].
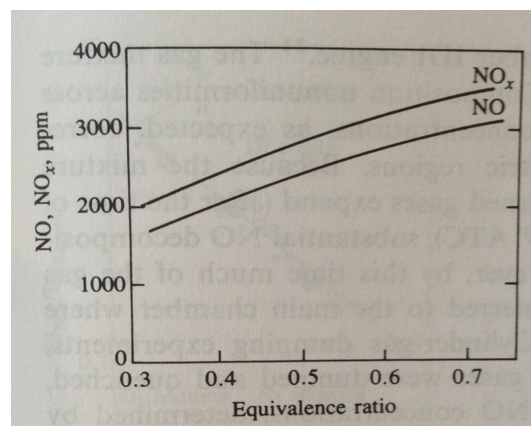
Figure 6: NO, NOx concentrations versus equivalence ratio [9]

As in the spark ignition engine a technique used for the control of nitrogen oxides is intake air dilution, which simply lowers the amount of free oxygen available to form NOx. This was explained previously as exhaust gas recirculation. However, as the mechanism simply involves lowering the concentration of oxygen any gas can be used for the dilution of the intake air. The effect of using nitrogen, carbon dioxide and exhaust gas as the diluents is shown in figure 7 below.
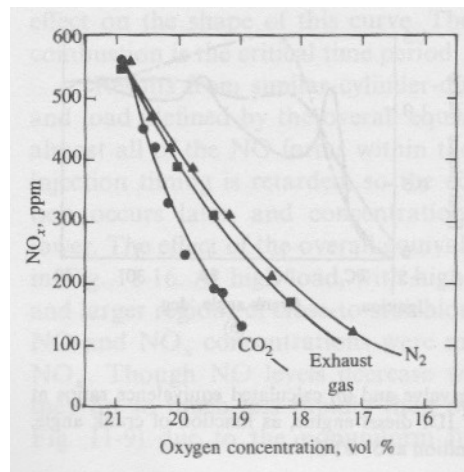
Figure 7: NO concentration versus oxygen concentration [10]

The best results are seen to occur using carbon dioxide as the oxygen concentration still remains high for the effective combustion of the fuel, thus providing the highest combustion efficiency [10].

4.3.2. Carbon Monoxides (CO)

The mechanisms governing the formation of carbon monoxide in the internal combustion engine are very closely linked to the air-fuel ratio that the engine is operating at. It is found that engines operating on the fuel rich side of stoichiometric will produce considerably higher carbon monoxide emissions than engines operating on the fuel lean side of stoichiometric. It is for this reason that excessive carbon monoxide emissions are only problematic for spark ignition engines as compression ignition engines, by virtue of their operating principle, will always function on the fuel lean side of stoichiometric. Hence, the production of carbon monoxide is not considered to be a major issue for compression ignition engines.

17

The preconceived belief may be that the carbon monoxide formed in the combustion chamber of the engine may easily oxidize with free oxygen at any point after the act of combustion. It is however, found not to be the case as the temperatures necessary for the oxidation of carbon monoxide to carbon dioxide are not achieved at any downstream point of the combustion process. Only with the aid of external devices such as oxidation catalysts is it possible to oxidise the carbon monoxide. However, from figure 8 below, it is seen that the best prevention against carbon monoxide production is to remain on the fuel lean side of stoichiometric. Figure 8 below also demonstrates the effect that differing H/C ratios, with respect to the fuel, have on the overall production of carbon monoxide. It is seen that fuels with lower ratios perform better [11] [8].
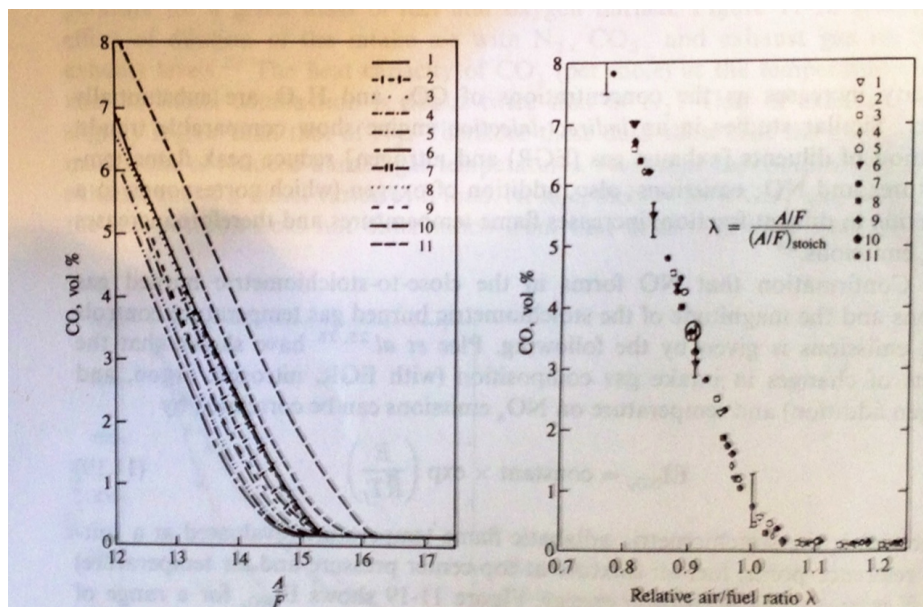
Figure 8: CO concentration versus air fuel ratio [11]

4.3.3. Total Hydrocarbons (THC)

Total hydrocarbons refer to any organic emissions resulting from the incomplete combustion of the hydrocarbon fuel. The form of the hydrocarbon may vary depending on the ratio of carbon to hydrogen, thus anything from methane to a loose carbon hydrogen pairs may be present. Collectively these emissions are grouped as total hydrocarbons. Various scenarios exist for the formation of these total

hydrocarbon emissions; a combination of these different formation mechanisms can be at play within the combustion chamber of an engine. The distinctions are made on whether the engine is operating on the spark or compression ignition principle as seen below.

4.3.3.1 THC in Spark Ignition Engines

As these emissions are a direct result of the incomplete combustion of the hydrocarbon fuel their concentration is very much linked to the fuel air ratio. The concentration of total hydrocarbons in the exhaust will increase when the mixture is on the fuel rich side of stoichiometric as there is excess fuel to be burnt. The concentration will also rise when the mixture becomes fuel-lean as this results in a deterioration of the combustion quality and thus the prevalence of misfire will increase. The fuel simply passes through the engine without being burnt. There exist numerous possible hydrocarbon formation mechanisms in spark ignition engines as explained below [8].

Flame Quenching

This mechanism involves the suppression of the progressive burn that takes place within the cylinder by the extinction of the flame front on the comparatively colder surface of the cylinder walls. Thus the flame extinguishes before all the fuel is burnt. The surface finish of the cylinder wall has been shown to affect the production of total hydrocarbons, with smooth walled combustion chambers showing less production than those with rough finishes. The thickness of this so called quench layer is of the order of 0.05mm to 0.4mm, it has been observed that subsequent oxidation after the diffusion of hydrocarbons into the burnt gas will occur. Thus this mechanism will result in a transient concentration of hydrocarbons in the cylinder as is seen in figure 9 below [12] [13] [8]
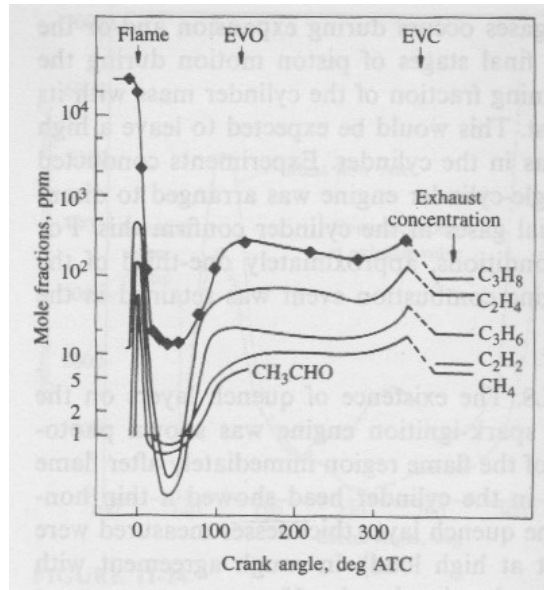
Figure 9: Transient concentration of THC [13]

Crevice Mechanism

This mechanism results from all the small cavities and spaces in which the air fuel mixture is able to 'hide' from the advancing flame front, thus it remains un-burnt. As a consequence of the operating procedure of the internal combustion engine the pressure rises during the cycle, which forces the fuel mixture into these crevices. The lack of combustion in the crevices is aided by the fact that the crevices usually, by their nature, have a high surface area to volume ratio and thus cool the mixture very effectively preventing easy combustion. The largest of these crevices is the space between the piston, top piston ring and cylinder wall. As cylinder pressure rises the mixture is forced in this space and segregated from the burning bulk. When the pressure drops during the exhaust stroke the motion of the bulk helps to dislodge this un-burnt charge, which is then able to enter the exhaust stream. Various visualisation methods have shown the major crevice sites to be, in addition to the one mentioned, the valve to valve-seat space and the sparkplug threads. Thus in-order to minimise the production of hydrocarbon emissions a good starting point would be to minimise these sites from a design point of view [14] [15] [8].

Engine Oil

Engine oil itself is not a direct source of hydrocarbon emissions as far as the tailpipe is concerned. It is rather its absorption of the fuel vapours that result in an increase in observed THC. During the intake stroke the fuel concentration is high as fresh charge is being admitted into the cylinder. The oil that is present for lubricating purposes on the cylinder walls will absorb fuel vapour until saturation occurs. During the compression stroke the ambient pressure rises allowing, by Henry's Law, the oil to further absorb fuel vapour [16]. After combustion has taken place the fuel vapour concentration in the combustion chamber is effectively zero. The absorbed fuel vapour will then be released into the burnt bulk gas body. This mechanism effectively allows for fuel to skip the combustion process and emerge on the other side as a pollutant [8].

Incomplete combustion

This results from what is called bulk gas quenching. This occurs during the expansion stroke were the bulk gas cools ahead of the flame front causing ineffective combustion of the hydrocarbon fuel. This phenomenon is most common at low loads and idle speeds. The very act of combustion will create localized areas where the bulk charge is diluted and thus does not burn effectively [8].

4.3.3.2.THC in Compression Ignition Engines

There are three main mechanisms that result in hydrocarbon emissions in the diesel engine. These occur when fuel is mixed to leaner than the combustion limit allows during the delay period. When the fuel leaving the fuel injectors undermixes late in the combustion process and from bulk charge quenching and engine misfire [10] [8].

Overleaning

As the fuel is injected the distribution of the fuel will change with time resulting in localised areas that will be leaner than what is required for ignition. The fuel moves from a core and spreads outwards. The spread radius is indicative of the air fuel ratio, thus fuel beyond a certain radius is unable to ignite, as it will be too lean. This is shown in figure 10 below. Other species such as aldehydes can exist in this region and could escape the burn process altogether. Factors that affect the amount of hydrocarbon emissions that are generated from this mechanism would be: the quantity of fuel that is injected during the ignition delay period [17] and the mixing rate, thus the spread of fuel from the nozzle which dictates the size of the so called shell outside which no ignition occurs.
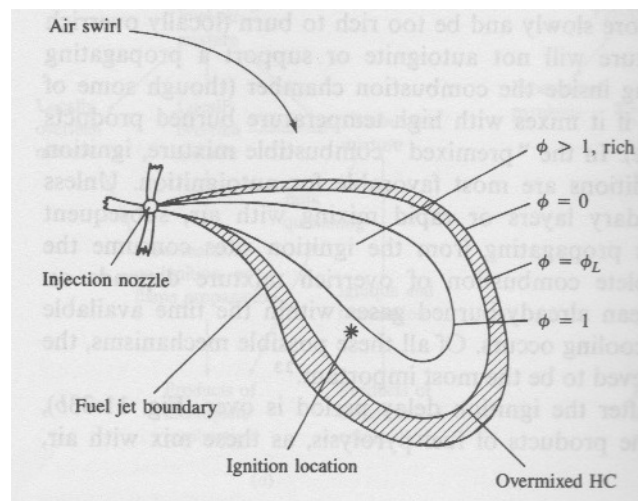
Figure 10: Diesel Injector Spray Pattern [17]

Undermixing

This occurs when fuel enters the cylinder during combustion and is not mixed sufficiently with the air. Two main sources of this so called undermixed fuel are: fuel that drips from the injector sac volume, and when the fuel injection system over-fuels the engine during high load conditions. The injector drip phenomenon is as a result of fuel accumulation in the space below the injector needle seat and the nozzle flute volume. When the fuel is heated, as a result of combustion during the expansion stroke, this trapped fuel vaporises moving into the combustion chamber. Various

design considerations are used to minimise this effect. Overfuelling of the engine will occur in transient conditions such as during the acceleration of the engine under high load. The overall fuel mixture will remain lean but there will be localised zones of fuel rich mixture and these will be responsible for increased hydrocarbon production [17] [8].

Flame Front Quenching

This is similar to the mechanism in the spark ignition engine where the quenching of the flame front will occur at the wall of the combustion chamber. This leads to a general loss in combustion quality. The lower combustion quality results in more of the hydrocarbon fuel escaping the burn process and emerging as pollution [8].

4.4. Particulates

4.4.1. Historical Treatments

An adequate prediction model for the formation of particulate matter does not exist [18]. Study was limited to simple measurements with smoke meters and opacimeters such as those described in Section 4.2.1. The understanding is that particulates vary in size greatly and are simply organic compounds resulting from the carbon based fuel combustion. Thus they are not unlike hydrocarbon emissions except they are present on a macroscopic level in the form of soot, liquid droplets, dirt or smoke. Acceptable levels of soot were well documented but these standards mainly referred to a visual impact, as measurement techniques offered no adequate means of determining the particle composition. The impact that particulates have on the surroundings is very different to their effect in the cylinder, thus samples are often diluted to approximate what the effect would be when the particulate emission had mixed with the atmospheric air post the tailpipe. Particulates could also form as a result of condensation of gaseous emissions in atmospheric air or by reacting with other emitted species [19]

It has also been shown that there exists a correlation between the amount of nitric oxide an engine emits and the particulates emitted. There appears to be a trade-off between these two emissions. This is clearly seen in figure 11, below, where the amount of NO increases for a reducing concentration of particulates.
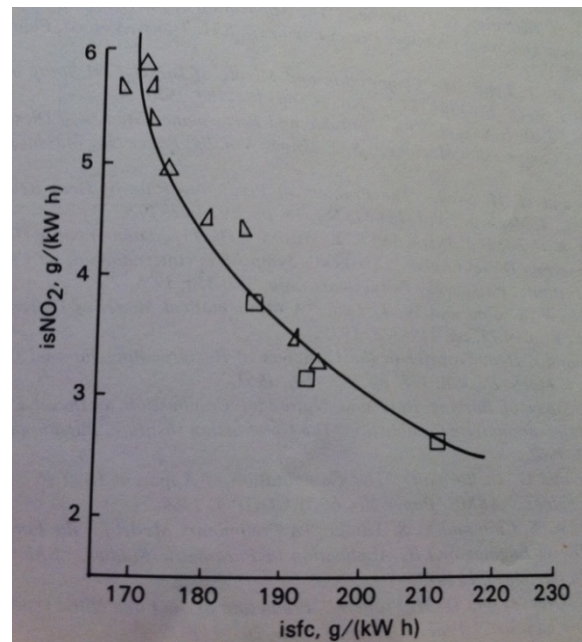
Figure 11: Relationship between Particulates and NO [18]

This indicates that the mechanisms at play that aid in the formation of nitric oxide must have a suppressive role on engine particulate formation and vice versa. It could also be an indication that both processes are highly susceptible to the engine's overall air-fuel ratio. Thus by moving the air-fuel ratio towards being leaner, until an optimum point, which is related to the stoichiometric air-fuel ratio, the engines output of nitric oxide will decrease. Thus, a fuel richer charge mixture will result in an increase in the particulate output of the engine, which is intuitively expected as particulates are derived from the carbon in the organic fuel [18].

4.4.2. Current Treatments

A greater understanding exists today as to what the actual compositions of these particulate emissions are. The particulate is at its base level formed from a loose

carbon that results from the burning of the organic fuel, as explained earlier. Onto this carbonaceous core multiple species attach, amongst others:

- Unburnt Hydrocarbons
- Oxygenated Hydrocarbons
- Aromatic Hydrocarbons
- Sulphates
- Sulphur Dioxide
- Nitrogen Dioxide
- Sulphuric Acid

Due to the size of these emitted particles, which is often less that 2 microns they present a health risk, as they are easily respired. These particulate emissions have also shown to be a causative factor for lung cancer [20].

An apparent contradiction exists as a result of the stated relationship between particulate output and a fuel rich combustion charge in a diesel engine, which has an overall fuel lean charge. This can be explained by understanding that the combustion chamber of a diesel engine will have localized areas of fuel rich mixture, see figure 10 [21].

The processes that particulates undergo during development are now understood and are illustrated below in figure 12. It is seen that a particulate will undergo three stages within the cylinder. These are nucleation where the particulate forms, surface growth were the particulate increases in size and agglomeration where many particulates combine. The next stage takes place out of the engine, namely in the exhaust system and the atmosphere downstream of the tailpipe. These are the stages of absorption and condensation. This is where the overall concentration of particulates can decrease as they oxidise or attach to hydrocarbons. These stages are fully explained in the following sections.
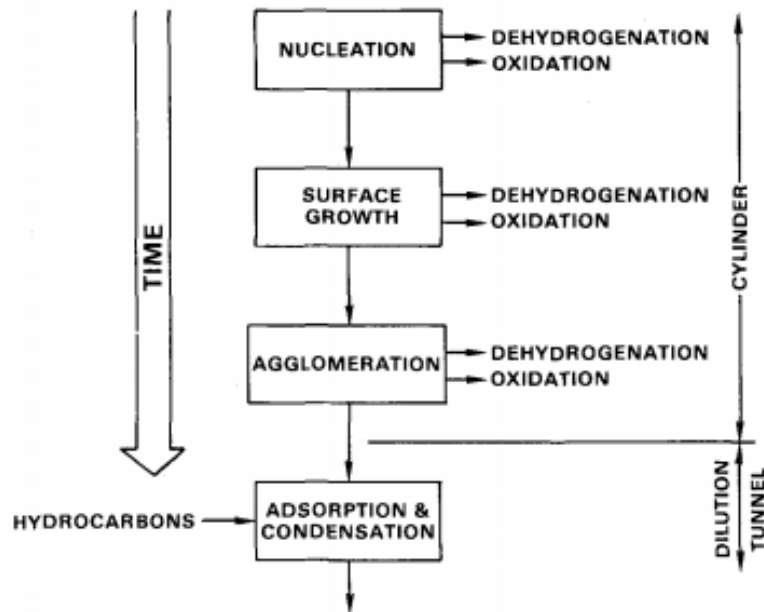
Figure 12: Particulate Formation Process [21]

4.4.3. Particulates of SI and CI Engines

4.4.3.1.Particulates in SI Engines

In modern gasoline engines, fuelled on unleaded gasoline and equipped with catalytic converters, the prevalence of particulates as a major emission is very low. However, in the past when lead was added to the fuel to act as an inhibitor of auto ignition and engine knock, the composition of particulate emissions was predominantly lead based. Another large contributor of particulates are sulphates. Gasoline can contain anything from 150ppm to 600ppm by weight sulphur. The sulphur is first oxidised during combustion to sulphur dioxide and then in the oxidation catalyst to sulphur trioxide, which then combines with water in the atmosphere to form a sulphuric acid aerosol, which is a very harmful particulate. By definition a particulate can be either soot or liquid droplets. Thus the sulphuric gas aerosol can be considered a particulate emission.

The almost standardised use of unleaded fuels has reduced the output of particulates by about 20mg/km in engines without catalysts. The reason why it is mentioned without a catalyst is that the catalyst will aid in the production of sulphuric acid, thus the net effect may be argued to be minimal. Thus there exists a trade off between the effectiveness of catalysts in reducing the outputs of many other partially oxidised species and the output of sulphuric acid. For this reason the introduction of low sulphur fuels has become such a prevalent topic. [22]

4.4.3.2.Particulates in CI Engines

The primary source of particulates in a compression ignition engine is unburnt or partially burnt hydrocarbon fuel. Thus the majority of the particulates in a diesel engine are actually soot. The partially burnt hydrocarbon fuel may result from the overfuelling that occurs under acceleration and when the engine is under heavy loads. As explained earlier the diesel engine never has an overall fuel rich mixture, rather localised pockets of fuel rich mixture exist. This is similar to the mechanism at play with regard to hydrocarbon emission production, as explained in section 4.3.2.

The sulphur content in diesel, which can lead to the production of sulphuric acid aerosols, is also an issue in diesel engine emissions. It is for this reason that the sulphur content of diesel fuel is strictly controlled to less than 50ppm. [8]

4.4.4. Particle Formation

This stage, often referred to as nucleation, is actually poorly understood. However, a few theories exist for the formation of the soot nuclei. The main distinguishing factor as to what route will be followed when the hydrocarbon fuel produces soot during burning will depend on the temperature of the reaction and the actual structure of the hydrocarbon fuel.

From an equilibrium standpoint, whether or not the hydrocarbon fuel will produce soot during combustion can be expressed by the following equation. It is seen that mixtures that are fuel rich are more likely to produce soot.

$$C_mH_n + yO_2 \rightarrow 2yCO + \frac{n}{2}H_2 + (m - 2y)C_{soot}$$
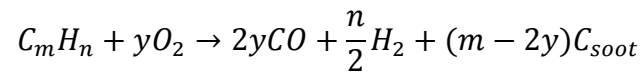
<div align="right">Equation 4</div>

When m is larger than 2y soot should be produced, that is when the C/O ratio exceeds 1. The resulting air fuel equivalence ratio is given by

$$\phi = 2\left(\frac{c}{0}\right)(1 + \delta)$$

<div align="right">Equation 5</div>

In reality the above rule is not often followed, and (C/O) ratios of about 0.5 to 0.8 are observed with soot production. It is also observed that soot production is strongly linked to temperature and will increase with increasing temperature [8]

A simple two-route mechanism model is suggested as an explanation for the formation of soot; this is illustrated below in figure 13. Aromatic hydrocarbons can either form soot via a quicker direct method where the aromatic rings are condensed into graphite structures. The aromatic hydrocarbons can also follow a more indirect method involving the fragmentation of the aromatic ring into a simpler hydrocarbon, which then polymerises and eventually forms carbon. The choice of which route will be followed is temperature dependant. If the temperature is lower, below about 1800K, the first route will be followed and if the temperature is above 1800K the latter route will be followed. If the hydrocarbon fuel is of the aliphatic type it will only follow the latter route described where the large molecules fragment and then polymerise finally forming carbon [21].
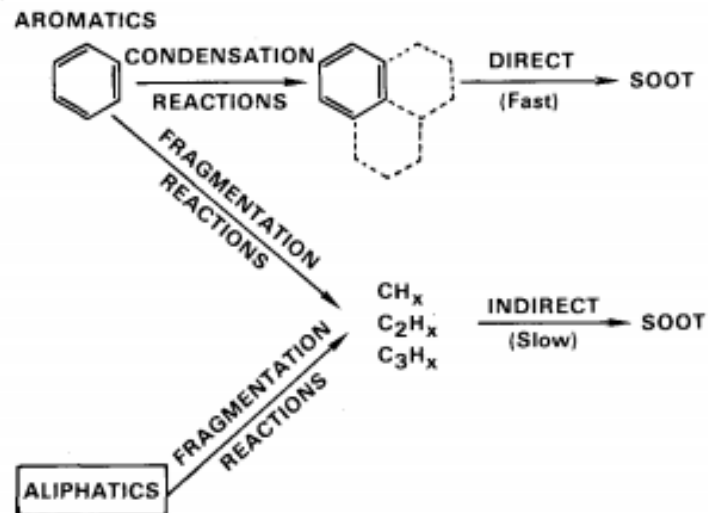
Figure 13: Nucleation routes for soot formation [21]

Many other formation models exist but it appears that none have been proved emphatically. Thus the comprehensive understanding of nucleation is still illusive.

4.4.5. Particle Growth

4.4.5.1. Surface Growth

After the process of nucleation has ceased the mass of soot formed will increase. Without this stage the soot loading solely attributed to nucleation would be low. The nuclei increase their mass and size by increasing their surface area. This is accomplished by deposition of gas-phase hydrocarbon intermediates. The actual nature of these intermediates can be explained by referral to figure 13, above. The fragmented hydrocarbons of the first more direct formation route could be the source of the simpler hydrocarbon intermediates. The deposition of the hydrocarbon intermediates will be in an even fashion, retaining the particle's spherical structure. At any time during the surface growth development phase the particles can combine or agglomerate with one another [21].

4.4.5.2.Agglomeration

This development stage will increase the size of the particles but it will decrease the number of particles. The way in which the particles combine can vary. While the sizes of the particles are still comparatively small, thus in the infancy of the surface growth stage, they can simply combine and coalesce or coagulate into a single spherical particle. If the collision occurs later in the surface growth development phase, thus with larger particles, the particles will simply combine to form a cluster of individually recognisable particles. These clusters can again combine to form long chainlike structures. This formation of chainlike structure suggests that the electrostatic forces have a significant role to play, and it was found that such chains have a positive charge.

The stages of particle size growth and the consequent impact of the number of particles and the overall hydrocarbon concentration is shown in figure 14, below. It is seen that the overall particle number density will increase until a maximum is reached. This is attributed to the transition between nucleation and agglomeration. Thus during agglomeration the number of particles decreases but the corresponding particle size increases. The surface growth stage terminates when the curves, indicative of particle size, diameter and volume, pass though the point of inflection. The decrease in the hydrocarbon concentration throughout the process can be attributed to the simple law of conservation of mass. The hydrocarbon fuel is the source of particles thus as the concentration of the particles increases the amount of hydrocarbon fuel decreases. Also the source of the hydrocarbon intermediates used in surface growth must be attributed to the fuel [21].
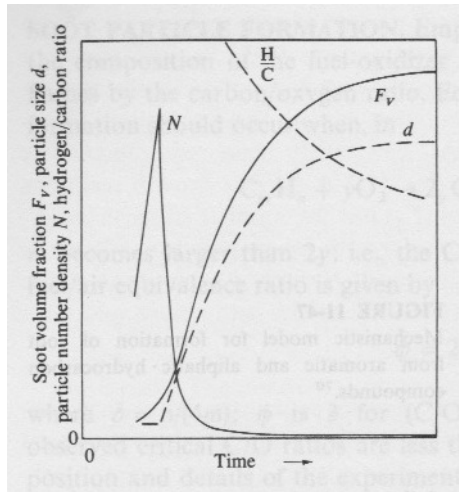
Figure 14: Interplay between soot concentration and size [21]

4.4.6 Particle Oxidation

The prevalence of soot particle oxidation is a strong one. Investigations have shown that combustion chambers that produce large soot loading sometimes do not expel such high soot concentrations in the exhaust, as the mechanisms for oxidation of the soot to CO and CO_2 are very good.

The amount of oxidation is seen to be a transient operation. The rate of oxidation can be indicated by the decrease or increase in carbon, or soot, in the cylinder – this is called carbon recession. In figure 15 below the rate of carbon recession is plotted against the engine's crank angle. It is seen that there is a maximum point reached after which the rate decreases. This maximum can be linked to the idea that the rate of oxidation freezes after some point. This oxidation freezing is linked to the cylinder temperature and is seen to occur at about 2000K, thus oxidation of the carbon soot will only occur at temperatures above 2000K [21].
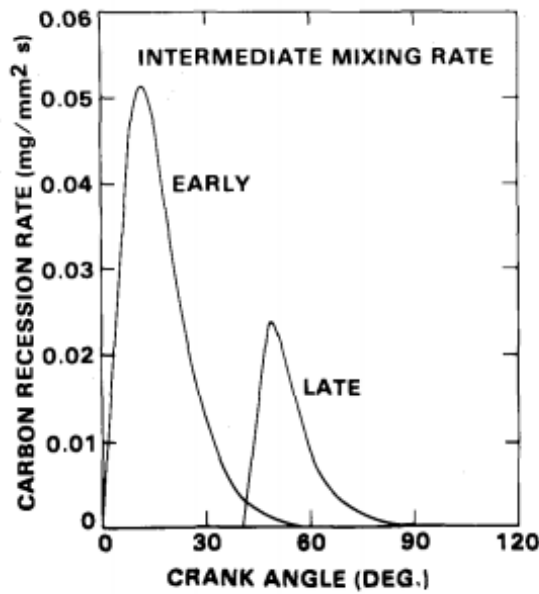
Figure 15: Carbon Recession versus Time in the Cylinder [23]

This idea of oxidation freezing being linked to temperature is illustrated clearly in figure 16 below, where the rate of carbon recession is plotted against temperature directly for various partial pressures of oxygen. The partial pressure of the oxygen is indicative of the concentration of oxygen. It is seen that with more oxygen, carbon recession will increase as expected but a consequent higher temperature environment will need to be maintained to reap this benefit. [21]
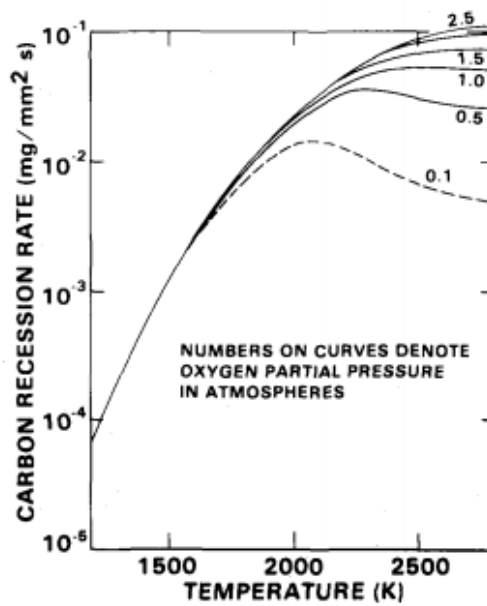
Figure 16: Carbon Recession versus Temperature [21]

4.5. Previous Relatable Works

Work has been done where the particulate emissions from a compression ignition engine running on dimethyl ether were compared to those of a conventionally fuelled diesel engine. XinLIng et al [24] found that the particulates emitted, by number, from an engine, while being fuelled with dimethyl ether decreased for engine speeds of 2200rpm, when compared to the same engine operating with diesel fuelling. The particulates emitted by number, increased for engine speeds of 1400rpm at high and medium loads, when dimethyl ether fuel was used. XinLing et al [24] also found that the geometric size of the particulates increased when diesel fuel was used and that more particulates of the nucleation mode where emitted when dimethyl ether was used, as compared to more accumulation occurring under diesel fuelling.

A study by Mitsuharu et al [25] found that the size distribution of the particulates emitted from a direct injection dimethyl ether fuelled engine, decreased when compared to a diesel fuelled engine. This means that smaller particles were found under dimethyl ether conditions. Mitsuharu et al [25] also found that the size distribution decreased with increasing load.

Work has also been done that relates the gaseous emissions of a compression ignition engine that is fuelled on dimethyl ether. Kim et al [26] found that NOx emissions were slightly higher under dimethyl ether fuelling conditions when compared with diesel fuelling. A reason for this is given to be that charge temperature in the combustion chamber was increasing as the dimethyl ether ignited faster than diesel. Carbon monoxide and hydrocarbon emissions were drastically lower with dimethyl ether fuelling as more free oxygen is released. Kim et al [26] also found that the indicated mean effective pressure was slightly higher with dimethyl ether fuelling and attributes this to the engine having a higher thermal efficiency under dimethyl ether fuelling, as less products of incomplete combustion were present allowing for lower heat radiation and better combustion efficiency.

4.6 Dimethyl Ether Characteristics

Diesel and dimethyl ether (DME) were both used to fuel the test engine, as outlined in the experimental objectives. The characteristics of this fuel need to be elaborated upon. DME is a colourless gas at room temperature; it must thus be compressed into a liquid prior to injection, as injection in the gaseous phase is problematic. The table below summarises the properties of DME and diesel for comparative purposes.

Table 2: Physical Properties of DME [29]

PARAMETER	DME	DIESEL
Chemical formula	C2H6O	C14.4H24.9
Mole weight (g)	46	>100
Boiling Point (^{0}C)	-24.9	180 – 350
Vapour Pressure @ 25^{0}C (bar)	5.1	<0.01
Liquid Density (kg/m^3)	668	840
Liquid Viscosity (cP)	0.15	4.4 – 5.4
Low Heat Value (MJ/kg)	28.43	42.5
Explosion Limit in air (vol %)	3.4 - 17	0.6 – 6.5
Ignition Temperature (^{0}C)	235	250
Cetane Number	55 - 60	40 - 55
%wt of Carbon	52.2	86
%wt of Hydrogen	13.0	14
%wt of Oxygen	34.8	0

It is seen that DME has on average a slightly higher Cetane number; this would suggest a smoother running engine and an easier starting engine. However the viscosity of the DME is considerably lower than that of the diesel. This accounts for the biggest challenge in DME fuelled engines. Unlike diesel, the low viscosity of DME offers virtually no lubricating properties. This also makes the compression of DME difficult, as its poor lubricating properties will destroy most pumps used to compress it.

5. Apparatus and Facilities

5.1 Test Cell Schematic

Shown in the figure below is the functional layout of the test cell used. The movement of information and matter is shown as well as energy output from the engine.
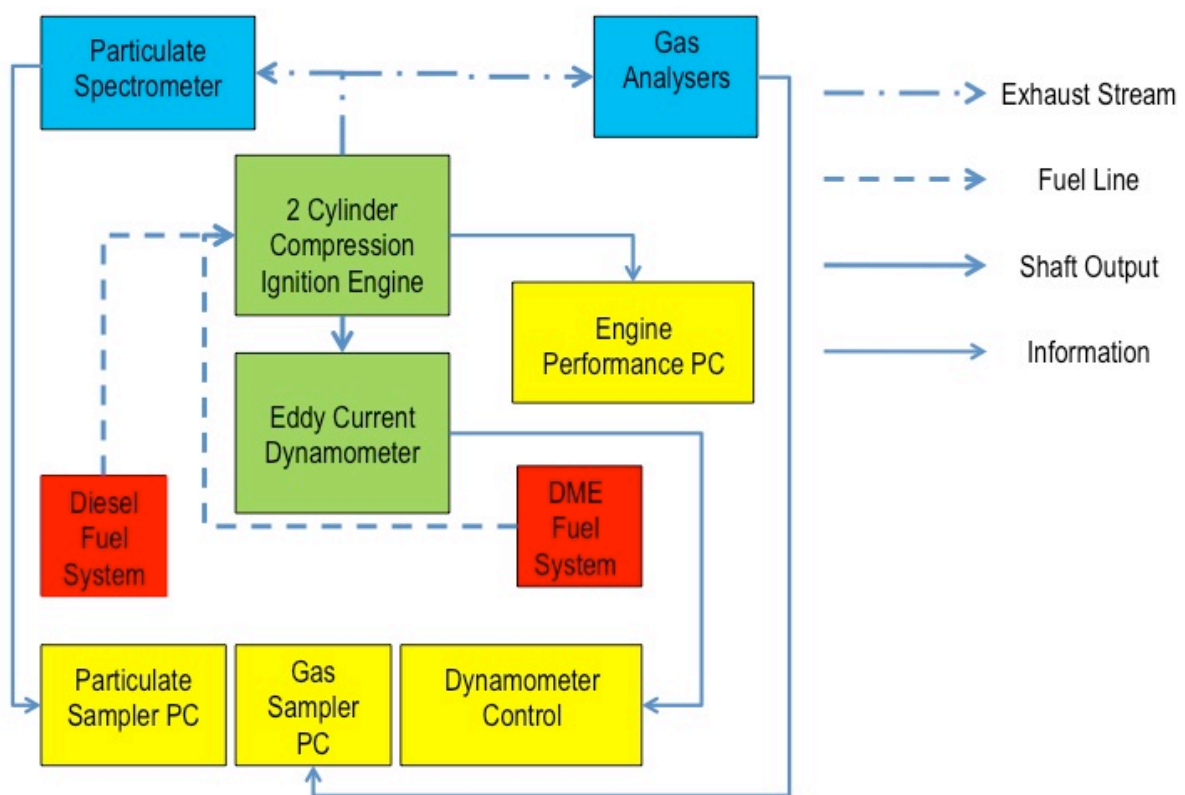
Figure 17: Functional Layout of Test Cell

5.2 Experimental Apparatus

5.2.1. Compression Ignition Engine

A Lister Petter 2-cylinder air-cooled compression ignition engine was used for this investigation. The engine had its air directing shrouds removed to allow for the installation of pressure transducers. The removal of the shroud covers necessitated the use of extra cooling fans to prevent the engine from overheating. The specifications of the engine are presented in the table below.

Table 3: Engine Specifications

PARAMETER	VALUE
Engine Model	R V19 PH2 40 9602
Manufacturer	Lister Petter
Displacement	1330cc
Cylinders	2
Bore	87.74mm
Stroke	110.0mm
Maximum Power	13.4Kw @ 2200rpm
Maximum Torque	59.4Nm @ 2200rpm
Compression Ratio	16.5:1

5.2.2. Dynamometer

A Borghi and Saveri water-cooled eddy current dynamometer is directly coupled to the engine. The water supply is re-circulated through a pumping system between the sump water storage in the Mechanical Engineering Laboratory basement and a header tank on the roof of the Laboratory. This header tank allows for water to be delivered to the dynamometer at the required pressure, and also incorporates an overflow system as the pump provides water at a flow rate that is in excess of what is required. The specifications of the dynamometer are presented in the table below.

Table 4: Dynamometer Specifications

PARAMETER	VALUE
Model	FE 150 S
Manufacturer	Borghi & Saveri
Maximum Input Speed	13000rpm
Maximum Input Torque	280Nm
Maximum Input Power	110Kw

5.2.3 Diesel Fuel System

The diesel fuelling system is the conventional system that is found on the standard 2 cylinder Lister Petter engine. The main feature being that it is a mechanical injection system with a cam driven injector pump and a mechanical injector per cylinder. The injectors have a return flow line that re-enters the main fuel line downstream of the fuel flow meter. The only modification to the system is that a 3-way valve is installed in the main fuel line before it splits to each injector pump. This 3-way valve allows the DME fuel to be introduced and the diesel fuel to be isolated.

5.2.4. DME fuel System

As mentioned previously the DME fuel enters the main fuel line before the line splits to each injector pump. Thus the DME is injected in the same manner as the diesel. The DME is supplied under pressure to the 3-way valve from a diaphragm pump. The DME is pressurised to prevent it from vaporising before it is injected, as the injection pumping system only works with liquid DME. The DME is supplied from a conventional propane type cylinder, except that it is drawn off from the bottom of the cylinder via a submerged pipe, to ensure that only liquid is removed. The DME flows from the bottle through a non-return valve, to prevent flash back, into a control regulator; the pressure is controlled to about 4 bar at this point. From the regulator the DME travels through a rotameter to measure its flow rate thus allowing a fuel consumption figure to be determined. From the rotameter the DME flows into a Hydracell diaphragm pump. The specifications of the pump are presented in the table below:

Table 5: DME Delivery Pump Specifications

PARAMETER	VALUE
Model	*F20, with X Cam*
Manufacturer	*Hydracell*
Rated Rotational Speed	*1750rpm*
Maximum Delivery Pressure	*70 Bar*
Rated Flow Rate	*3.79 l/min*
Maximum Inlet Pressure	*7 Bar*
Diaphragm Material	*Buna-N*

This type of pump is specially designed to pump highly corrosive substances like DME at relatively low flow rates but at high pressures. However, the pump still delivers DME at a flow that is in excess of what the engine consumes. The pump is thus fitted with pressure relief valve that allows the operating pressure to be set. This pressure relief valve then vents excess DME into a return line that re-enters the pump inlet. The return line incorporates a cooling coil that removes excess heat from the DME as it is re-circulated. This cooling coil is submerged in a dry ice and water bath. The excess heat, if not removed, would accumulate in the system and bring the DME to boiling point, thus vaporising it, and nullifying the whole pumping operation.

The injector overflow is gaseous as the DME is venting to atmospheric pressure at this stage. This flow is led through a second rotameter. The difference in flow rates between these two rotameters, the primary at the bottle and the secondary at the injector overflow, is representative of the consumption of DME.

5.3 Experimental Instrumentation

5.3.1. Gas Analysers

Four gas analysers are used in this investigation, namely:

- Signal Series 7000 GFIR Carbon dioxide, CO_2
- Signal Series 7000 GFIR Carbon monoxide, CO
- Signal HM Total hydrocarbons, THC
- Signal 4000 VM Heated Vacuum Nitrous Oxides, NO_x

The gas analysers are set up to sample through the same heated line. The use of a heated line is needed as many species such as NO_x are dependant on temperature when they form or decay, thus conditions found at the exhaust must be carried forward into the sampler, and maintaining this heated atmosphere also prevents water in the exhaust from condensing. The heated line terminates in an oven chamber, which freezes the decay or formation of these species through temperature control. The oven also has a particulate filter, as particulate matter can damage the analysers. From the output of the oven chamber the sample splits into those that are analysed hot and those that need to be cooled. The species that are analysed hot are:

- NO_x
- THC

The remaining sample is cooled and dried before entering the analysers. This is performed in a cooler and drier unit; this unit dissipates excess heat though a heat exchanger system connected to large heat sinks. These heat sinks have air directed over them to allow for heat loss by forced convection. Removing condensate, which forms as the sample is cooled, through a tube pumping system, dries the sample. The condensate forms in tubes, which are squeezed by rotating rollers that force the condensate out and vent it to atmosphere. The layout of the analyser arrangement is shown in the figure below:
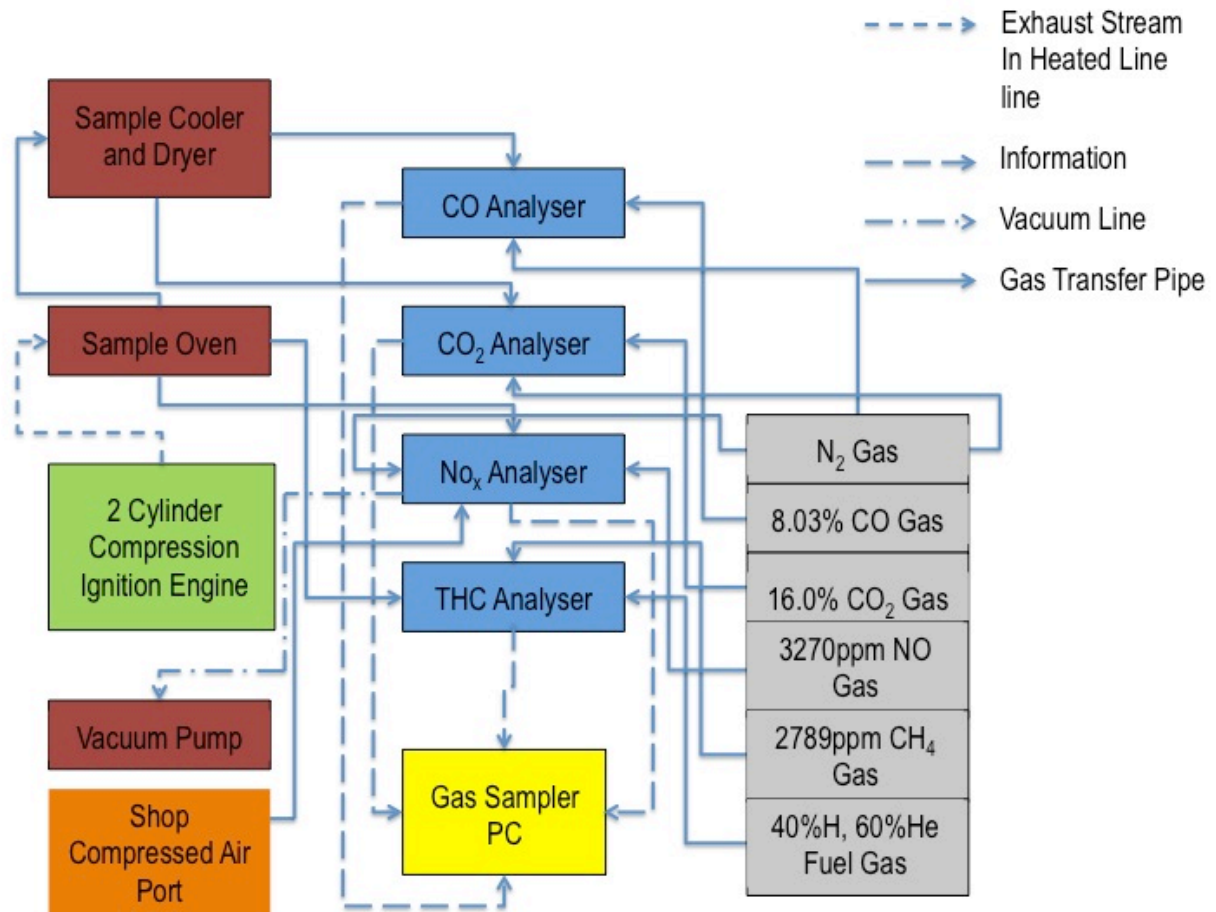
Figure 18: Signal Gas Analyser Layout

5.3.2. Particulate Spectrometer

This instrument is a:

- Cambustion DMS500 Fast Particulate Spectrometer

The device is used to measure various parameters to do with particulate matter, including:

- Transient spectral changes in particulate size with concentration.
- Time averaged size spectral density of particulates.
- Time averaged cumulative particulate distribution.
- Minimum and maximum particle sizes.
- Geometric mean particle diameter and the deviations.

40

- The total particle concentration, thus number of particles per cubic centimetre.

This instrument also operates with a heated line to prevent any changes to the sample with decreasing temperature. The instrument has a mechanism to dilute the sample. This is particularly useful with engine testing, as the high concentration of particulates would quickly damage the instrument. A primary diluter is used in conjunction with a secondary diluter; the primary allows dilution of up to 10:1, while the secondary allows for dilution of up to 500:1. This allows for a maximum dilution of 5000 parts of dry air to 1 part sample stream. In this investigation the diluters were set as follows for diesel:

- Primary dilution at between 7 and 9
- Secondary dilution at 500

And for DME:

- Primary dilution at 5
- Secondary dilution at between 10 and 50

The amount of dilution is fine-tuned by referring to a dynamic range scale provided on the instrument-operating window in the software. This scale is colour coded and should always be in the green range. The layout of the instrument is shown in the figure below as follows:
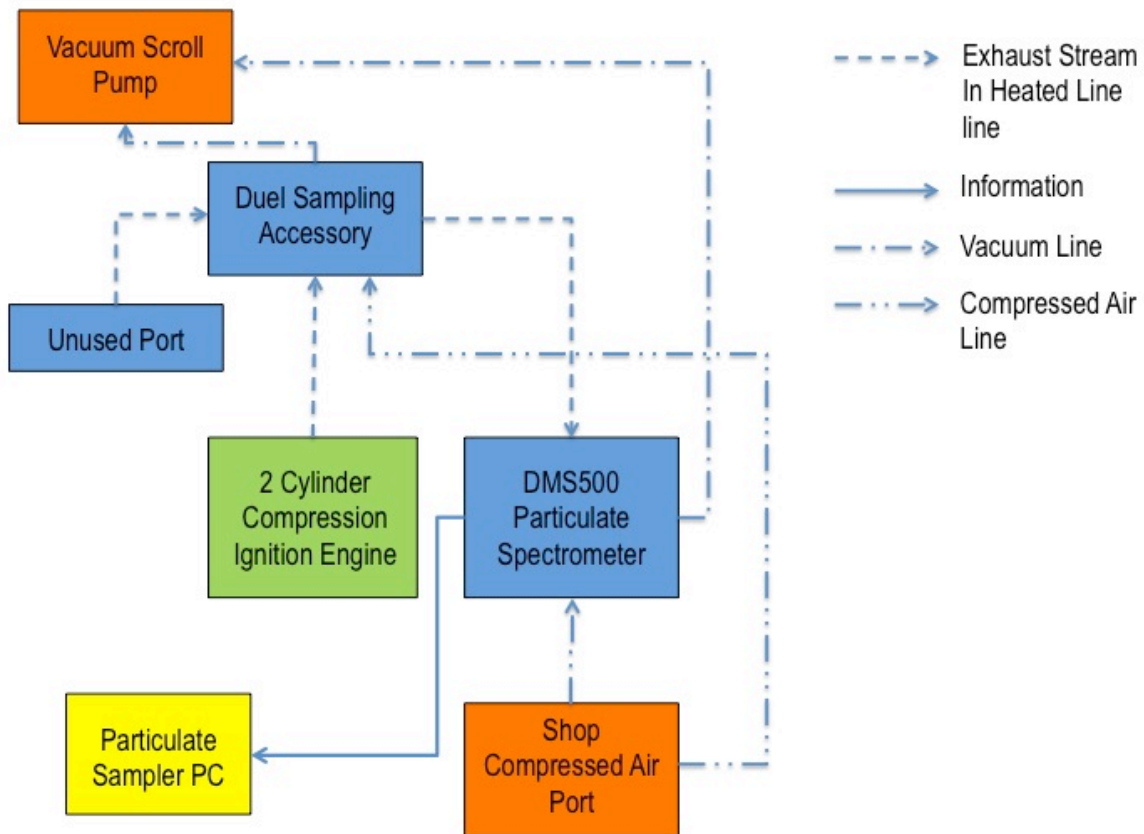
Figure 19: DMS500 Layout

5.3.3. Engine Test Instrumentation

5.3.3.1. Diesel Fuel Flow

The diesel fuel consumption is measured using a *Pierburg PLU 106* analogue flow meter. The signal is amplified and displayed on an analogue dial. This signal is split at this point and converted to a digital signal, using a DAC, and input into the data acquisition PC for recording, via one of the steady state channels.

5.3.3.2. Barometric Pressure

The ambient barometric air pressure is measured using a digital barometer; this signal is directly input into the data acquisition PC via a steady state channel and recorded.

5.3.3.3. Engine Air Flow

The engine draws in air through a plenum chamber that has a *BS 1042 Standard* orifice plate as its inlet. The pressure drop across this orifice plate is measured using a digital manometer. This manometer outputs a proportional voltage, which is fed into a steady state channel on the data acquisition PC for recording and interpretation.

5.3.3.4. Torque

A load cell at the end of an arm measures the torque applied to the engine as a result of the control current. The load cell, which is of the *S-Type,* outputs a voltage that is input, via a steady state channel, to the data acquisition PC and recorded.

5.3.3.5. Ambient Temperature, Exhaust Temperature and Engine Inlet Air Temperature

All three of these temperatures are measured using *K-Type thermocouples*. All output a pre-calibrated voltage, which are input into the data acquisition PC via steady state channels.

5.3.3.6. Fuel line and Cylinder Pressure

In both cases *Piezoresistive* pressure transducers are used. A *Kistler 4065A1000A1* is used for the fuel line and a *Kistler 6121A1* for the cylinder pressure. These are dynamic instruments and their outputs are fed into the data acquisition PC via high-speed channels. The voltage in each case is amplified, via a separate charge amplifier before being sent to the PC. The cylinder pressure transducer is enclosed with a water jacket to maintain a relatively low temperature while sampling. The water jacket, which surrounds the transducer, has tap water running through it and thus this constant flow removes heat that would otherwise accumulate.

5.3.3.7. TDC Marker and Crank Angle

The TDC signal is used as the trigger point for all the instrumentation. It is determined via an *AVL Pulse Multiplier*, and this signal is fed directly into the data acquisition PC. A shaft encoder that measures every 0.2^0 CA determines the crank angle that has elapsed since the TDC trigger; this is fed to the data acquisition PC via a high-speed channel.

6. Instrumentation Setup

6.1 Signal Gas Analysers

The Signal Gas Analysers were serviced and calibrated as follows:

- Replacing all filters in the units
- Renewing pump diaphragms and seals
- Changing faulty electronic control boards
- Cleaning all sample pipes and chambers
- Ensuring that all gas suppliers were adequate, including span gases, fuel gases and zero gas, which in this case was nitrogen.
- Calibration of all analysers.

6.2 Cambustion Fast Particulate Spectrometer

This instrument was a new acquisition by the Thermodynamics Engine Testing Department. It was thus necessary to set up and commission all components, including:

- Provision of airlines for the instrument's diluter.
- Set up of the vacuum scroll pump, which draws the sample through the instrument and provides vacuum to operate control valves.
- Set up of the DMS500 instrument including wiring for electrical supply to the instrument.

Only the manufacturer in England can perform the calibration of the instrument. A calibration certificate accompanied the instrument ensuring that it would perform as required. The instrument was tested by drawing a sample from the engine exhaust and comparing basic trends with those described in the instrument's user manual. In all cases it was found that the instrument behaved as expected.

7. Calibrations

7.1 DMS500 Fast particulate Spectrometer

The DMS500 was calibrated at the factory and supplied with a calibration certificate, for a period of 18 months. The 18 months is based on the assumption that the instrument is used on a daily basis. Although it must be noted that a regular calibration must be performed at least every 2 years as the calibration points of the sensing elements will drift with time.

7.2 Signal Gas Analysers

The calibration procedure needs to be completed at every start up. The procedure is detailed below:

1. Ensure all gas cylinders have adequate gas this includes the nitrogen (zero air), the span gases and the fuel gas for the THC analyser.
2. Open the compressed air supply to the analyser rack.
3. Start up all analysers, the vacuum pumps, the oven, heated line and cooler/drier.
4. Allow all analysers, which are now in the standby mode to warm up for 60-90 minutes.
5. Enter Zero mode on all analysers and allow time to settle.
6. Adjust the zero calibration potentiometer on all analysers until zero is seen on the output.
7. Enter the span mode on all analysers and allow time to settle.
8. Adjust the span calibration potentiometer on all analysers until the correct reading is seen based on the concentration of the span gas used.
9. Ensure all span values are correct under settings on each analyser.
10. Press the calibration button and allow time for the calibration to be performed.

7.3. Data Acquisition Software.

The engine parameters are captured on the engine test computer. A number of high speed and steady state channels are used. The following calibration values were used:

Table 6: Engine Test Channels Calibrations

	Channel Number	Description	Units	Conversion Factor (MU/Volt)	Calibration Factor (MU)
High Speed Channels	1	Trigger	None	Not Applicable to High Speed Channels	
	2	Fuel Line Pressure	MPa		
	3	Cylinder Pressure	MPa		
	4	Not Used			
	5	Crank Angle Encoder	Degrees		
	6	Top Dead Centre Indicator	None		
Steady State Channels	2	Diesel Fuel Flow Meter	g/s	0.9709	-0.0067
	3	Barometric Pressure	Bar	1.0000	0.00000
	4	Air Flow	mmH_2O	4.1111	0.1166
	5	Engine Speed	Rpm	994.86	4.6838
	7	Engine Torque	Nm	27.819	0.7247
	9	Ambient Temperature	^{0}C	98.0200	1.8629
	10	Pre Catalyst Exhaust Temperature	^{o}C	98.5030	-2.5197
	11	Post Catalyst Exhaust Temperature	^{0}C	98.891	-0.7402
	12	Air Temperature	^{o}C	98.9710	1.1938

7.4.DME Rotameters

The rotameters used were calibrated using a software program provided by the manufacturer. The calibrations for the primary and secondary rotameters are given as follows:

- Primary, $y = 0.0005x^2 + 0.1009x - 0.1192$
- Secondary, $y = 0.015x$

Where: y = mass flowrate in (g/s)

And: x = scale reading on rotameter

The models of the rotameters are given as follows:

- Primary: FP-1/8-25-G-5/81, for liquid DME
- Secondary: FP-1/4-40-G-6/81, for gaseous DME

8 Procedure and Precautions

The procedure and necessary precautions are presented below for each of the major apparatus areas, namely the gas analysers, particulate spectrometer, engine and DME fuelling system.

8.1 Procedure

8.1.1 Signal Gas Analyser

1. Open all cylinder valves to span gases, nitrogen and fuel gas.
2. Open compressed air supply.
3. Switch on vacuum pumps.
4. Switch on all analysers and allow 60 minutes to warm up.
5. Calibrate analysers as outlined in section 7.2.
6. Start up signal program on the control computer.
7. Enter a name and location for the tests to be saved.
8. Enter sample mode on the analysers.
9. Take tests as outlined below.

8.1.2 DMS500

1. Open compressed air supply.
2. Switch on main power switch on analyser.
3. Switch on vacuum pump.
4. Switch on duel sampling accessory and select heated line to be used.
5. Start up Cambustion program on the control computer.
6. Select instrument status ON in the Cambustion program.
7. Allow instrument to warm up.

8. Select auto zero mode in the Cambustion program and allow instrument to zero.

9. Select sample mode in the Cambustion program.

10. Take tests as outlined below.

8.1.3 Engine Set Up

1. Start up dynamometer cooling water pump.

2. Switch header water tank status light, and wait for it to illuminate, this indicates the tank is full.

3. Open all water valves to the dynamometer.

4. Open pressure transducer cooling water valve.

5. Switch on dynamometer controller.

6. Enter mode M, constant control current, using the mode selector knob.

7. Select zero control current.

8. Start engine.

9. Increase the control current until a torque of 20Nm is attained.

10. Adjust speed on engine governor until 1500rpm is attained.

11. Allow the engine to warm up until an oil temperature of 50^0C is attained.

12. Take tests as outlined below.

8.1.4 Extra Instructions for DME Testing

1. Close DME regulator.

2. Close DME primary rotameter valve.

3. Switch 3-way fuel selection valve to DME fuel.

4. Submerge return line cooling coiling in 2 kilograms dry ice and water.

5. Fill the DME pump with oil via the breather port.

6. Open DME dump valve.

7. Open liquid valve on DME cylinder.

8. Slowly open DME regulator valve fully and about 4,5 bars is reached.

9. Slowly open DME primary rotameter valve until nearly fully open.

10. Close DME dump valve when liquid DME has begun to appear in the gas stream.

11. Let the inlet pressure build up to 4,5 bars.

12. Open DME dump valve again, liquid DME should appear in a strong stream.

13. Slowly close DME dump valve.

14. Open the pressure relief valve about 3 turns.

15. Switch on the DME pump.

16. When delivery line pressure builds, slowly close the pressure relief until 50 bar is reached.

17. Ensure pressure is stable at 50 bar

18. Start the engine.

19. Wait for fuel change over, characterised by a change in tone of the engine and the expulsion of diesel under the high pressure from the injector overflow line, this takes about 5 minuets.

20. Open throttle wide at change over, and then release it back.

21. Fit the secondary rotameter pipe to the injector overflow line.

22. Check that DME can be smelt from the output pipe of the secondary rotameter, this signifies the engine is indeed running on DME.

23. Continue on from section 8.1.3, step 9.

24. After the testing is complete switch off the DME pump

25. Close the DME cylinder.

26. Vent the DME out from the dump valve.

27. Close the DME dump valve once all DME has vented out of the pumping system.

28. Close the DME regulator.

8.1.5 Experiment

The outline of the experiment is illustrated in the table below:

Table 7: Experimental Matrix

		TORQUE					
		20	25	30	35	40	45
SPEED	1300	1a	2a	3a	4a	5a	6a
	1400	1b	2b	3b	4b	5b	6b
	1500	1c	2c	3c	4c	5c	6c
	1600	1d	2d	3d	4d	5d	6d
	1700	1e	2e	3e	4e	5e	6e
	1800	1f	2f	3f	4f	5f	6f

The readings of gas concentrations, particulates and engine performance are taken in sets as shown, set 1 – 6, at the torques shown and speeds a – f. This is done for both DME and diesel fuels.

1. Using the control current dial, on the dynamometer controller, set the control current to produce the torque needed.
2. Using the engine governor dial set the speed needed.
3. Adjust the current dial, if the torque has changed with the speed change.
4. Allow the engine to settle for about 10 seconds.
5. Set the desired file name and save path in the Signal program.
6. Start logging the gas analyser readings.
7. Set the desired file name and save path in the Cambustion program
8. Start logging the particulate readings.
9. Stop logging the particulate readings once the gas readings have stopped.
10. Set the desired file name and save path in the Engine Test Program.
11. Set the speed trigger point appropriate for the test.
12. Flip the cylinder pressure transducer charge amplifier from reset to operate.
13. Start the test and accept it.
14. Flip the cylinder pressure transducer charge amplifier back to reset mode.
15. Open the HRCA program and load the test and ensure that the test contains data, repeat if necessary.
16. Repeat steps 2-14 for all the desired speeds.

17. Set the next torque needed and continue with steps 2-14 for the speeds within that torque bracket.
18. Repeat all the above for DME fuel.

8.2 Precautions

8.2.1. Engine and Dynamometer

1. Ensure that the water supply to the dynamometer is running this can be checked with the status lamps on the front of the dynamometer controller.
2. Ensure that the over-speed dial is set to maximum; this will prevent the control current from being switched off at high speeds.
3. Make sure that the battery is fully charged.
4. Never allow the engine speed to exceed 2500rpm for an excessive period of time.
5. Injector opening pressure must always be at 210 bar.

8.2.2. Instrumentation

1. The cooling water to the cylinder pressure transducer must be on at all times.
2. The pressure transducer charge amplifier must remain in the reset mode at all times expect when a test is being taken.

8.2.3. DME Fuel System

1. The DME pump must not be started until liquid DME vents out of the dump valve, if gas is still in the system it will cause cavitation in the pump.

2. Ensure that the DME return-line cooling-coil is always submerged in water and dry ice when DME test are being done.

3. Ensure that the dry ice and water bath never exceeds 5^0C, add more dry ice if it does.

4. Ensure that the engine and DME pump oil level is correct.

5. After DME tests have been done be sure to run the engine on diesel for a period of 2 minutes, this will ensure that all DME, which is highly corrosive, is not left in the system.

9. Experimental Observations and Difficulties

9.1. DME Fuelling Problems

The use of DME as a fuel for internal combustion engines, although having many advantages with regard to emissions, has numerous practical challenges. Many of these are associated with the fuel's need to be compressed into the liquid phase to allow for its injection into the engine. The DME is also highly corrosive and causes excessive wear to pump seals and this is aggravated by the high pumping pressures, such as an input pressure of 4 bar and an output pressure of 40-50 bar. The pump used to pressurise the DME, as expanded upon earlier, is of the diaphragm type. On several occasions the diaphragm burst and the pump had to be serviced. The reason for the diaphragm bursting was believed to be the DME vaporizing at the diaphragm surface resulting in cavitation. Fitting larger inlet pipes to the pump rectified this. Previously the pump inlet fitting of a ½ " BSPT, was reduced to a ¼ " BSPT fitting and to a 1/8" fitting at a point further along. These small fittings were believed to be mimicking the effect of an orifice and expanding the DME, causing vaporization. Another reason for the bursting of the pumping diaphragm was that the incorrect material was specified. The pump agents suggested that a Viton diaphragm be used but this failed on numerous occasions. A Buena-N diaphragm was tried and this eliminated the bursting problem.

Other problems encountered with the DME fuelling apparatus was at one point the pump motor seized due to the high pressures and consequent in-pump forces. The cause of this was believed to be a faulty pressure relief valve that would, under normal operating conditions not allow a build-up of pressure followed by a sudden release, but rather a consistent release. The problem was rectified by greasing the pressure relief valve well and regularly, as seen in the procedure.

9.2 Data Acquisition Problems

Due to a well-used set-up that was in place, many instruments and amplifiers were showing signs of wear and tear. The pressure transducer charge amplifier was one case in point. The amplifier built up a residual charge and would cause an offset of the pressure waveforms in an ever-increasing trend. Keeping the amplifier in the 'Reset' position between successive readings rectified the problem and it was only switched to the 'operate' position shortly before the reading was to be taken. The significance of this was not well understood in the initial stages. It is for this reason that this preventative measure is included in the normal operating procedure.

9.3 Signal Gas Analysers

While overall these instruments proved to be very robust and reliable, the THC analyser, which is a flame ionization type instrument, proved very difficult to ignite. The flame used is a hydrogen flame in a helium carrier gas. Initially the reason for the difficulty in igniting the flame was believed to be due to the hydrogen and helium gas mixture separating in the cylinder, over the extended period that it had been standing. A new cylinder was ordered; however, the problem prevailed. The final theory on this was that on colder days the ambient air was not conducive to the hydrogen flame igniting, as the instrument gave little resistance on warmer days of operation. It must also be noted that colder days in Johannesburg are generally drier and the lack of water vapour in the air may have contributed in some manner to the flame not igniting. However it was found that if the instrument warm up period was extended to 60 minutes, as stated previously, as opposed to the recommended 30 minuets the problem was often resolved by numerous attempts at igniting the flame, with a 25 second purge of the instrument following each unsuccessful attempt.

10. Raw Experimental Data

The data acquisition on the experimental rig is largely automated with the sampling systems recording the data to either a .csv file or an .xls file. The raw data is largely in the same form for either the diesel tests or the DME test, thus one explanation for each type will be given.

10.1. Particulate Data

The Cambustion Fast Particulate Spectrometer automatically records data in a .dms file format that is easily converted to .xls format by the data processing Excel macro provided. The data acquired after each test has the format shown in the figure below:
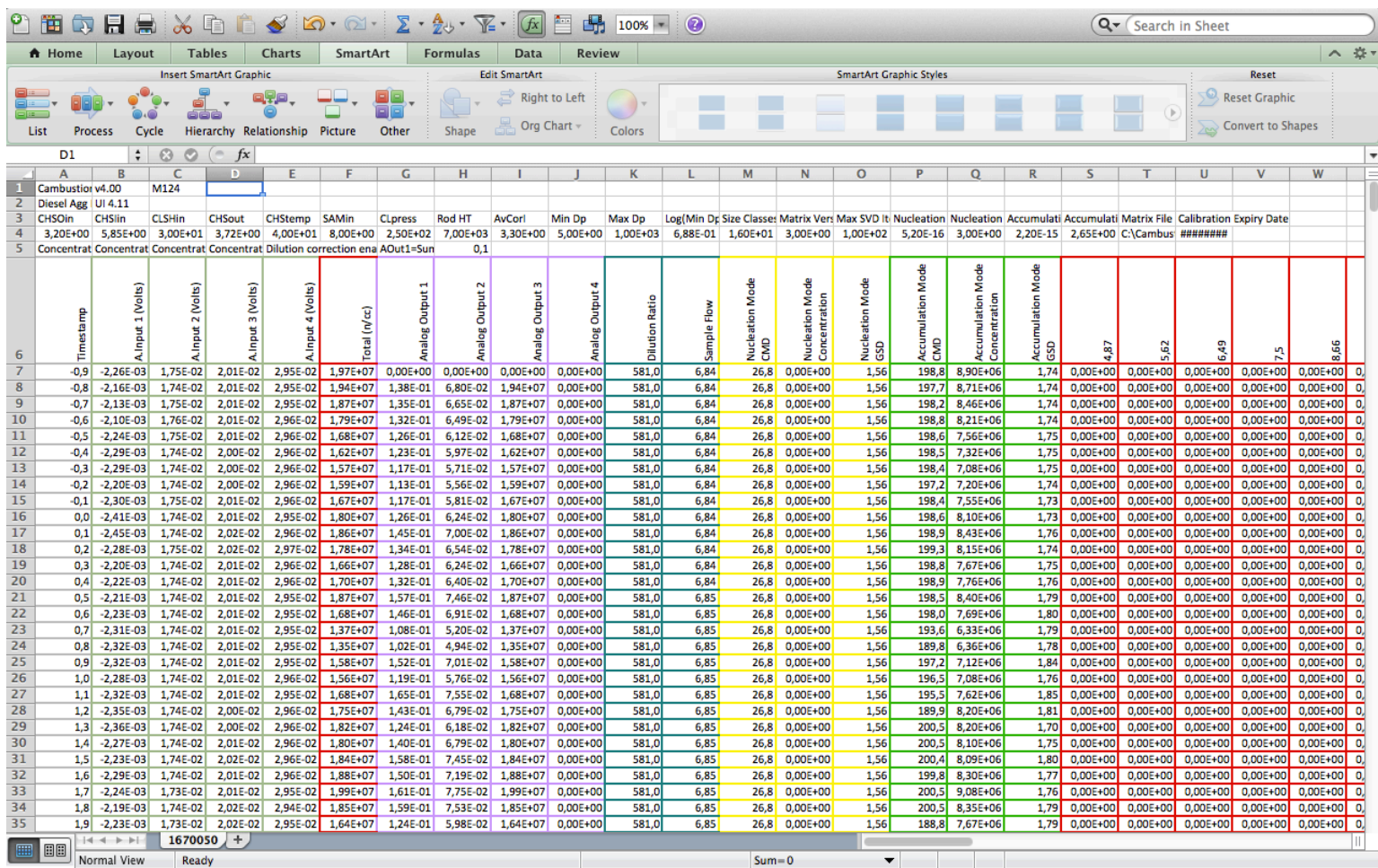
Figure 20: Screen Shot of the Cambustion Data

A multitude of information is given in the above spreadsheet. The instrument records information about the particulates that it is sampling at 0.1 second intervals, thus each line of data represents the sample every 0.1 seconds. The tests that were conducted in this investigation were steady state tests so the fluctuations in data every 0.1 of a second were not important, as an average was taken over the entire interval. The classifier column ring currents represent the basic experimental information; these are the electrical signals that the vortex of particulates creates while being spun in a vertical column. The classifier has at its core a high voltage coil set that induces currents in the classifier column receiving coils. The particulates interrupt these electrical signals thus they are detected. As the particulates are spinning, different sizes of particulates end up at different elevations in the column, based on their mass.

10.2. Gaseous Emissions Data

The signal gas analysers send information about the gas sample to a computer that measures at a 1 second interval, the information is sent as a digital signal. The data is compiled for all 4 analysers and saved to a .csv file, which can be opened in Excel. Fifty readings are taken per test and automatically averaged at the end of each data set. These averaged results are used in the further processing steps. The output information for the gas readings per test is shown in the figure below.

Figure 21: Screen Shot of Raw Gas Data

10.3. Engine Performance Data

The engine is instrumented to give information from various sensors, the details of which are explained in the preceding sections. The engine performance information is recorded on a dedicated computer for later processing with various fixed

geometric parameters of the test engine. The information is split into two sections namely the high-speed data channels and the steady state data channels as shown in the table below.

Table 8: Engine Performance Data Channels
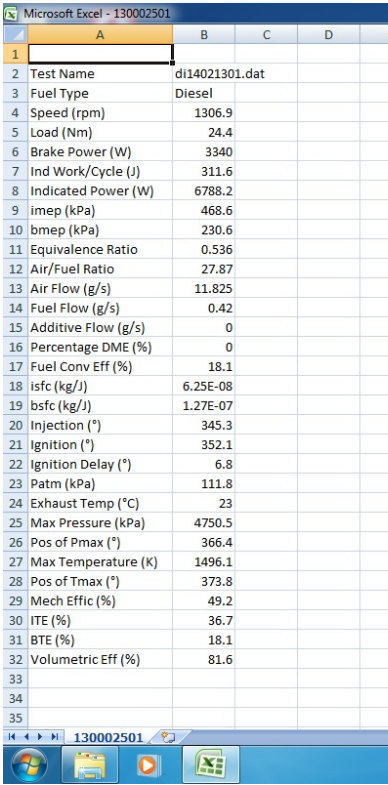
	Channel Number	Description
High Speed Channels	1	Trigger
	2	Fuel Line Pressure
	3	Cylinder Pressure
	4	Not Used
	5	Crank Angle Encoder
	6	Top Dead Centre Indicator
Steady State Channels	2	Diesel Fuel Flow Meter
	3	Barometric Pressure
	4	Air Flow
	5	Engine Speed
	7	Engine Torque
	9	Ambient Temperature
	10	Pre Catalyst Exhaust Temperature
	11	Post Catalyst Exhaust Temperature
	12	Air Temperature

The acquisition software is programmed to acquire data for a period of 7 engine cycles, for later averaging. The high-speed channels sample every 0.2 degrees of crank angle. The information is recorded as volts from all the channels and converted based on the calibrations, explained in a previous section, into the appropriate mechanical unit. The raw information is graphed and presented for the 7 cycles per test and is later converted to a format that can be read into Excel and combined with the other information.

11 Results Processing

11.1. Performance Summary Data

Custom written software, developed as part of several previous Master's and Final Year projects, is used to compute all the required performance data for a particular test. The software, called HRCA, is based on the finite heat release principle in thermodynamics. This coupled with various known fixed parameters of the engine are combined to present information as shown in the figure below.

Figure 22: Screen Shot of Raw Performance Data

The above information is saved as a .csv file for easy manipulation. The .csv file is opened with Excel where it is combined with information from others tests within the particular experiment. This operation is simply performed by copying and pasting the data from one spreadsheet into another, as shown in figure below.

	25							30							35					
	1300	1400	1500	1600	1700	1800		1300	1400	1500	1600	1700	1800		1300	1400	1500	1600	1700	1800
Speed (rpm)	1331,2	1408,9	1491,5	1608,1	1724,7	1807,2		1306,9	1418,6	1510,9	1603,2	1690,7	1792,7		1316,6	1408,9	1510,9	1598,4	1705,2	1802,4
Load (Nm)	25,6	25,6	25,2	25,2	25,5	25,2		30,5	30,5	30,4	30,2	29,8	30,1		35,5	35,5	35,1	35	35,3	35,1
Brake Power (W)	3572,4	3781	3939	4246,9	4603,9	4772,9		4176,5	4533,6	4807	5077,9	5282,7	5652,4		4900,5	5244	5559,3	5858,2	6298,4	6631,7
Ind Work/Cycle (J)	315,5	317,7	331,7	335,8	327,2	328,4		306,3	321,1	312,2	344,3	333,6	354,4		307,5	317,8	326,1	334,4	347,5	339,8
Indicated Power (W)	7000,5	7461,1	8245,3	8999,4	9406	9892		6672	7591,6	7861,2	9200,8	9400,8	10589,5		6747,2	7463,1	8212,5	8907,4	9877	10208,5
imep (kPa)	474,5	477,8	498,8	504,9	492,1	493,9		460,6	482,8	469,4	517,8	501,7	533		462,4	477,9	490,4	502,8	522,6	511
bmep (kPa)	242,1	242,1	238,3	238,3	240,9	238,3		288,3	288,3	287,1	285,8	281,9	284,5		335,8	335,8	332	330,7	333,3	332
Equivalence Ratio	0,527	0,552	0,612	0,673	0,666	0,684		0,51	0,589	0,669	0,699	0,693	0,742		0,814	0,689	0,703	0,743	0,759	0,846
Air/Fuel Ratio	28,34	27,18	24,41	22,22	22,4	21,87		29,38	25,34	22,31	21,36	21,53	20,12		18,37	21,74	21,23	20,12	19,69	17,68
Air Flow (g/s)	11,752	12,046	12,552	13,115	13,115	13,115		11,488	11,951	12,639	13,115	13,115	13,115		9,274	11,905	12,532	13,115	13,115	13,115
Fuel Flow (g/s)	0,41	0,44	0,51	0,59	0,59	0,6		0,39	0,47	0,57	0,61	0,61	0,65		0,5	0,55	0,59	0,65	0,67	0,74
Additive Flow (g/s)	0	0	0	0	0	0		0	0	0	0	0	0		0	0	0	0	0	0
Percentage DME (%)	0	0	0	0	0	0		0	0	0	0	0	0		0	0	0	0	0	0
Fuel Conv Eff (%)	19,8	19,6	17,6	16,5	18	18,3		24,5	22	19,5	19	19,9	19,9		22,3	22	21,6	20,6	21,7	20,5
isfc (kg/J)	5,92E-08	5,94E-08	6,24E-08	6,56E-08	6,22E-08	6,06E-08		5,86E-08	6,21E-08	7,21E-08	6,67E-08	6,48E-08	6,16E-08		7,48E-08	7,34E-08	7,19E-08	7,32E-08	6,74E-08	7,27E-08
bsfc (kg/J)	1,16E-07	1,17E-07	1,31E-07	1,39E-07	1,27E-07	1,26E-07		9,36E-08	1,04E-07	1,18E-07	1,21E-07	1,15E-07	1,15E-07		1,03E-07	1,04E-07	1,06E-07	1,11E-07	1,06E-07	1,12E-07
Injection (°)	346,1	347,7	348,7	348,1	348,5	349,9		345,9	346,9	347,1	348,5	348,9	349,5		346,5	347,1	348,5	347,3	348,9	350,1
Ignition (°)	351,5	352,5	352,7	353,7	352,5	353,1		352,1	352,3	352,1	352,5	357,9	352,7		351,3	351,9	352,7	355,5	353,3	353,5
Ignition Delay (°)	5,4	4,8	4	5,6	4	3,2		6,2	5,4	5	4	9	3,2		4,8	4,8	4,2	8,2	4,4	3,4
Patm (kPa)	139,2	138,7	138,7	138,7	139,2	138,7		138,7	138,2	138,2	138,2	138,2	138,2		138,2	137,7	137,7	137,7	137,7	137,2
Exhaust Temp (°C)	22,5	22,5	22,5	22,5	23	22,5		23	23	23	23	23	23,9		23	23	23	23	23	23
Max Pressure (kPa)	5114,7	5006,8	5021,5	5055,7	5085,4	5011,7		5089,8	5050,3	5016,1	5133,3	4972,2	4947,8		5064,9	5025,4	5059,6	5064,5	5001	4922,4
Pos of Pmax (°)	366	367	366,8	367,8	367	367,2		366,4	367	366,6	368,4	367,8	368,4		365,4	366,8	366,4	367,2	368,4	368,8
Max Temperature (K)	1615,6	1657,4	1705,8	1776	1899,2	2000,4		1616,7	1684,3	1679,3	1821,3	1867,8	2016,1		1989,5	1681,1	1728,1	1774,2	1907	1973
Pos of Tmax (°)	372,4	373,8	374,2	374,8	374,4	374,8		372,6	373,4	373,2	375,4	375,2	377,6		374,6	374,8	373,8	374,8	377,8	377
Mech Effic (%)	51	50,7	47,8	47,2	48,9	48,2		62,6	59,7	61,1	55,2	56,2	53,4		72,6	70,3	67,7	65,8	63,8	65
ITE (%)	38,7	38,6	36,8	35	36,9	37,8		39,1	36,9	31,8	34,4	35,4	37,3		30,7	31,3	31,9	31,3	34	31,6
BTE (%)	19,8	19,6	17,6	16,5	18	18,3		24,5	22	19,5	19	19,9	19,9		22,3	22	21,6	20,6	21,7	20,5
Volumetric Eff (%)	79,7	77,1	75,9	73,6	68,6	65,5		79,3	76	75,5	73,8	70	66		63,6	76,2	74,8	74	69,4	65,7

Figure 23: Screen Shot of Compiled Engine Performance Data

11.2. Gaseous Emissions

The gas data, as mentioned previously, is automatically averaged for 50 data points per test, and saved in a .csv format. The average readings from the tests, making up the particular experiment, are combined into one spreadsheet. This is done again by simply copying and pasting the required data from one spreadsheet into the combined spreadsheet. The result of this is shown in the figure below.

		NOx	THC	CO	CO2
25	1300	200,906	96,318	39,38	26741,2
	1400	211,412	92,052	53,5	28266
	1500	205,224	88,89	67,38	28268,6
	1600	204,278	77,514	87,06	29817,4
	1700	223,818	81,536	106,58	31885,2
	1800	232,742	95,66	117,46	31371,4
30	1300	194,292	68,66	110,42	24982,6
	1400	478,56	114,566	124,1	73806
	1500	450,64	101,66	128,5	72328
	1600	439,54	87,184	132,54	69644
	1700	414,46	96,992	138,32	69808
	1800	405,54	111,46	158,18	72886
35	1300	523,5	67,294	285,28	82662
	1400	522,08	61,974	360,78	81528
	1500	503,12	63,342	225,82	77008
	1600	466,82	63,3	186,98	78100
	1700	451,06	63,502	207,66	75666
	1800	411,3	73,658	247,78	78020
40	1300	497,04	143,28	203,52	71684
	1400	501,78	87,96	95,18	73616
	1500	528,64	66,884	164,3	76482
	1600	513,06	59,138	547,92	80436
	1700	529,76	62,162	569,48	84412
	1800	460,86	61,004	654,22	85624

Figure 24: Screen Shot of Combined Gas Data

11.3. Particulate Graph Generation and Maximum Concentration

The processing of the raw data for the particulate tests is done easily using a custom written Excel add in, called DMS utilities, provided by Cambustion. The first step is to create a summary sheet for the entire test. This is because the tests are all steady state so the data collected at the 0,1 second intervals needs to be averaged over the test period. The summary sheet has the following format, as shown in the figure below.

DMS Summary Data

	A	B	D	E	F	G	H	I	J	K	L	M	N	O	P	S	T	U	V
1	DMS Summary Data																		
3	weighting	0																	
4		number																	
5	shape factor	1,000	In size range:																
6	density		min	5	nm														
7		kg /m^0	max	1000	nm														
8	density factor																		
10	Start time	End time	Total N/cc	Geometric Mean Diameter	Geometric Standard Deviation of Diameter	Count Median Diameter nm	A.Input 1 (Volts)	A.Input 2 (Volts)	A.Input 3 (Volts)	A.Input 4 (Volts)	Total N/cc	Analog Output 1	Analog Output 2	Analog Output 3	Analog Output 4	Nucleation Mode CMD	Nucleation Mode Concentration	Nucleation Mode GSD	Nucleation mode surface a (µm^2/c
11	-0,9	44,3	2,10E+07	189,04	1,28	188,54	-0,002	0,017	0,020	0,030	2,10E+07	1,80E-01	8,59E-02	2,10E+07	0,00E+00	#DIV/0!	0,00E+00	#DIV/0!	0,00E-

Figure 25: Screen Shot of the Particulate Summary Sheet for a Test

At this point it is required to select the base of comparison, the Excel macro allows for either concentration of:

- Particulates by Number
- Particulates by Volume
- Particulates by Size
- Particulates by Mass

It was decided to use Particulates by Number, as this is the format specified by the Euro Standards, thus the results could be tied back to this if required. The summary sheet allows for the creation of a number of useful graphs, such as the cumulative concentration of particulates as shown in the figure below:

Cumulative Concentration
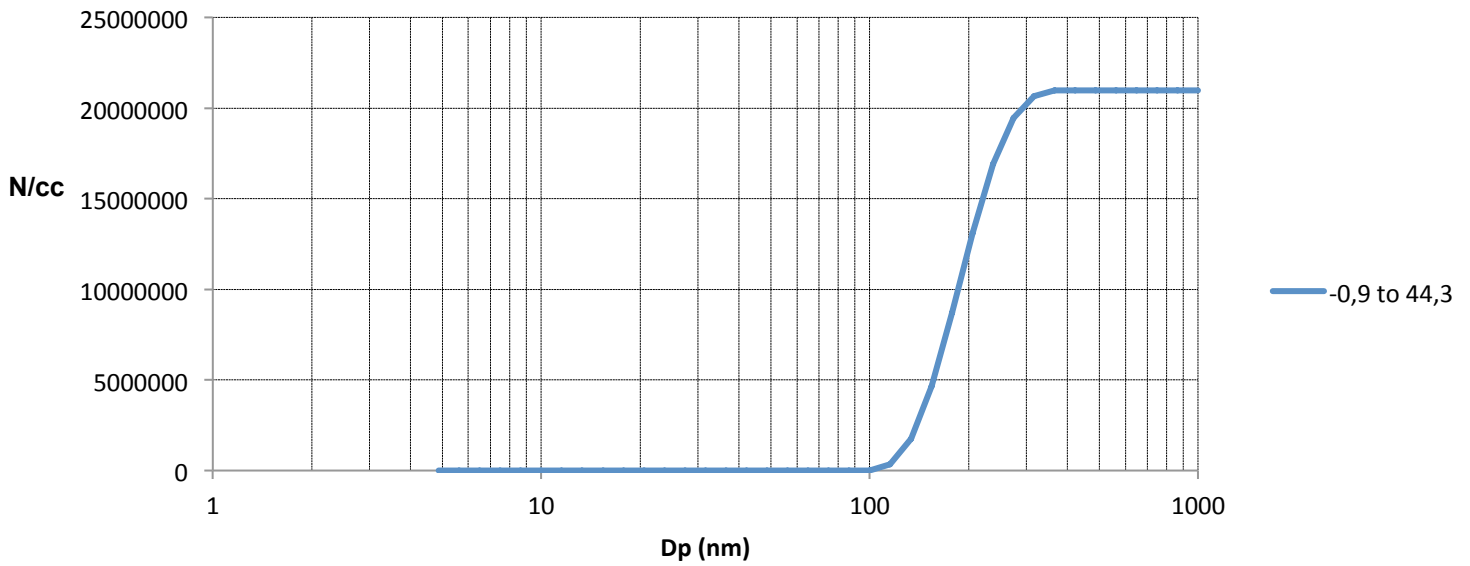
Figure 26: Example graph of Particulate Cumulative Concentration

The above graph shows the number of particulates per cubic centimetre of flow, N/cc, thus the concentration at various sizes, along the logarithmic x-axis. It is clear that a means of comparison is needed and a smooth line graph does not provide for one number per test which is what would be required. The graph gradient is at its maximum for a certain size of particle, in this case it is seen to be about 180nm at about 10000000 N/cc, thus the maximum concentration of particulates is about 10-million, 180nm sized particles per cubic centimetre of flow.

Another graph that can be created is the size spectral density of particulates. This is shown in the figure below.

Size Spectral Density
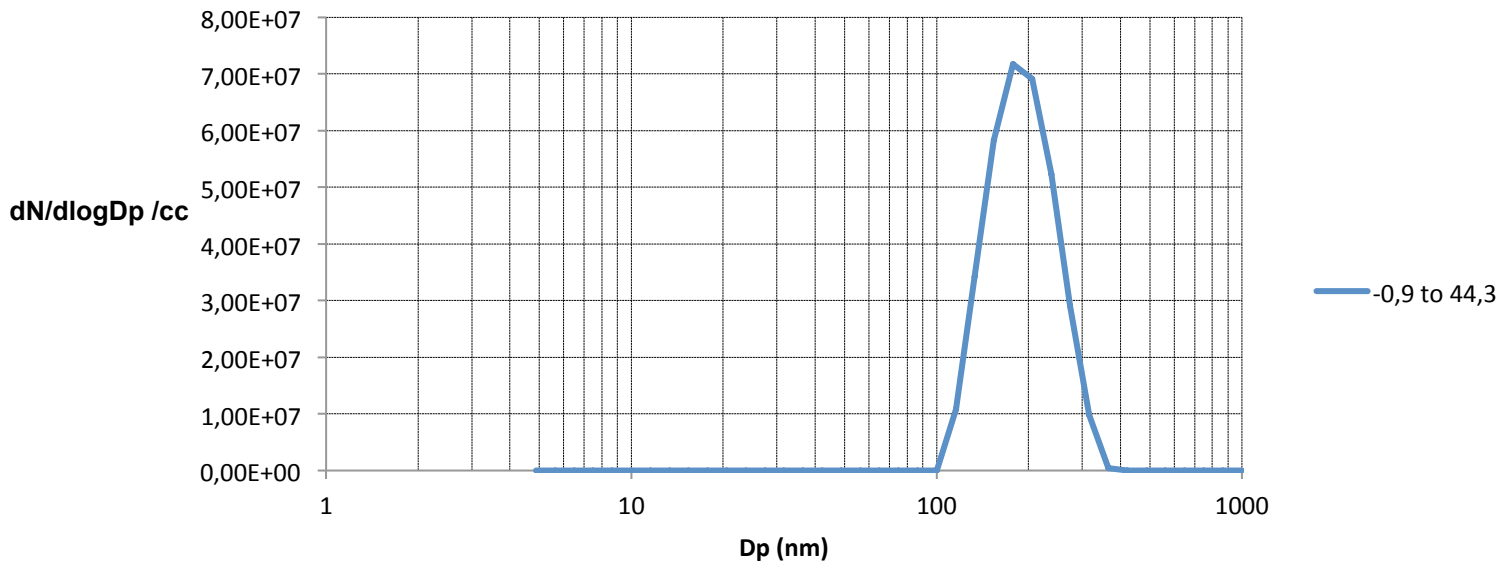
Figure 27: Example graph of Particulate Size Spectral Density

This graph shows the distribution of particles over a size range of 1 to 1000nm. Thus according to the above graph most particles are about 180nm having a concentration of 7,1E+7 dN/dlogDp/cc. This can be interpreted as the gradient of the previous graph, the cumulative concentration. Thus the slope was at a maximum at about 180nm, before it began to decrease. This number is recommended for comparative purposes as it gives a clearer indication of the maximum particulate concentration. Thus one can clearly deduce that most particulates were in a particular size range, having a particular count per cubic centimetre of flow. This maximum number in the size spectral density graph is used as the indicator for each test. The count of particulates at the maximum size is extracted for comparison. This number exists in the summary sheet, as this was the information originally used to construct the graph. The concentration at size intervals is recorded and used to construct this smooth line graph. The information is contained in cells AS11 to BP11, the maximum number, which is of interest, is extracted using the following Excel formulae:

$$Max\ Concentration = MAX('SummarySheet'!AS11:BP11)$$

Equation 6

66

This is done for each test within a particular experiment. Summary Sheets are created and the information is copied into one consolidated Spreadsheet as shown in the figure below:
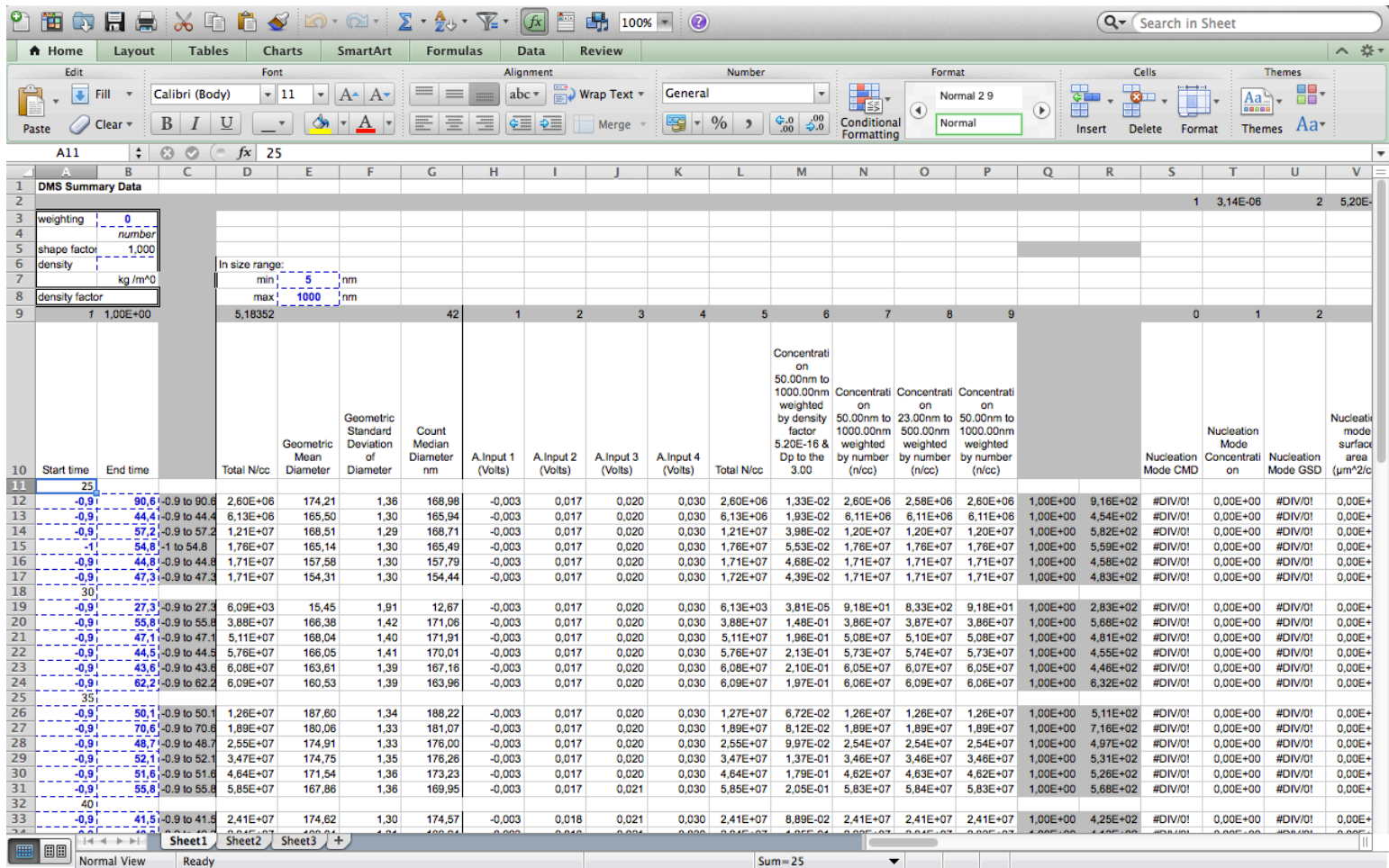
Figure 28: Screen Shot of Compiled Particulate Data

Following this, equation 6 is applied to extract the comparative number. This is shown in the figure below.
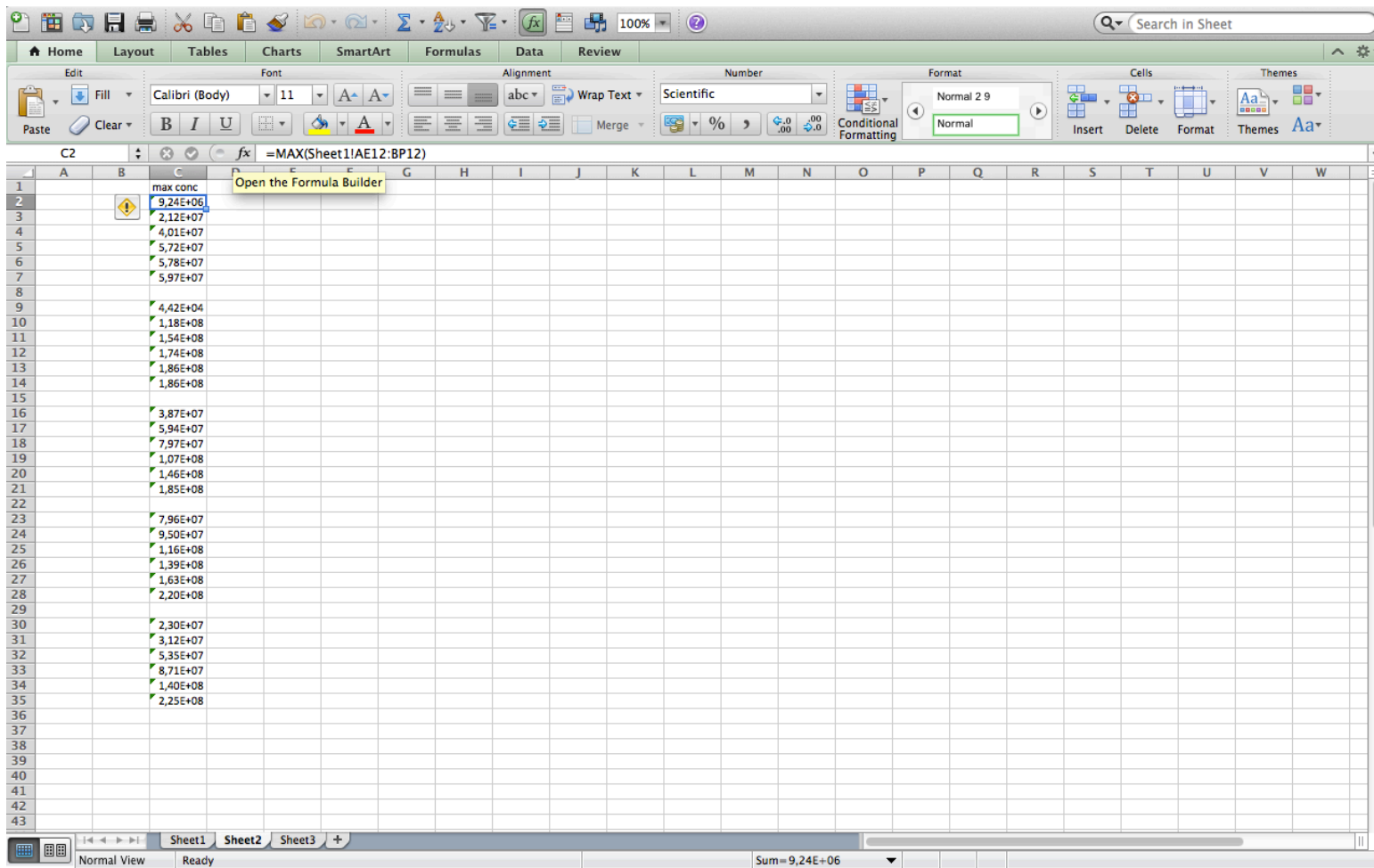
Figure 29: Screen Shot of Comparative Particulate Data

11.4 Data Compilation

The final step in the processing of the data for each experiment is to combine all the end results of the previous sections into a spreadsheet that can be used to construct graphs as needed and to compare data from the different groups. This is done simply by copying and pasting the information from the various subsections into one final spreadsheet. An example of a spreadsheet is shown in the figure below.

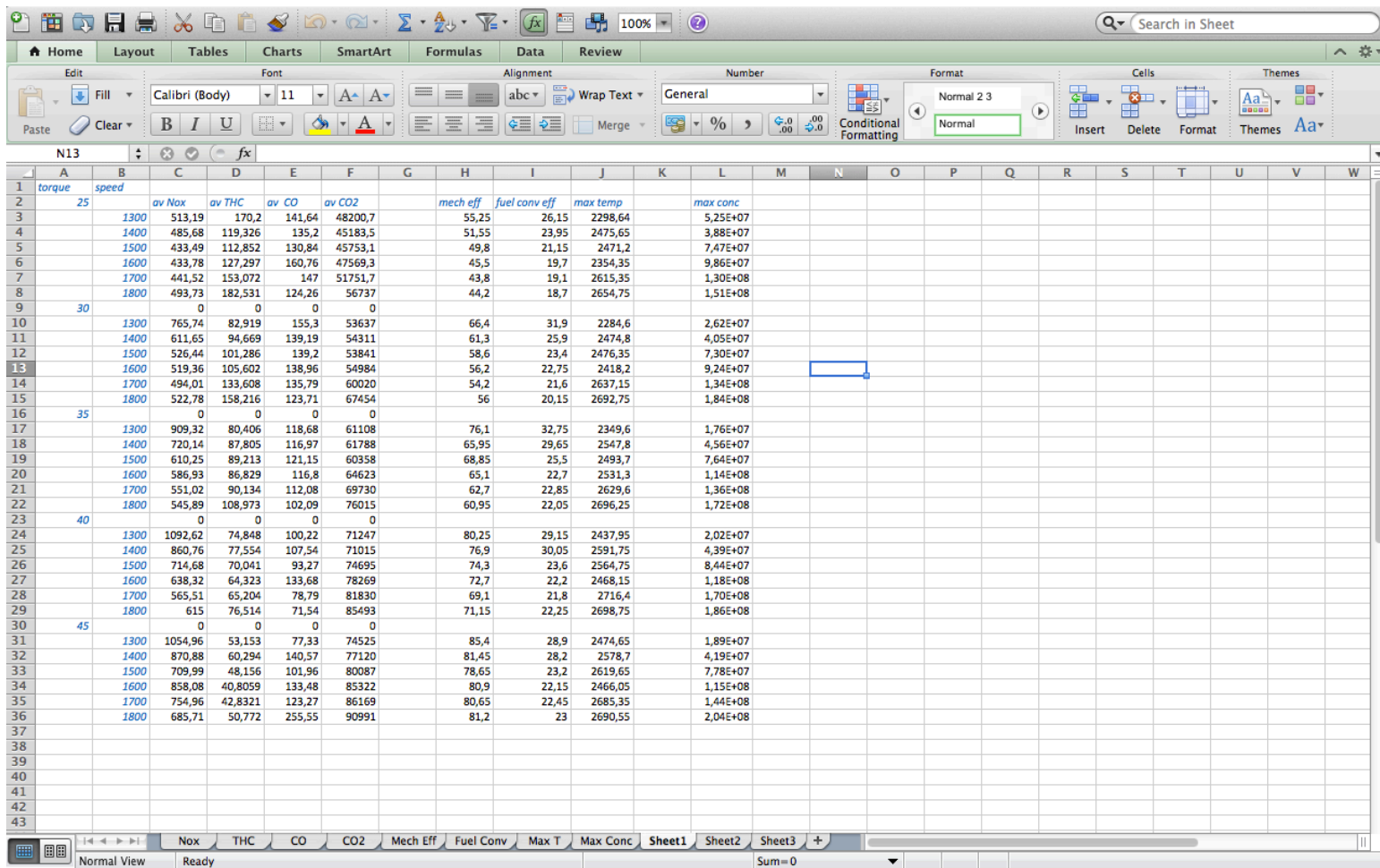| torque	speed	av Nox	av THC	av CO	av CO2		mech eff	fuel conv eff	max temp		max conc
25											
	1300	513,19	170,2	141,64	48200,7		55,25	26,15	2298,64		5,25E+07
	1400	485,68	119,326	135,2	45183,5		51,55	23,95	2475,65		3,88E+07
	1500	433,49	112,852	130,84	45753,1		49,8	21,15	2471,2		7,47E+07
	1600	433,78	127,297	160,76	47569,3		45,5	19,7	2354,35		9,86E+07
	1700	441,52	153,072	147	51751,7		43,8	19,1	2615,35		1,30E+08
	1800	493,73	182,531	124,26	56737		44,2	18,7	2654,75		1,51E+08
30		0	0	0	0						
	1300	765,74	82,919	155,3	53637		66,4	31,9	2284,6		2,62E+07
	1400	611,65	94,669	139,19	54311		61,3	25,9	2474,8		4,05E+07
	1500	526,44	101,286	139,2	53841		58,6	23,4	2476,35		7,30E+07
	1600	519,36	105,602	138,96	54984		56,2	22,75	2418,2		9,24E+07
	1700	494,01	133,608	135,79	60020		54,2	21,6	2637,15		1,34E+08
	1800	522,78	158,216	123,71	67454		56	20,15	2692,75		1,84E+08
35		0	0	0	0						
	1300	909,32	80,406	118,68	61108		76,1	32,75	2349,6		1,76E+07
	1400	720,14	87,805	116,97	61788		65,95	29,65	2547,8		4,56E+07
	1500	610,25	89,213	121,15	60358		68,85	25,5	2493,7		7,64E+07
	1600	586,93	86,829	116,8	64623		65,1	22,7	2531,3		1,14E+08
	1700	551,02	90,134	112,08	69730		62,7	22,85	2629,6		1,36E+08
	1800	545,89	108,973	102,09	76015		60,95	22,05	2696,25		1,72E+08
40		0	0	0	0						
	1300	1092,62	74,848	100,22	71247		80,25	29,15	2437,95		2,02E+07
	1400	860,76	77,554	107,54	71015		76,9	30,05	2591,75		4,39E+07
	1500	714,68	70,041	93,27	74695		74,3	23,6	2564,75		8,44E+07
	1600	638,32	64,323	133,68	78269		72,7	22,2	2468,15		1,18E+08
	1700	565,51	65,204	78,79	81830		69,1	21,8	2716,4		1,70E+08
	1800	615	76,514	71,54	85493		71,15	22,25	2698,75		1,86E+08
45		0	0	0	0						
	1300	1054,96	53,153	77,33	74525		85,4	28,9	2474,65		1,89E+07
	1400	870,88	60,294	140,57	77120		81,45	28,2	2578,7		4,19E+07
	1500	709,99	48,156	101,96	80087		78,65	23,2	2619,65		7,78E+07
	1600	858,08	40,8059	133,48	85322		80,9	22,15	2466,05		1,15E+08
	1700	754,96	42,8321	123,27	86169		80,65	22,45	2685,35		1,44E+08
	1800	685,71	50,772	255,55	90991		81,2	23	2690,55		2,04E+08

Figure 30: Screen Shot of the Compiled data from an Experiment

Using the above data, graphs comparing various aspects of the data can be constructed as needed. These graphs are presented in the Results section.

12. Presentation of Results and Discussion

The results obtained from this investigation which was aimed at determining what fuel and setting, with regard to speed and applied load, a compression ignition engine should be operated at to produce the lowest particulate emission possible, are presented below.

12.1. Diesel Fuelled Tests

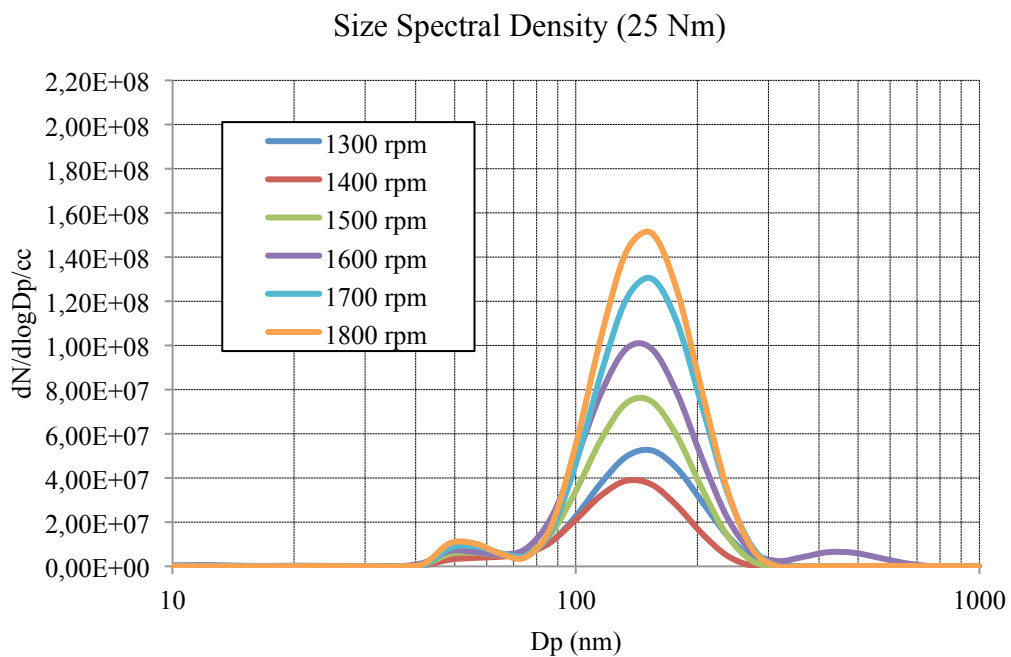### *12.1.1. Diesel Particulate Spectral Distributions*
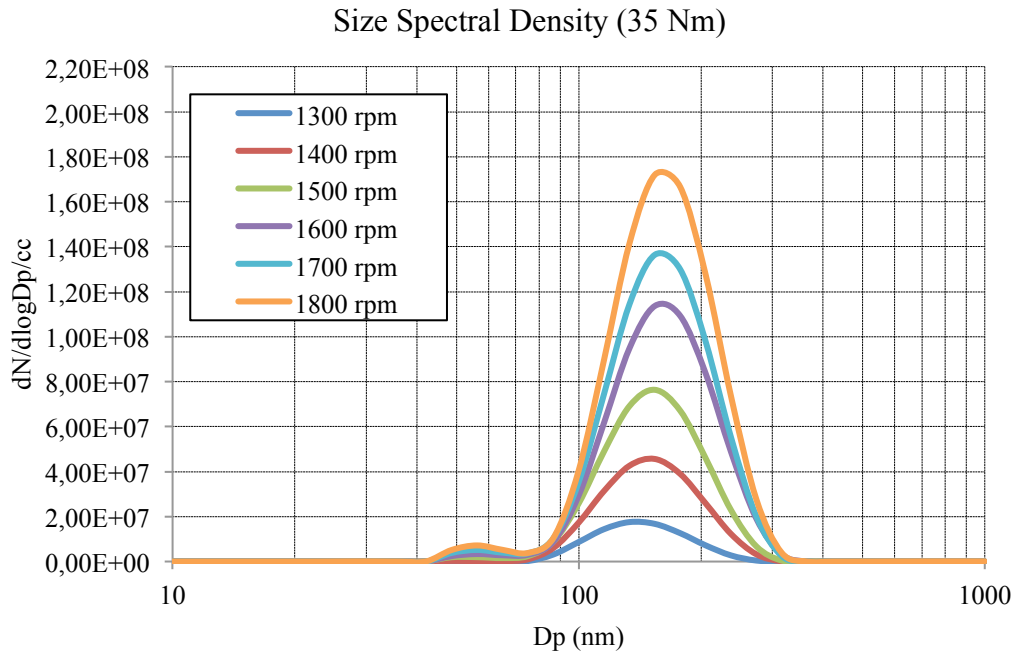

Figure 31: Diesel Particulates Size Spectral Density at 25Nm

Figure 32: Diesel Particulates Size Spectral Density at 35Nm
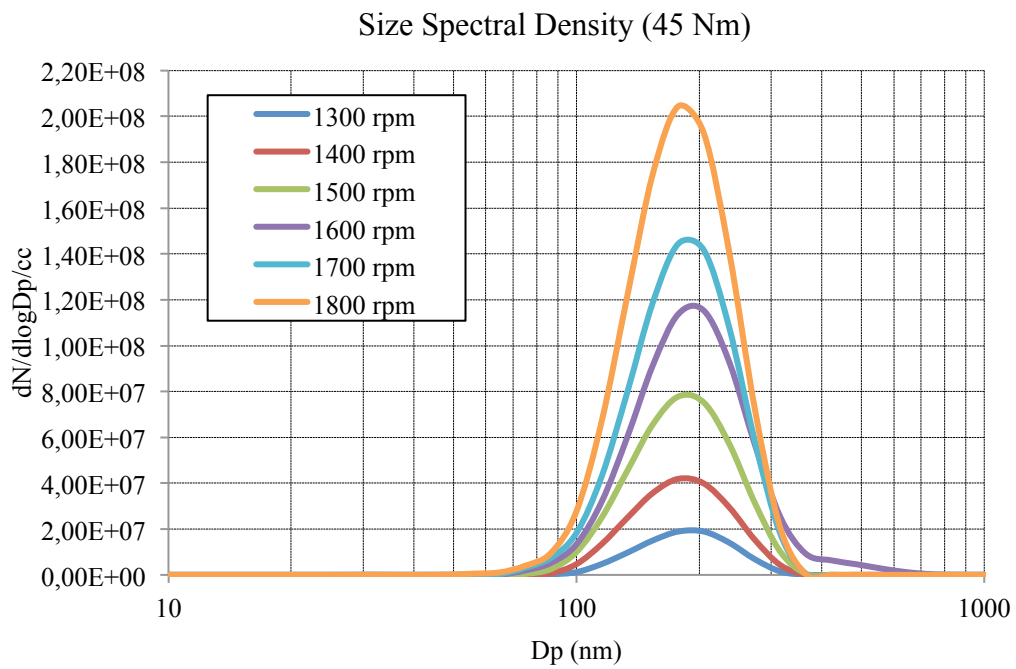
Figure 33: Diesel Particulates Size Spectral Density at 45Nm

Figures 31 to 33 demonstrate that increasing speed at all torques increases the maximum concentration of particulates. This is the case for all except the lowest torque of 25Nm. Figure 31 shows that the lowest maximum concentration is achieved at 1400rpm, and not the lowest speed of 1300rpm. This is an indication that there exists some minimum point between 1300rpm and 1500rpm, at 25Nm, for particulate output. This is believed to be relevant to the particular setup and engine used under the given conditions. This is unlikely to be a general rule for all engines.

The applied torque is seen to have little effect on the maximum concentration of particulates. By observing figures 31 to 33 it can be concluded that the concentration of particulates obtained at various speeds, from one torque to the next, has little variation. However, increasing torque appears to shift all peaks slightly to the right. From figure 31 it can be seen that there was a maximum concentration of particulates of about 150nm at 25Nm whereas figure 33 shows a maximum concentration of particulates of about 190nm at a torque of 45Nm.

The effect of increasing torque on the general spectral distributions is also seen. At lower torques, as in figure 31, there are two peaks shown, a high peak of about 150-170nm and a low peak of about 50nm. This low peak disappears at higher torques, as in figure 33. Thus the higher peak dominates at higher torques, which is an indication that there are a higher number of larger particulates produced, but at lower torques a less distinct maximum is observed, as two maximums, a primary and secondary, are expressed in the data. Although the idea of an even spread is used lightly. These two peaks are probably an indication of two formation mechanisms at play at lower torques and only one dominating at higher torques.

The complete set of data for diesel size spectral densities can be found in Appendix 1.

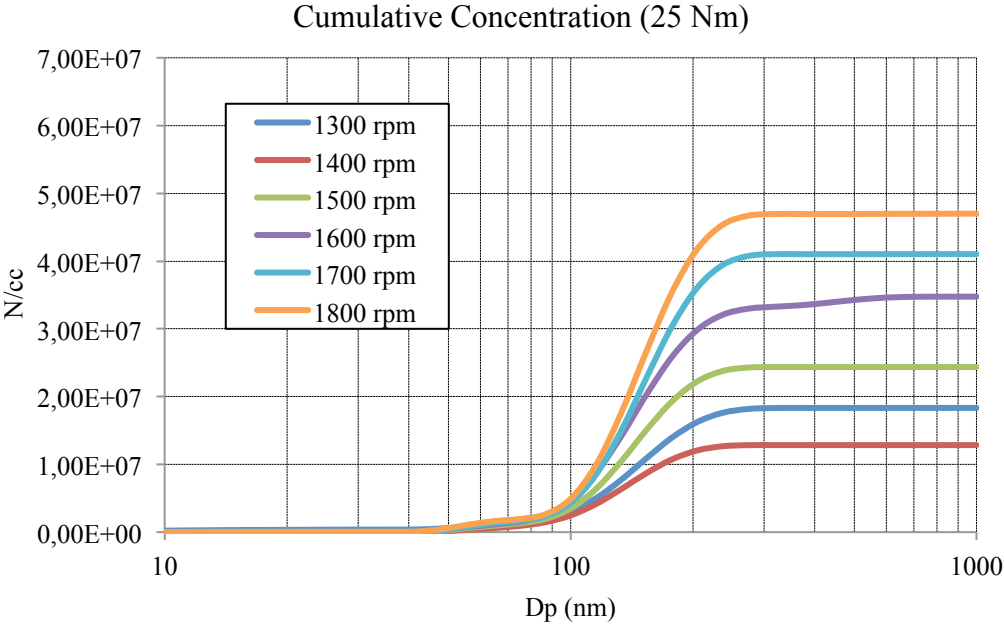## 12.1.2. Diesel Particulate Cumulative Concentrations

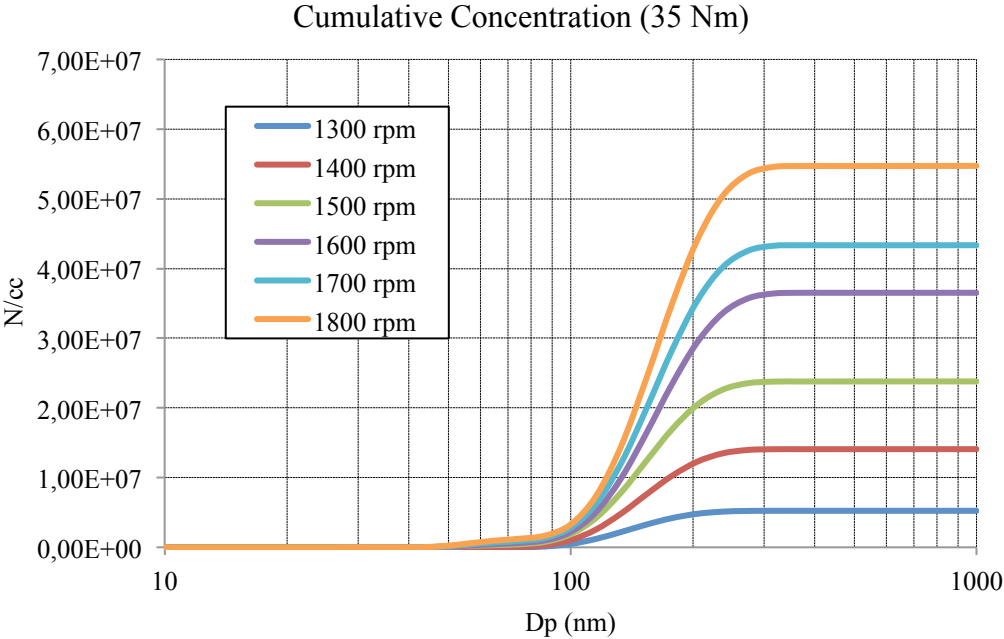Figure 34: Diesel Particulates Cumulative Concentration at 25Nm

Figure 35: Diesel Particulates Cumulative Concentration at 35Nm
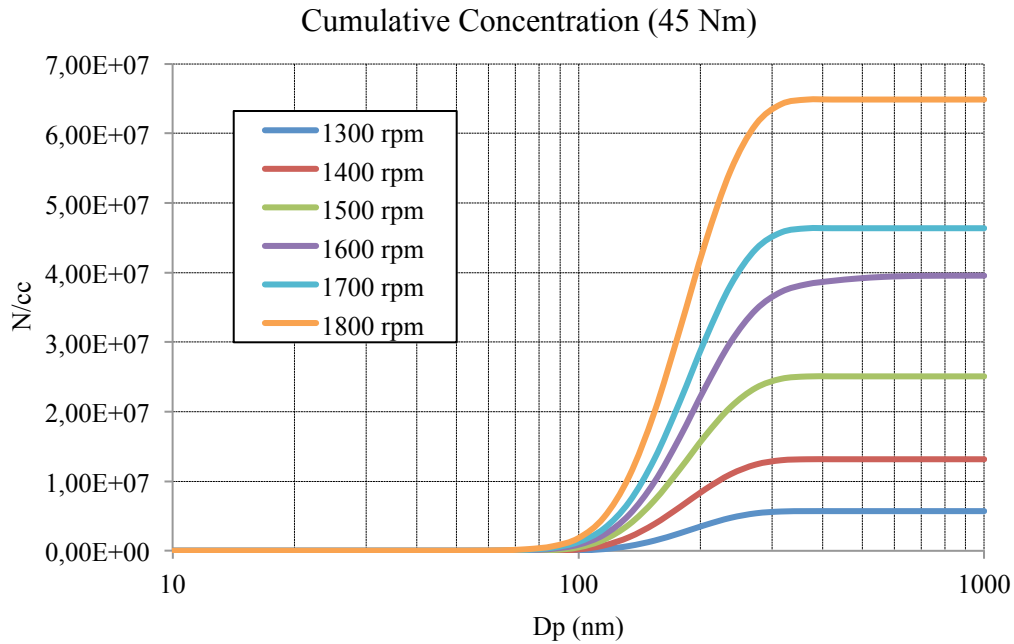
Figure 36: Diesel Particulates Cumulative Concentration at 45Nm

From figures 34 to 36 the effects of speed and torque on particulate output can be observed. Again it is observed that increasing speed has a large effect on the output of particulates as the figures show noticeable increases from one speed to the next at all torques. The effect of increasing engine torque with regard to particulate concentration and size is emphasized more clearly in this set of results. It is seen, from figures 34 to 36, that at high speeds the effect on changing torque in nearly all cases causes an increase in the output in particulates. It is, however, noticed that at 1700rpm the output decreases for 40Nm to 45Nm. This is again believed to be some indication of a minimum point for that speed. This type of optimal point was also observed for the lower torques. From figure 35 it is seen that for 1300rpm the minimum particulate output is at 35Nm. Thus the expected upward trend is deviated by a sudden decrease in particulate output.

Again it must be stated that these observed optimal points, with regard to minimum particulate production, are believed to be very specific to the given test apparatus and test conditions. It is, however, useful to understand that such optimums of minimum particulate output exist. It is believed that a link between the engine's optimal operating point with regard to cam and valve design probably exists.

The complete set for diesel cumulative distribution can be found in Appendix 1.

12.1.3. Diesel Particulates and Gaseous Emissions

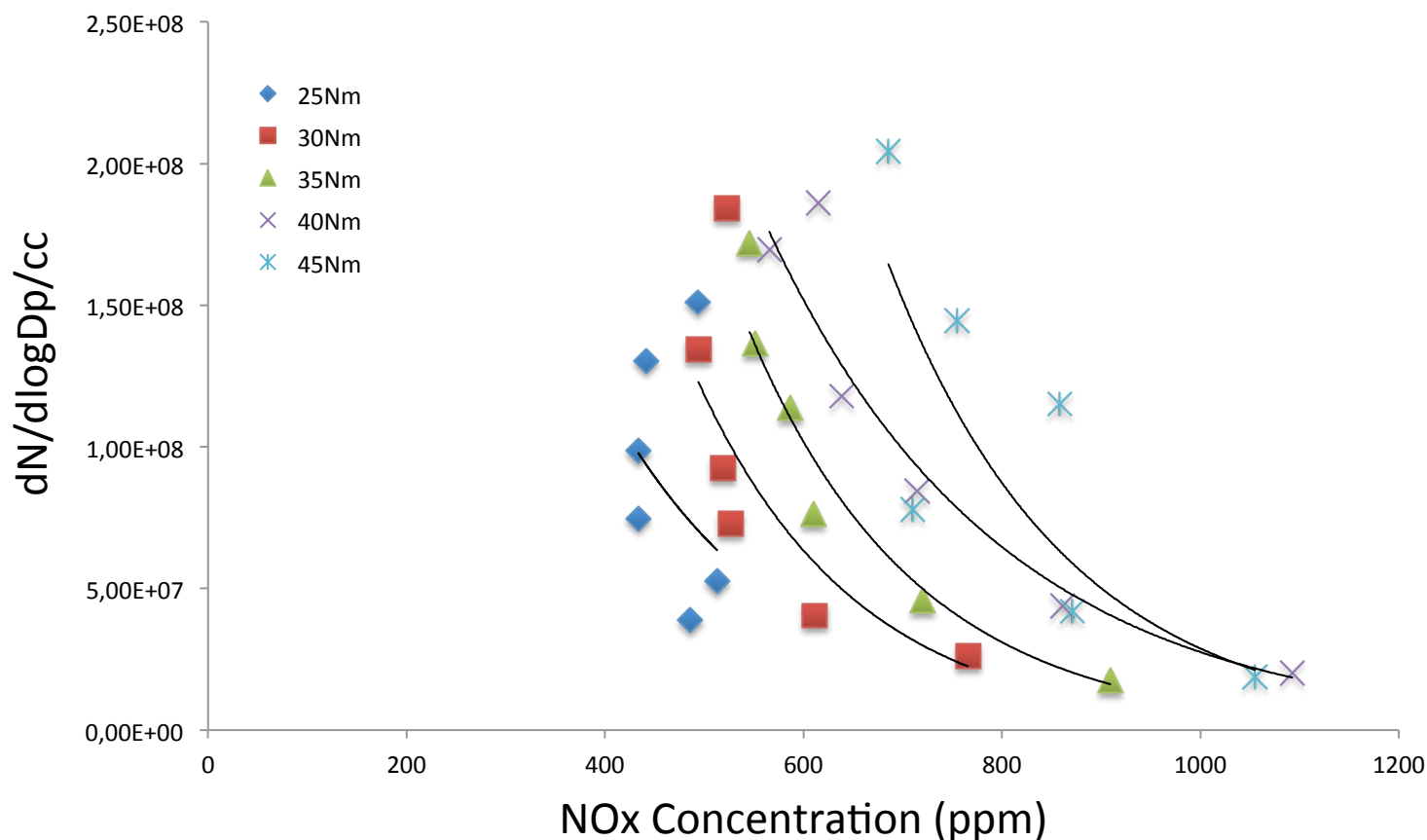### 12.1.3.1. NOx Output and Particulates

Figure 37: Maximum Concentration of Diesel Particulates vs. NOx Concentration

Figure 37 shows the link between the engine's output of NOx and its output of particulates. It can be observed, from the shape of all the curves, that an inversely proportional relationship between NOx output and particulate output exists. This conclusion is in support of findings in theory. It was noted in the literature survey Section 4.4.1 [18] that a clear trade-off between an engine's output of particulates and NOx exists. This finding is clearly an indication that the experimental method used is correct as the findings can be verified by an unrelated external source [18]

Increasing torque has little effect on the output of particulates, as discussed in the above section, but the effect of torque does have a considerable effect on the NOx

concentration. The trend lines move to the right with increasing torque, which suggests that torque has more of an impact on NOx formation than engine speed. This would suggest that the formation of NOx is independent of time whereas particulates have a strong dependence on time. By time, it is meant the cylinder transit time, thus the time that the charge spends undergoing its cycle, which is indicated by the engine speed. A slower speed means more cylinder transit time and consequently less particulates are output and vice-versa. This is an indication that particulates are a result of a less efficient, rushed, burn process. This result is logical in its inception and agrees with the very definition of a particulate being a remnant of an incomplete combustion cycle, an improperly oxidised carbon particle stemming from the fuel.
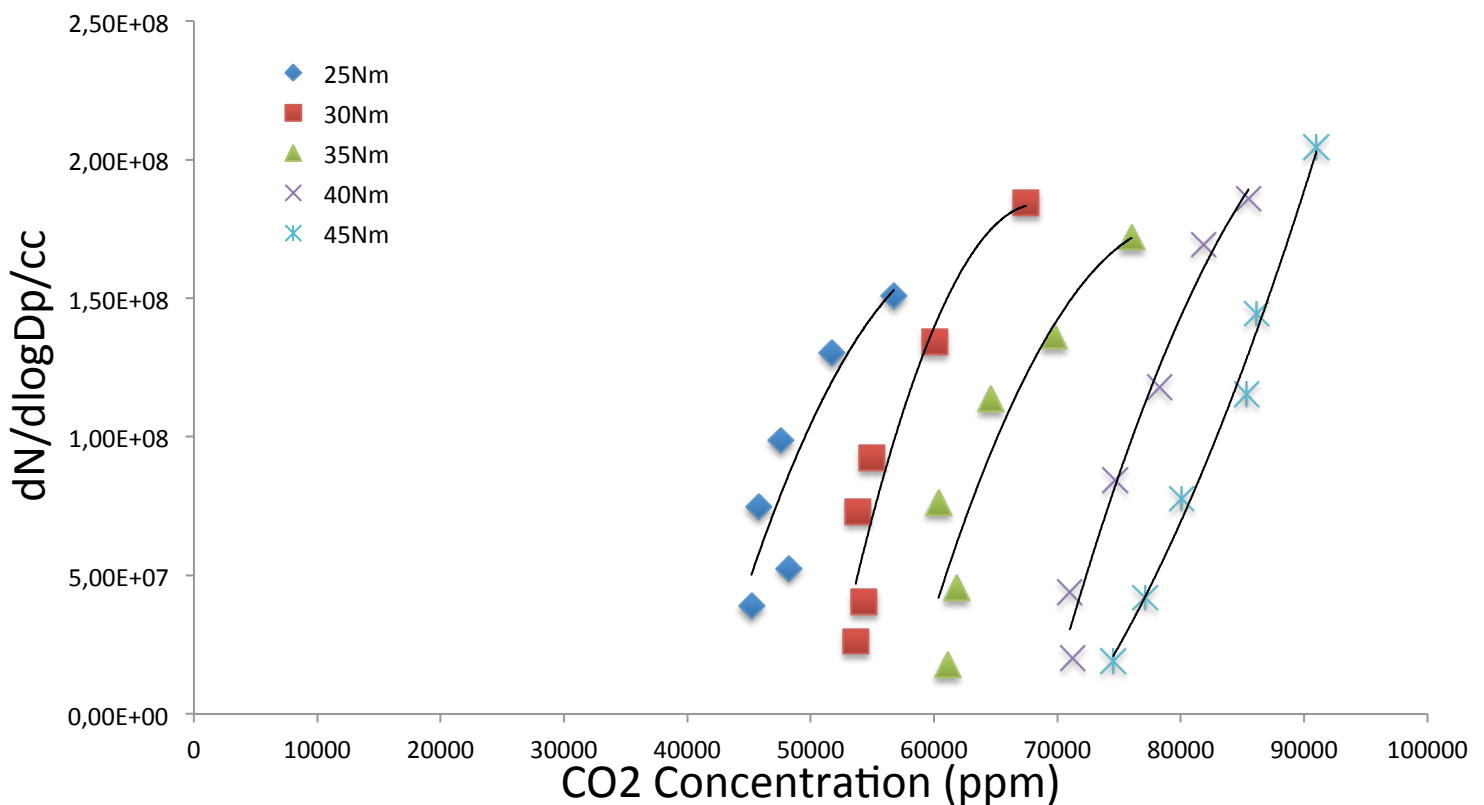
12.1.3.2. Carbon Dioxide and Particulates

Figure 38: Maximum Concentration of Diesel Particulates vs. CO_2 Concentration

Figure 38 demonstrates that a fairly straight-line relationship exists between the engine's output of particulates and carbon dioxide. It is again seen that torque has little effect on the output of particulates but rather engine speed is the primary driver, as discussed above. This is evidenced by the series of somewhat parallel lines, each representing a different load applied to the engine. It is, however, noted that torque affects carbon dioxide output as it increases with each successive parallel line. Each successive increase in 10Nm causes an increase in carbon dioxide of about 10000ppm or 10%.

These lines are very close to the vertical; this is an indication that speed plays little role in the engines output of carbon dioxide. Thus it is observed that, like NOx gases above, carbon dioxide is not dependent on cylinder transit but rather on applied engine load unlike particulates. The near vertical lines indicate no apparent relationship between particulate output and carbon dioxide output.
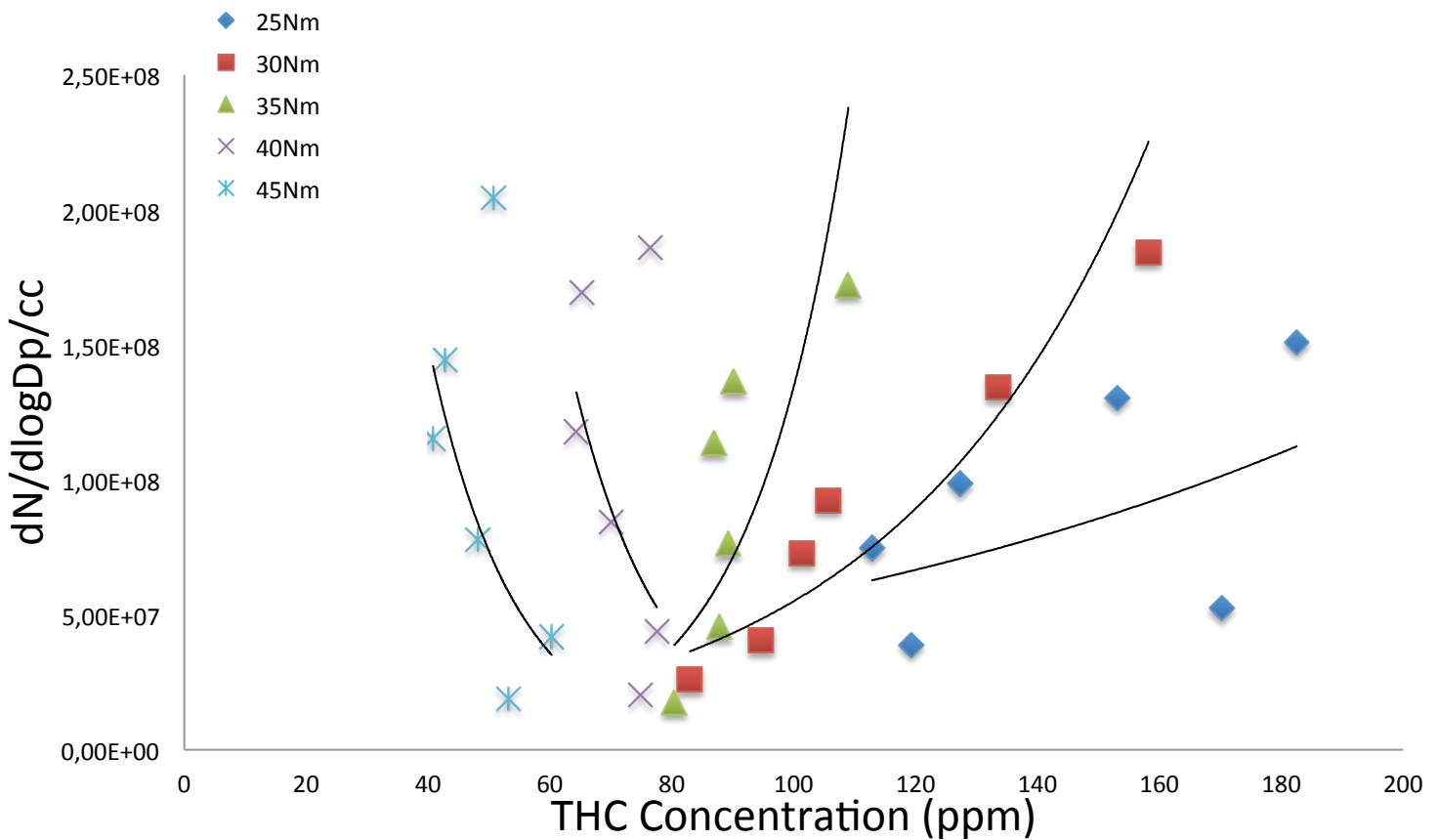
12.1.3.3. Total Hydrocarbons and Particulates

Figure 39: Maximum Concentration of Diesel Particulates vs. THC Concentration

It is seen from figure 39 that engine torque has a significant effect on THC and its relationship to the output of particulates. From the figure it is evident that at higher torques THC output decreases. This is observed from the scatter of points, and their general trend towards the left, which decrease with increasing torque.

The relationship between engine speed and THC output also changes with increasing torque. At lower torques increasing engine rotational speed causes an increase in THC. It is clear that cylinder transit time is more relevant at lower torques, but overall the engine load is still seen to be the greatest indicating factor of THC output.

The relationship between THC and particulates is seen, from figure 39, to depend largely on the applied engine torque. At lower torques this relationship is fairly linear with an increase in THC resulting in an increase in particulates. Thus the cylinder

transit time is seen to be relevant to both THC and particulates. At medium torques the output of THC is fairly independent of the particulate output. This is evidenced by the vertical nature of the scatter. The effect of cylinder transit time is relevant for particulates, as it always is, but irrelevant for THC. This again corroborates the finding that engine load is a more powerful indicator of THC than engine speed. This finding suggests that at higher loads the engine is outputting more useful work. This is evidenced by the increase in mechanical efficiency at higher loads. Thus less waste in the form of THC is outputted. At high torques the relationship between THC and particulates is seen to become inversely proportional, meaning that when the engine outputs more THC it outputs less particulates. This trend is similar to what was observed for particulates and NOx. The shape of this high torque data set also ties up with the previously stated observation that when more power is produced; there is less waste in the form of THC. This inverse relationship also suggests that THC and particulates are made from the same basic building blocks, meaning that both THC and particulates are products of incomplete combustion; and by conservation of mass one or the other increases at high engine load.

12.1.4. Diesel Particulates and Engine Performance

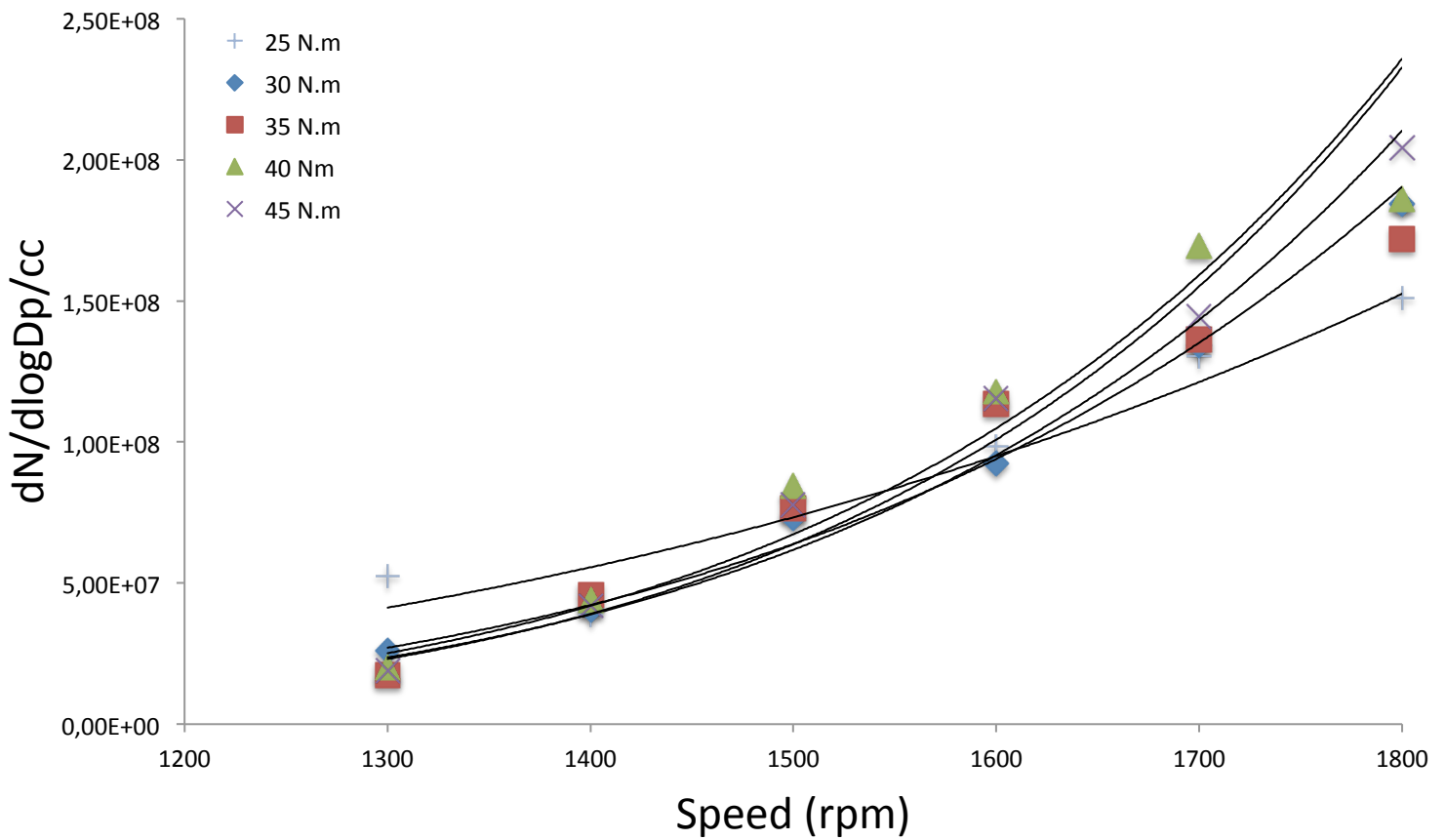### 12.1.4.1. Engine Speed, Load and Particulates

Figure 40: Maximum Concentration of Diesel Particulates vs. Engine RPM
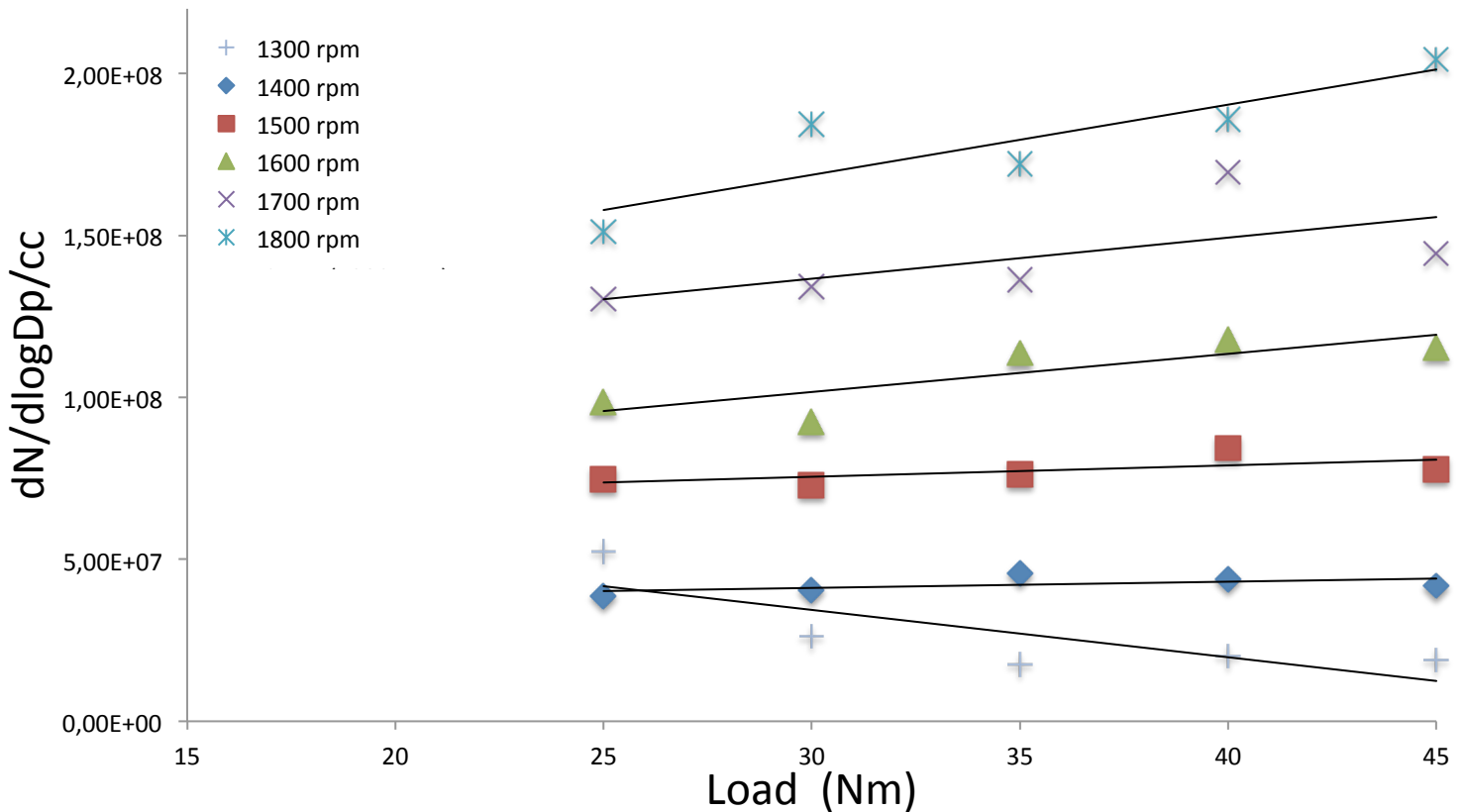
Figure 41: Maximum Concentration of Diesel Particulates vs. Engine Torque

Figure 40 is a plot of all of the peaks of figures 31 to 33 versus engine operating speed. The various loads that were applied are also shown. The curves obtained illustrate the finding that particulates are influenced largely by engine speed. It is noticed that the various data series, which are the engine loads, overlay one another suggesting that torque is of little significance with regard to particulates, as discussed previously. This graph clearly illustrates particulate's relationship to cylinder transit time and again reinforces the idea that particulates are a consequence of incomplete combustion. It is restated that the engine speed is directly indicative of the time the charge spends in the cylinder. The relationship between engine speed and particulates is seen to exhibit a fairly exponential shape. Thus the effect of increasing speed is seen to compound the production of particulates. Thus transitions at lower speed result in moderate increases in the particulate output while transitions at higher speed result in larger increases in the particulate output from one speed to the next. A reason for this may be because at lower speeds the energy that is used to overcome the friction needed to motor the

engine is comparable to its power output. Thus the change in fuel consumption becomes more comparable at higher speeds to the actual speed change.

Figure 41 is a plot of the same data except with the torque along the independent axis and the engine speeds are the various data series. The effect of torque on particulates is clearly illustrated by this graph. All the lines are virtually horizontal indicating that changing torque at a particular speed has little effect on the output of particulates. This indicates that an optimal operating point for an engine, under the variables replicated in this experiment, would be at high load and low speed. This would produce the required output power while minimizing the output of particulates. This is relevant to large stationary diesel engines as gearing could be used to adjust the output speed and torque. However, it is believed that this hypothesis might breakdown under the extreme operating limits of the engine, with regard to engine rpm, but within the normal speed ranges it should hold. This is believed as during experimentation the engine exhibited instabilities in performance, when running at excessively high or low speeds.

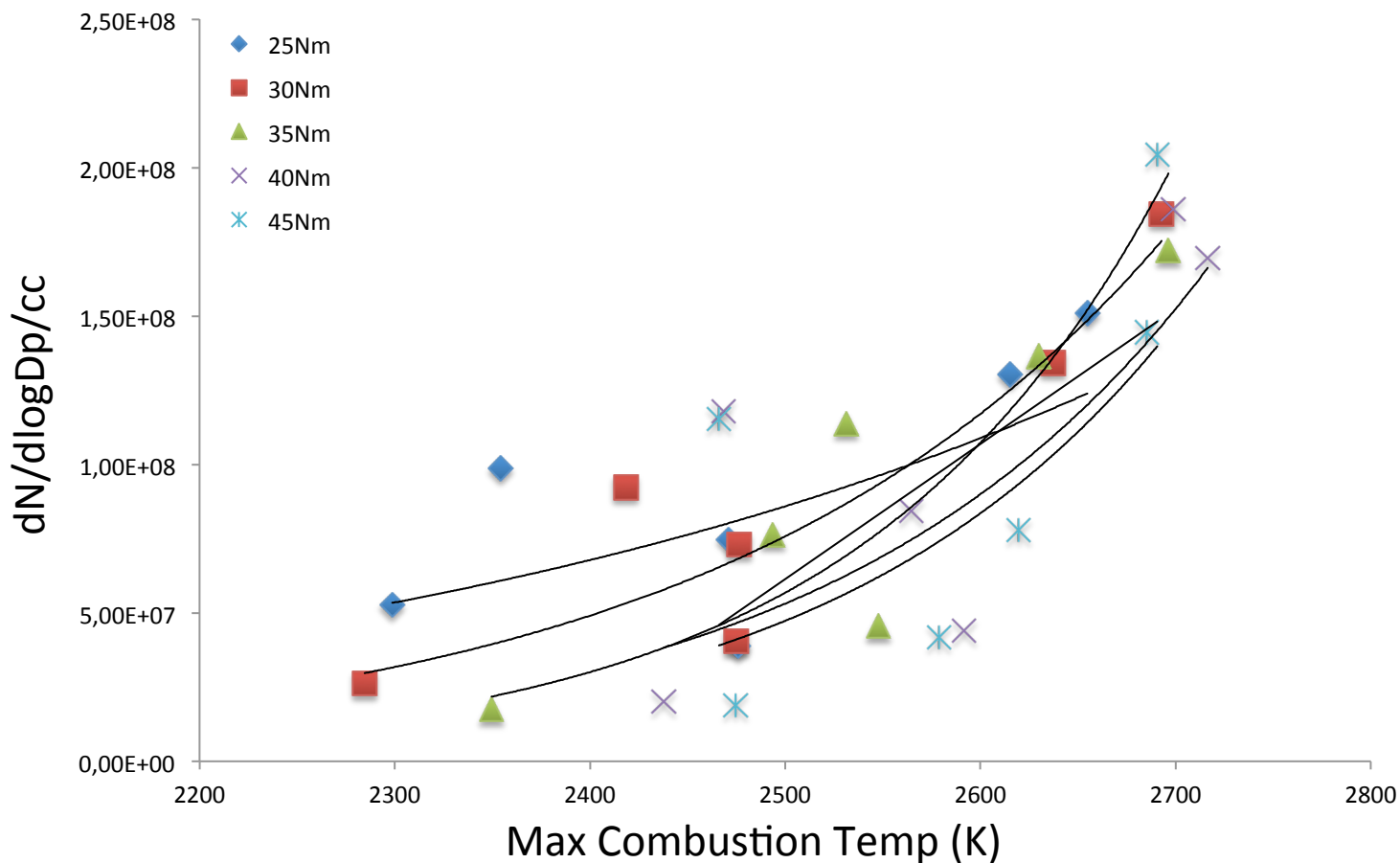## 12.1.4.2. Maximum Combustion Temperature and Particulates

Figure 42: Maximum Concentration of Diesel Particulates vs. Peak Combustion Temperature

The peak combustion temperature, from figure 42, is seen to relate to the maximum particulate concentration in a directly proportional, exponential fashion. It is seen that at high combustion temperatures the output of particulates is high and the opposite is also true. By comparing figures 40 and 42, it is noted that engine speed is a good indicator of peak combustion temperature as both figures have similar shapes and scatter. It is seen from the figure that peak combustion temperature is not very dependent on engine torque but rather on engine speed.

The engine's temperature is highest at high engine speeds thus short cylinder transit time for the charge. This is believed to be due to the decreased time for cylinder heat transfer, meaning that the gas temperature remains higher than if there were time for heat to dissipate after the moment of ignition. This creates a link between the maximum output of particulates and the available energy in the cylinder. Thus in high-energy environments many particulates will be produced, thus higher charge temperature means more particulates. This leaves the question as to why this higher energy environment does not translate to better energy conversion of the fuel and consequently a lower output in particulates? If one considers conservation of energy for the cylinder and the fact that the fuel itself is the source of potential energy, then it is plausible that in a hotter higher energy environment more fuel is available to form particulates in an already stunted, in terms of burn time, combustion cycle.

12.1.4.3. Fuel Conversion Efficiency and Particulates
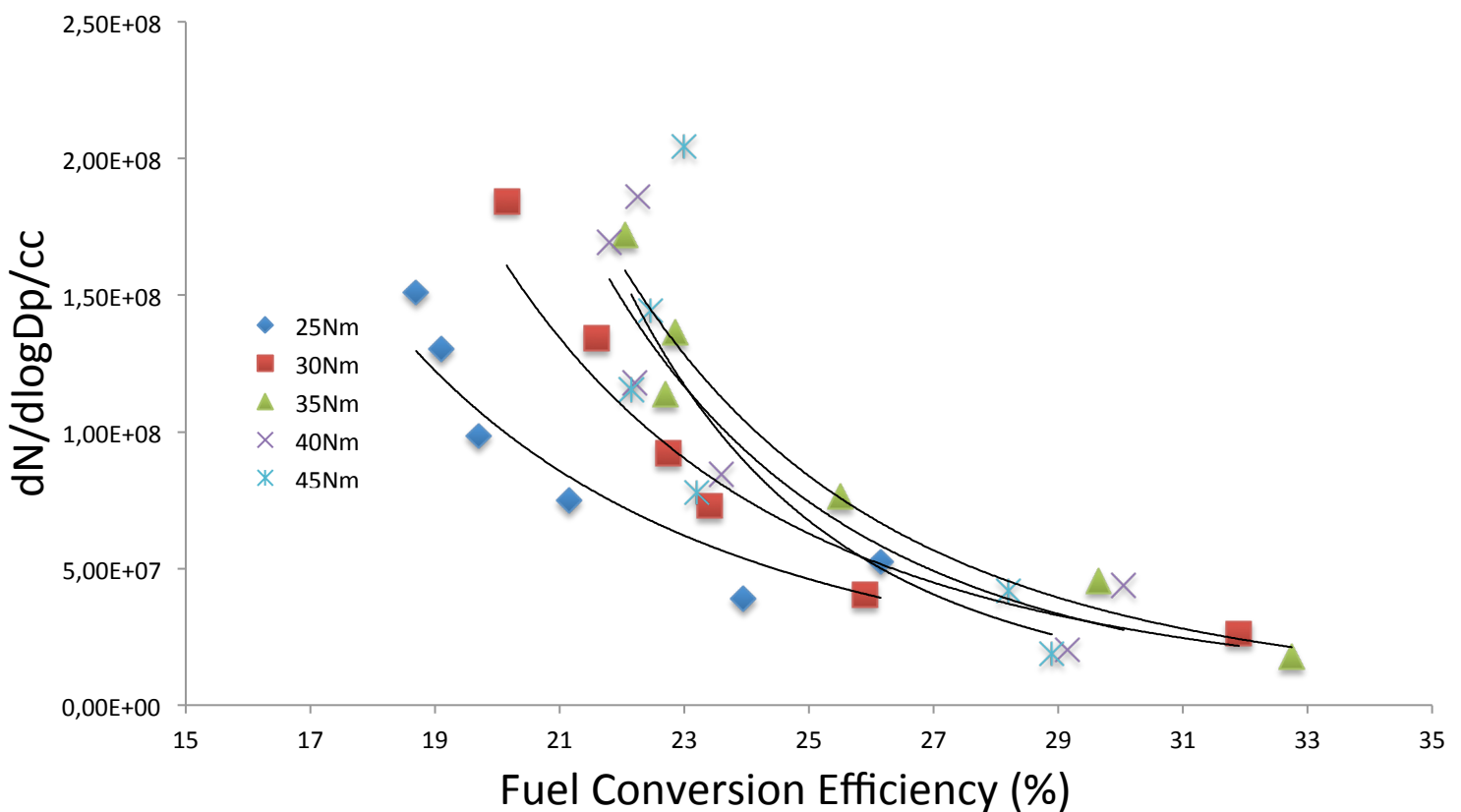

Figure 43: Maximum Concentration of Diesel Particulates vs. Engine Fuel Conversion Efficiency

The fuel conversion efficiency is a measure of how well the chemical potential energy of the fuel is converted into mechanical energy in the combustion chamber. Thus it is a measure of how well the fuel has burnt. It is known that a perfect combustion reaction would only result in water, carbon dioxide and nitrogen, as apparent air. It is therefore logical to assume that anything less than perfect reaction will result in the formation of substances that are partly oxidised species of carbon or plain carbon itself. A particulate can be derived from carbon, thus low fuel conversion efficiency should be indicative of high particulates, and this is seen to be the case. This is not to say that particulates only result from partly oxidised fuel, a particulate can be an aerosol of completely un-burnt fuel or lubricating oil.

Figure 43 shows that fuel conversion efficiency and the maximum particulate concentration are linked in an inversely proportional manner. Thus for a low fuel conversion efficiency a large output in particulates is observed and vice-versa. This relationship is seen to have a slight link to the engine torque as it is seen that the scatter for a lower torque remains slightly left of a scatter for a higher torque, but the relationship is not as pronounced as it is with the effect of engine speed. Although the speeds at which each data point was captured are not plotted, it is known from the raw data that fuel conversion efficiency decreased with increasing speed. It is also known that a higher maximum particulate concentration means a higher speed. These findings tie up well with the figure.

The fuel conversion efficiency is linked to the air-fuel ratio of the engine. As the engine under consideration is a diesel engine it is known that the amount of air inducted with each intake stroke remains close to equal, considering a factor that will be representative of the change in volumetric efficiency with changing engine speed, but rather the fuel quantity increases with increasing speed. As fuel conversion efficiency is an indirect measure of the amount of partly oxidised carbon species that are present, it follows that with more air and less fuel, as is expected at lower speed, it will be higher, which it is. It is also believed that the engine could benefit from turbo-charging, as the amount of air would increase without changing the amount of fuel. This would move the optimal operating point of high load at low speed to high load at high speed, which would result in a higher power output with less particulate output.

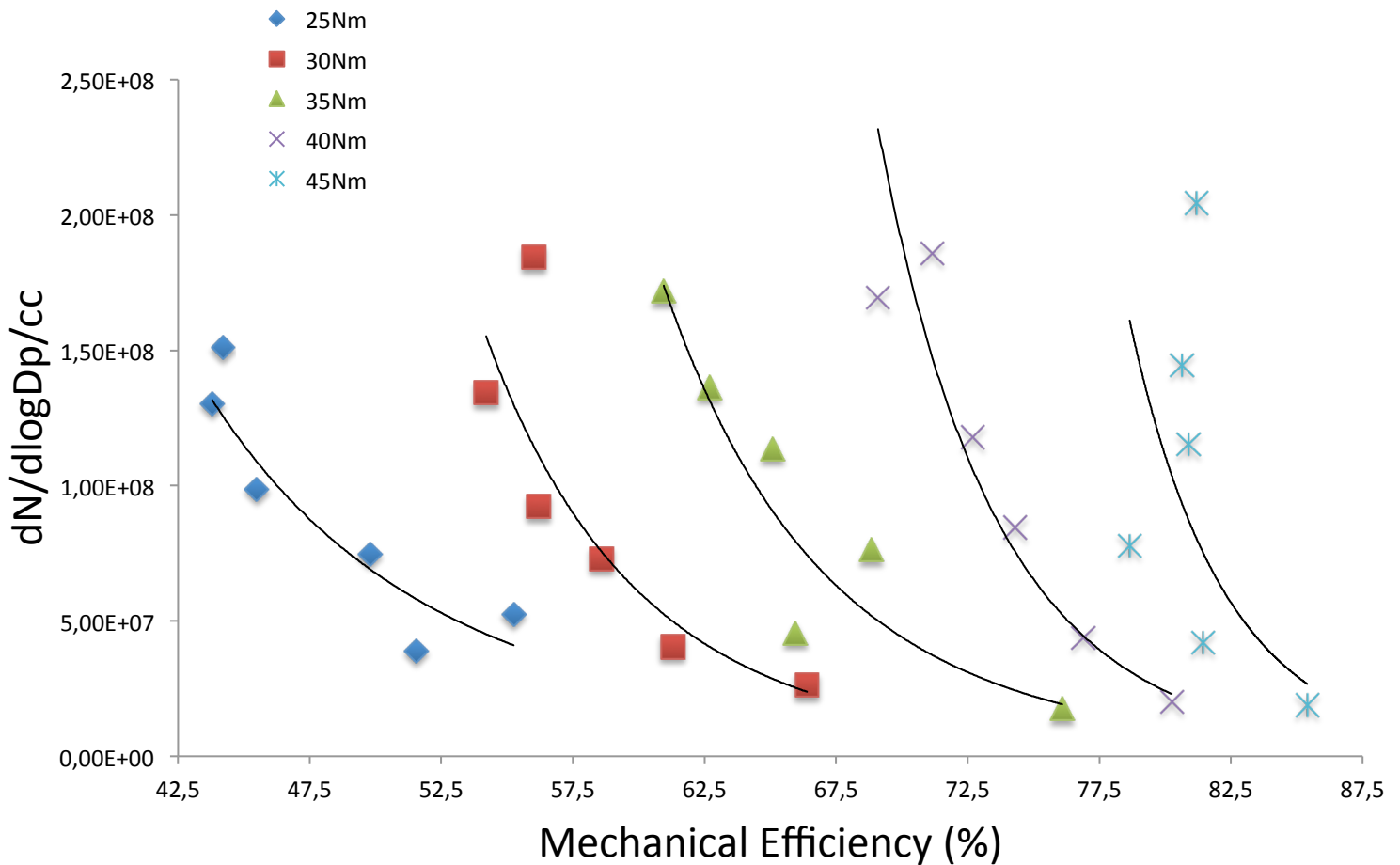## 12.1.4.4. Mechanical Efficiency and Particulates

Figure 44: Maximum Concentration of Diesel Particulates vs. Mechanical Efficiency of the Engine

Figure 44 demonstrates that the mechanical efficiency is linked to the maximum particulate output by a relationship that is dependant on applied load. The mechanical efficiency is seen to depend mostly on the engine load with increasing engine torque causing an increase in mechanical efficiency. This is due to the fact that there exists a certain amount of energy that is used to change the combustion charge each time, the energy for pumping, and to overcome the mechanical friction of the engine. Mechanical efficiency is obtained by dividing brake power by indicated power, thus at higher brake power, characterised by higher torque, the energy fraction that is used for pumping and to overcome friction is less, thus efficiency improves.

The relationship between mechanical efficiency and the maximum particulate output is seen to depend more on speed than engine load. The increasing load has the effect of changing the type of relationship from an almost linear inversely proportional one with a slope approaching -45 degrees to a slope that approaches the vertical at higher loads. Thus at lower torque the relationship between maximum particulates and mechanical efficiency is more prevalent. The vertical distribution of each set of points remains constant with increasing torque, thus engine speed has less of an effect on mechanical efficiency. From the figure it is seen that an engine that is operating at a high mechanical efficiency, thus a high load, will have a low maximum particulate output at a low speed. This corresponds with previous findings and again suggests an optimal operating point where the engine can maximise brake power and minimize particulates exists.

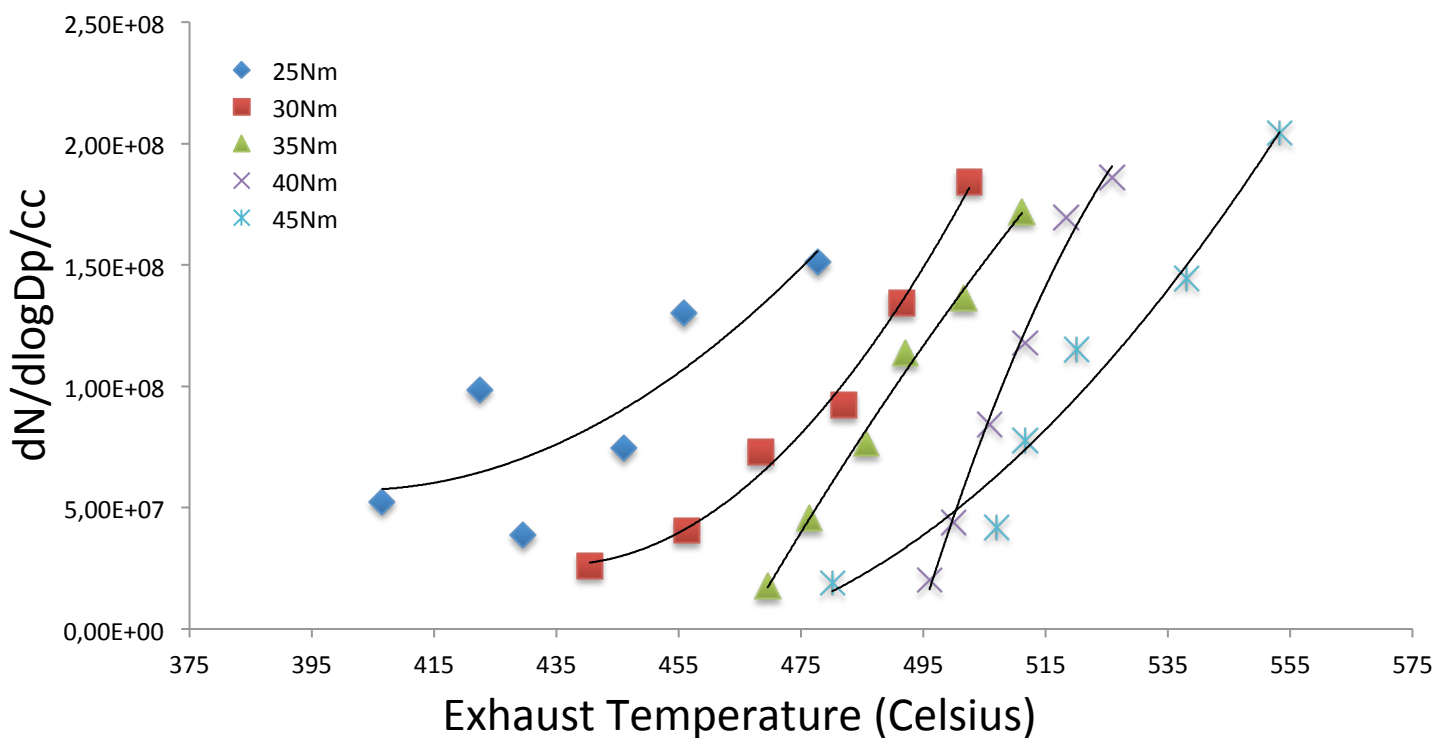## 12.1.4.5. Exhaust Temperature and Particulates

Figure 45: Maximum Concentration of Diesel Particulates vs. Engine Exhaust Gas Temperature

Figure 45 illustrates that increasing exhaust temperature also increases the maximum particulate concentration. The shape of the relationship is seen to remain fairly constant for changing engine torque. Increasing engine torque causes an increase in the exhaust temperature at that maximum particulate concentration.

It is noticed that exhaust temperature increases for both engine speed and engine torque, thus it is believed that it responds in general to a change in brake power. This is unlike the maximum particulate concentration that only seems to be responsive to engine speed, or cylinder transit time.

The fact that exhaust temperature is a function of engine brake power is indicative that an increase in output power must be met with an increase in cylinder temperature for it to translate into an increase in exhaust temperature. This is possible as at higher power outputs an engine would consume more fuel and this increase in fuel would translate into more chemical potential energy being released. The increase in fuel used causes an increase in particulates as it has been established that particulates stem from the hydrocarbon fuel.

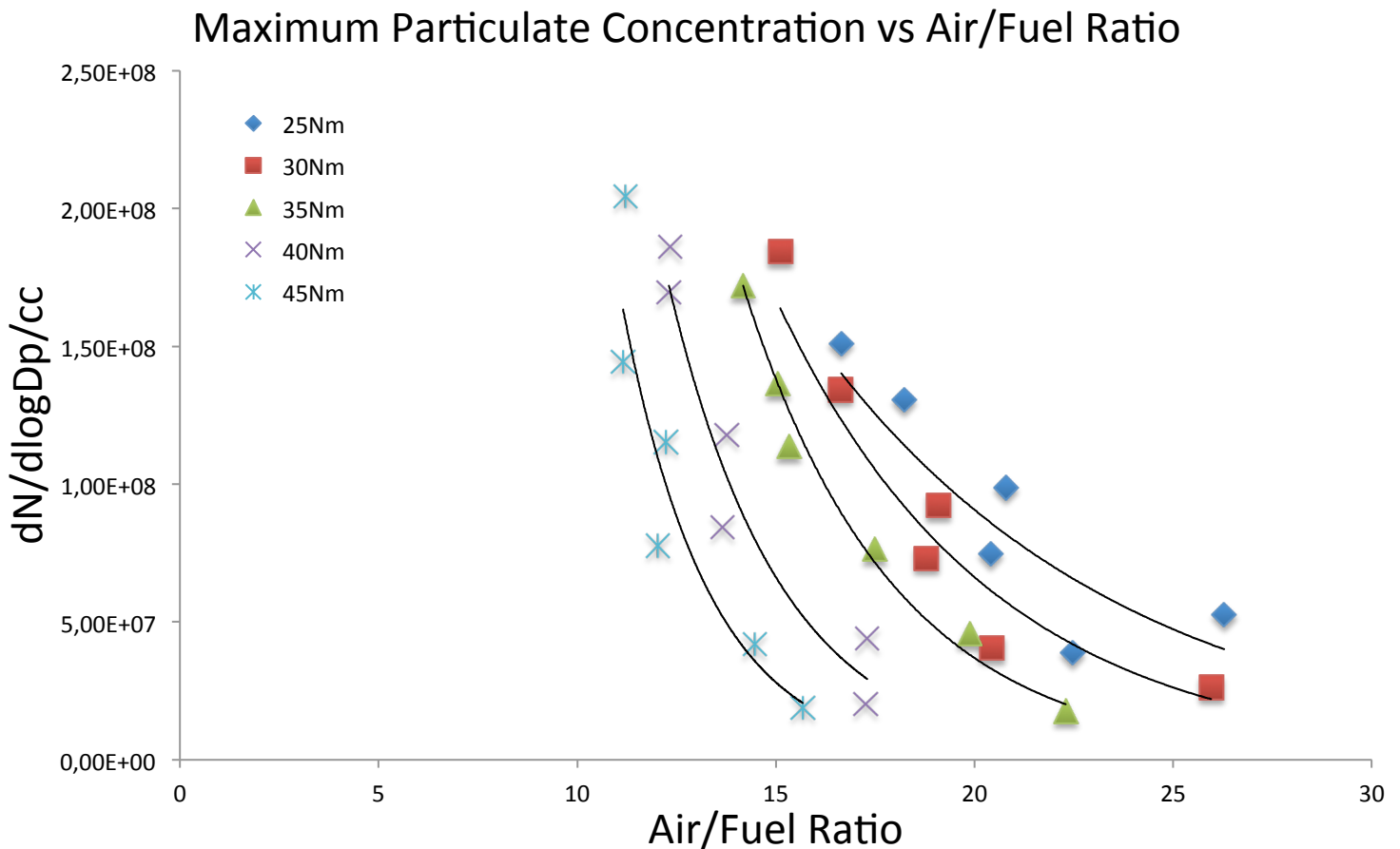## 12.1.4.6. Air/Fuel Ratio and Particulates

Figure 46: Maximum Concentration of Diesel Particulates vs. Actual Engine Air/Fuel Ratio

The relationship between air/fuel ratio and the maximum particulate output is seen, from figure 46, to be inversely proportional, whereby an increase in air/fuel ratio results in a decrease in the maximum particulate concentration. It is clear that increasing air/fuel ratio translates into a decrease in the engine's fuel flowrate. It is fully expected that less fuel would translate into less particulates, as is observed, in the previous sections.

The relationship changes slightly with changing torque. The curves flatten out slightly with decreasing torque. Thus the link between particulates and air/fuel ratio is observed to be less so at higher torques. Increasing torque also results in the data series moving toward the left, thus decreasing the air/fuel ratio, which means that higher engine loads demand more fuel. A consequence of the changing angle of slope is that at a lower torque the relationship between engine speed and air/fuel

ratio is stronger. The speed link can be used because of the previously established link between particulate output and engine speed.

This figure also demonstrates that the previously defined optimal operating point for the engine of high load at low speed has the drawback of an increase in fuel consumption. At a lower torque setting, where less fuel will be used, less brake power is produced, thus the operating point still makes sense but it should be noted that high power outputs demand more fuel.

Presented in Appendix 3 is a completed set of processed diesel data in tabulated form.

12.2. DME Fuelled Tests

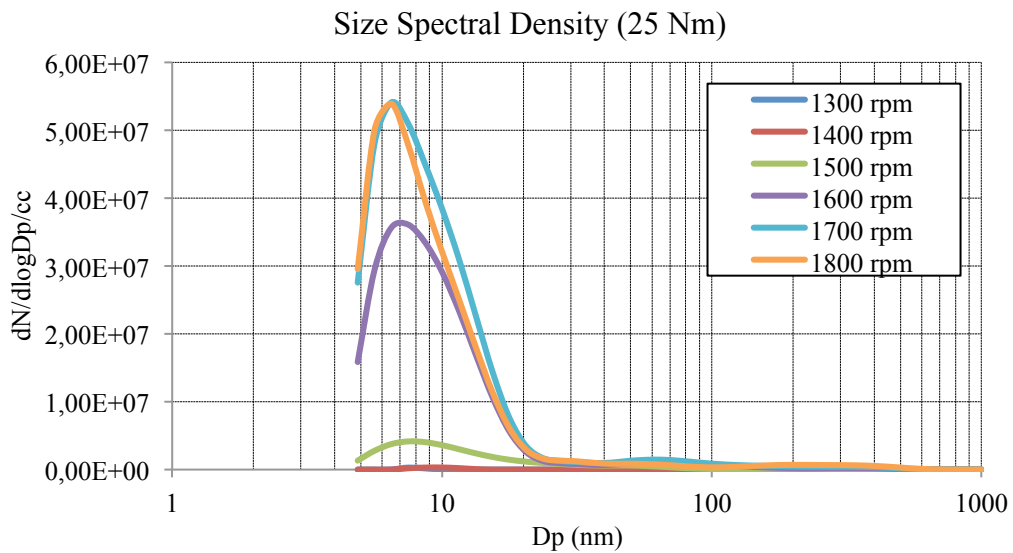### *12.2.1. DME Particulate Size Spectral Density Distribution*

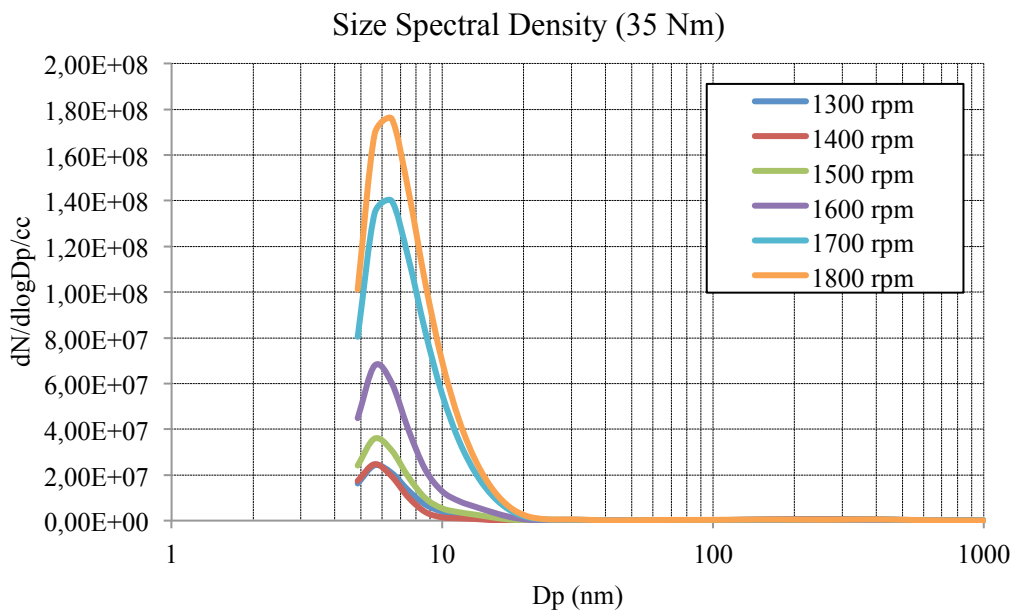Figure 47: DME Particulates Size Spectral Density at 25Nm

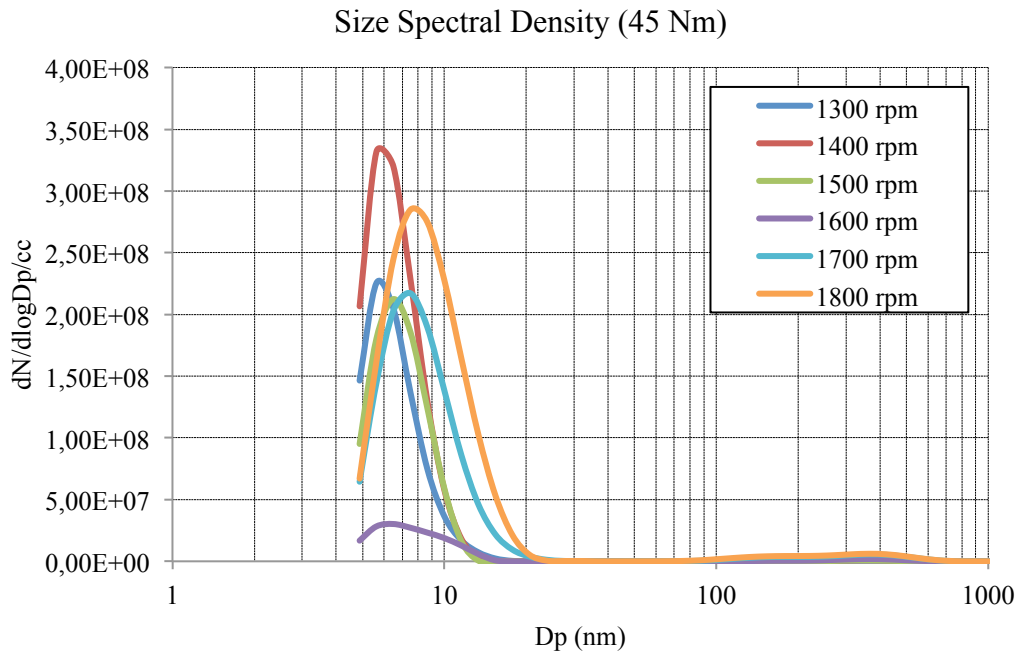Figure 48: DME Particulates Size Spectral Density at 35Nm

Figure 49: DME Particulates Size Spectral Density at 45Nm

Figures 47 to 49 illustrate that the size of the majority of particulates emitted by the engine while fuelled with dimethyl ether is constant at about 6nm. This appears to be independent of the engine load. However, variations in consistency are observed at the lowest load of 25Nm and the highest load of 45Nm, in figures 47 and 49 respectively. This may be due to the rpm instability of the engine at these extreme cases, where the engine governing mechanism had difficulty regulating the engine speed and speed drift occurred during the sample time.

The trends, however, clearly show that the increase in rotational speed of the engine causes a considerable increase in the concentration of these 6nm particles. This is clearest with figure 48, at 35Nm where the lowest concentration of particles is at 1300rpm while the highest is at 1800rpm. This lowest point seems to drift with increasing torque. The lowest concentration is shared between 1300rpm and 1400rpm at 35Nm, and the lowest concentration is at 1600rpm followed closely by 1500rpm at 45Nm. This could be an indication of some kind of optimal operating point for the engine in each case. However, the trend of increasing particulate concentrations with increasing speed is clear.

If the peak concentrations at particular speeds are compared with their counterparts from different torques, it is clear that engine load also increases the concentration of these 6nm particles. By examining figures 47 to 49, 1700rpm and 1800rpm in particular, this can be seen to be the case.

From figures 47 to 49 it is observed that all distribution curves are cut-off at 5nm. This is due to the instrument design which measures particles of 5nm to 2500nm. Instruments that can detect smaller particles were not available.

The full set of dimethyl ether size spectral densities is shown in Appendix 2.

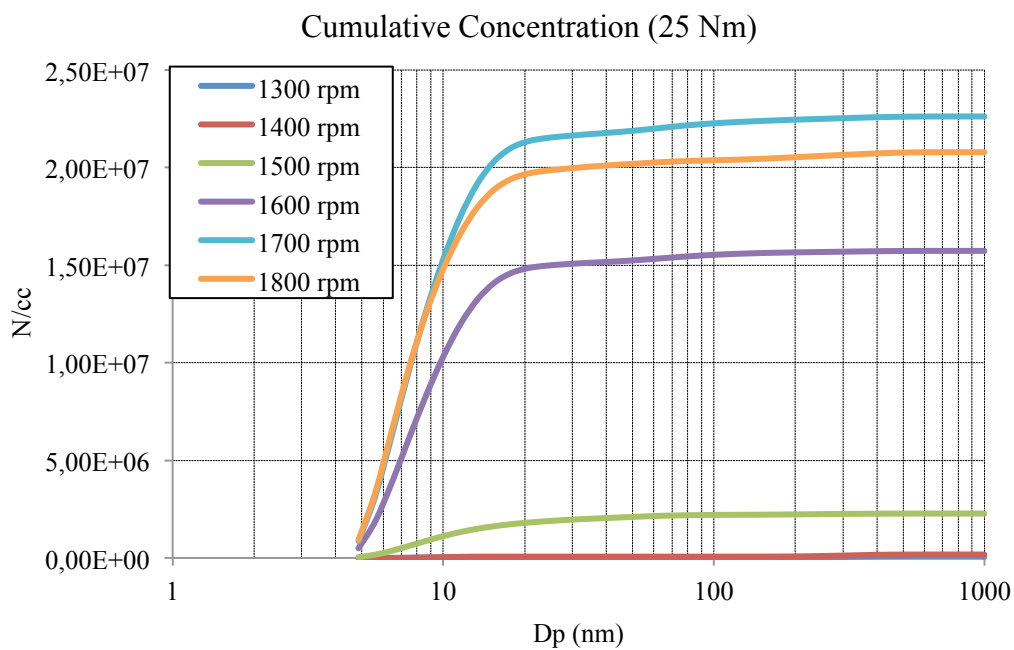## 12.2.2. DME Particulate Cumulative Concentrations

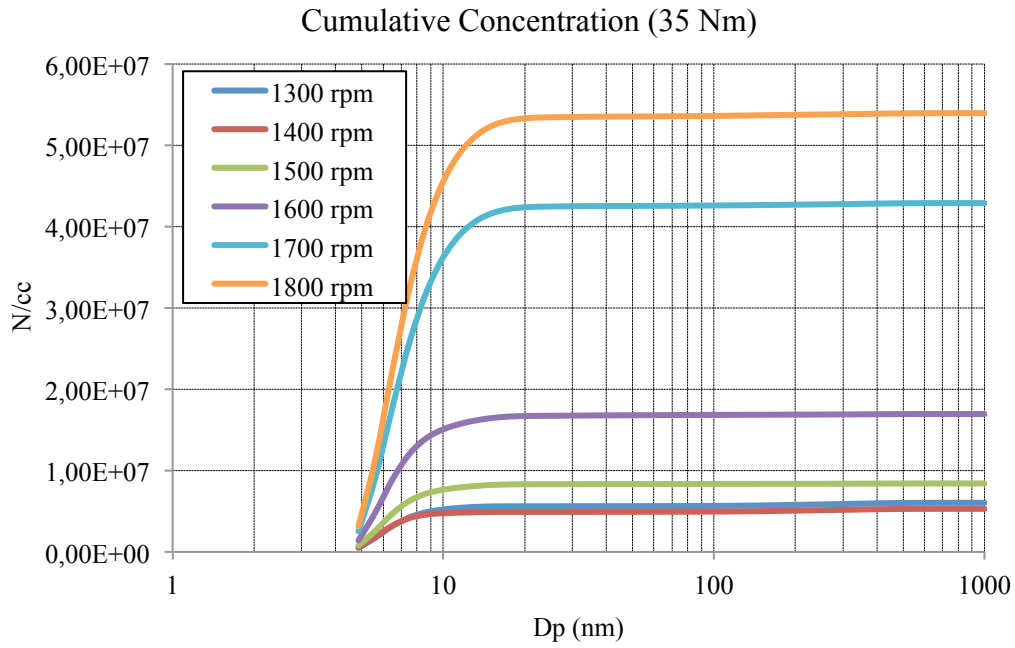Figure 50: DME Particulates Cumulative Concentration at 25Nm

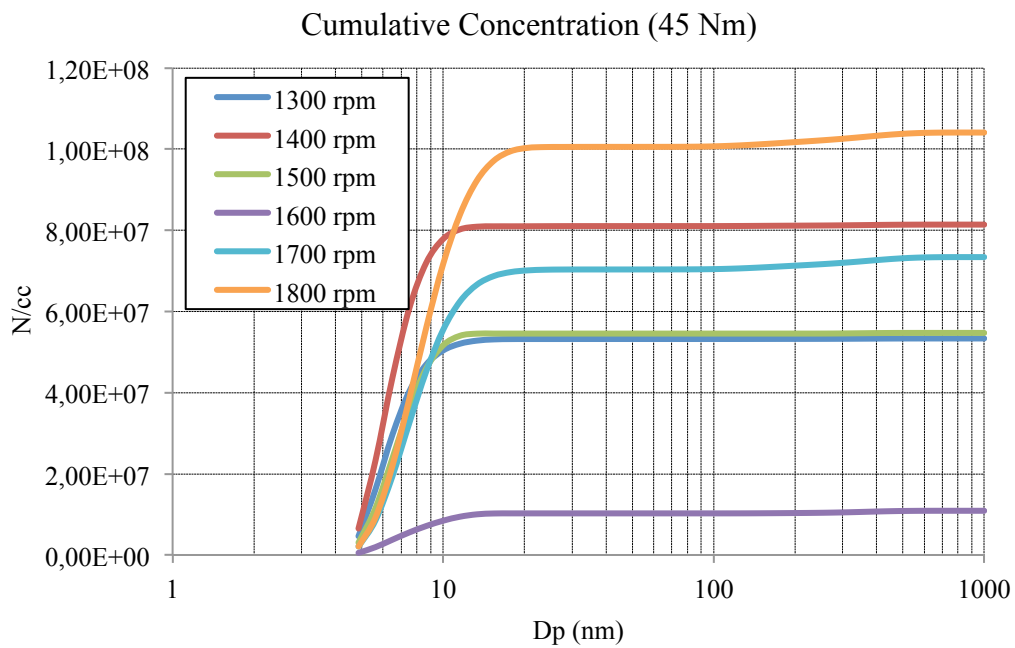Figure 51: DME Particulates Cumulative Concentration at 35Nm

Figure 52: DME Particulates Cumulative Concentration at 45Nm

Figures 50 to 52 present the information of figures 47 to 49 in an alternative form. Whereas figures 47 to 49 show a distribution curve of the particles by size and concentration per cubic centimetre, figures 50 to 52 show the data as a number

count of the particles by size in a cumulative fashion. The particles with the highest concentration are seen at the steepest gradient. These graphs illustrate that although the maximum concentration was thought to be of 6nm-sized particles, this is actually not the case. Increasing speed causes a slight increase in the size of the particulate of maximum concentration. Thus increasing speed not only increases the concentration of particles but also the size of the particle of maximum concentration.

By studying figure 51, 35Nm, it can be seen that the particulate size is increasing. Although this trend is clearest in figure 51 it can also be seen in the other figures. The observation of a lack of engine speed stability at these extreme loads must be recalled and its effect on the results not overlooked. The idea that larger particulates would be produced is a possible indication of more particle agglomeration being present or of more time for particle surface growth. But at higher engine speeds the transit time of the charge is reduced, thus the time for surface growth in the cylinder would be reduced. If agglomeration was the mechanism, then the amount of particulates being detected should decrease, which is not the case. It is thus most plausible that more nucleation is present during higher speeds along with surface growth of the particles outside the cylinder, or the increase in cylinder temperature at higher speeds could mean that surface growth in the cylinder is a more probable mechanism at play. The fact that higher speeds demand more fuel also corresponds with this notion.

12.2.3. DME Particulates and Gaseous Emissions

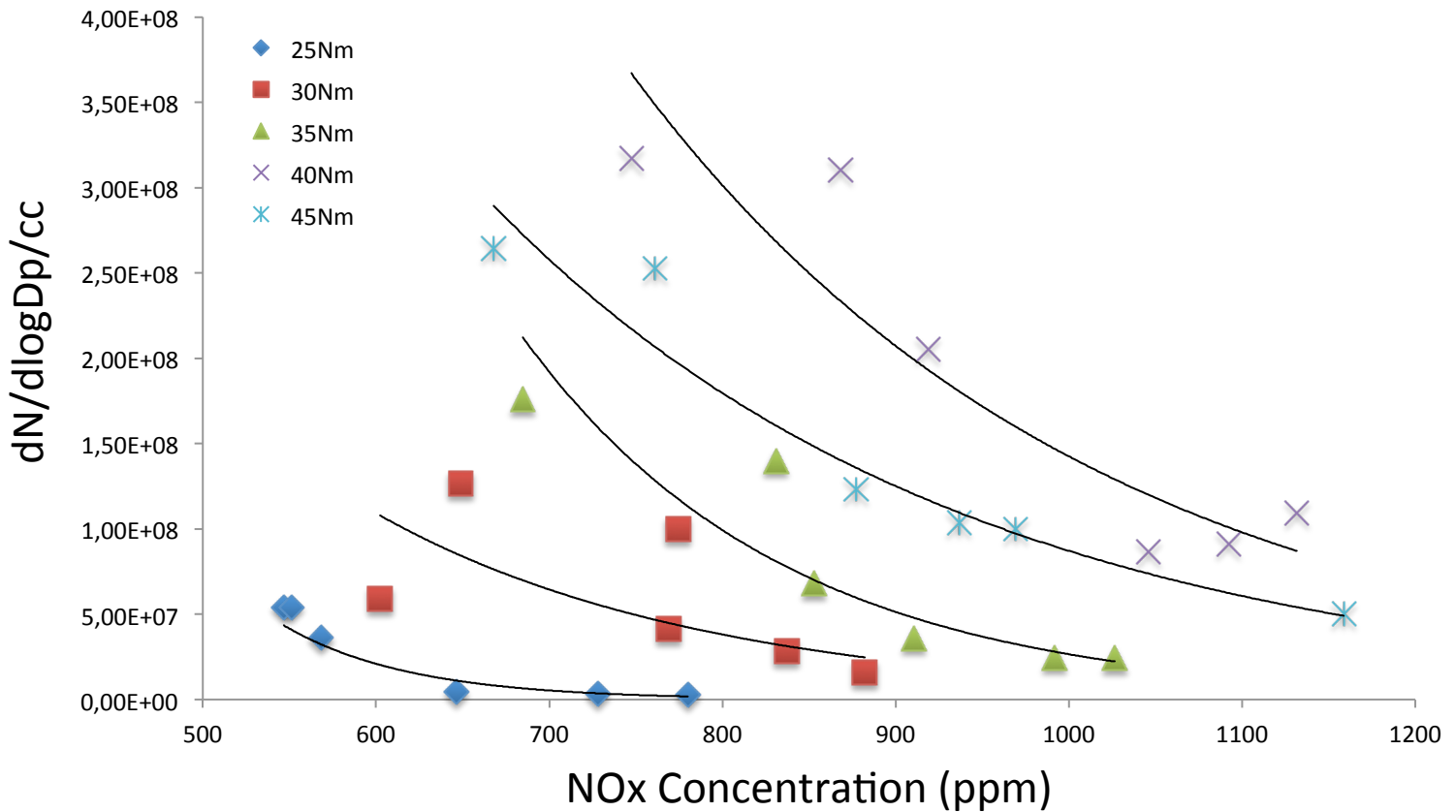### 11.2.3.1. NOx Gas Output and Particulates

Figure 53: Maximum Concentration of DME Particulates vs. NOx Concentration

In figure 53, the link between NOx output and maximum particulate concentration of the engine while fuelled on dimethyl ether can be observed. It can be concluded from the plot that NOx output and particulate output are linked in an inversely proportional manner, the degree of this changes with increasing engine load. The relationship is closest to being inversely proportional at high engine loads. At lower engine loads the relationship is less pronounced with large changes in NOx output producing smaller changes in the particulate output. It is noticed however, that the closest series to 135 degrees is 40Nm, and not 45Nm, thus this is indicative of an optimal point where the relationship is most pronounced and it tapers off towards both extremes. It was noted in the literature survey, Section 4.4.1, [18], that a trade-off is

known to exist between an engine's particulate and NOx output. Although this trade-off is well known for conventional fuels, it is noteworthy to find that it also exists with dimethyl ether fuelling. This clearly indicates that the factors that are conducive to forming particulates are not the same as those for NOx gases.

It is known that particulate concentration increases with increasing engine speed, thus the dependent axis is directly linked to engine speed. Therefore it can be observed that the engine produces more NOx at lower speeds. This could be linked to the higher temperatures at higher speeds causing the NOx species to dissociate back into nitrogen and oxygen. It is then plausible to assume that more oxygen is present in the combustion chamber at higher speeds and that a higher content of free oxygen is needed for the production of particulates.
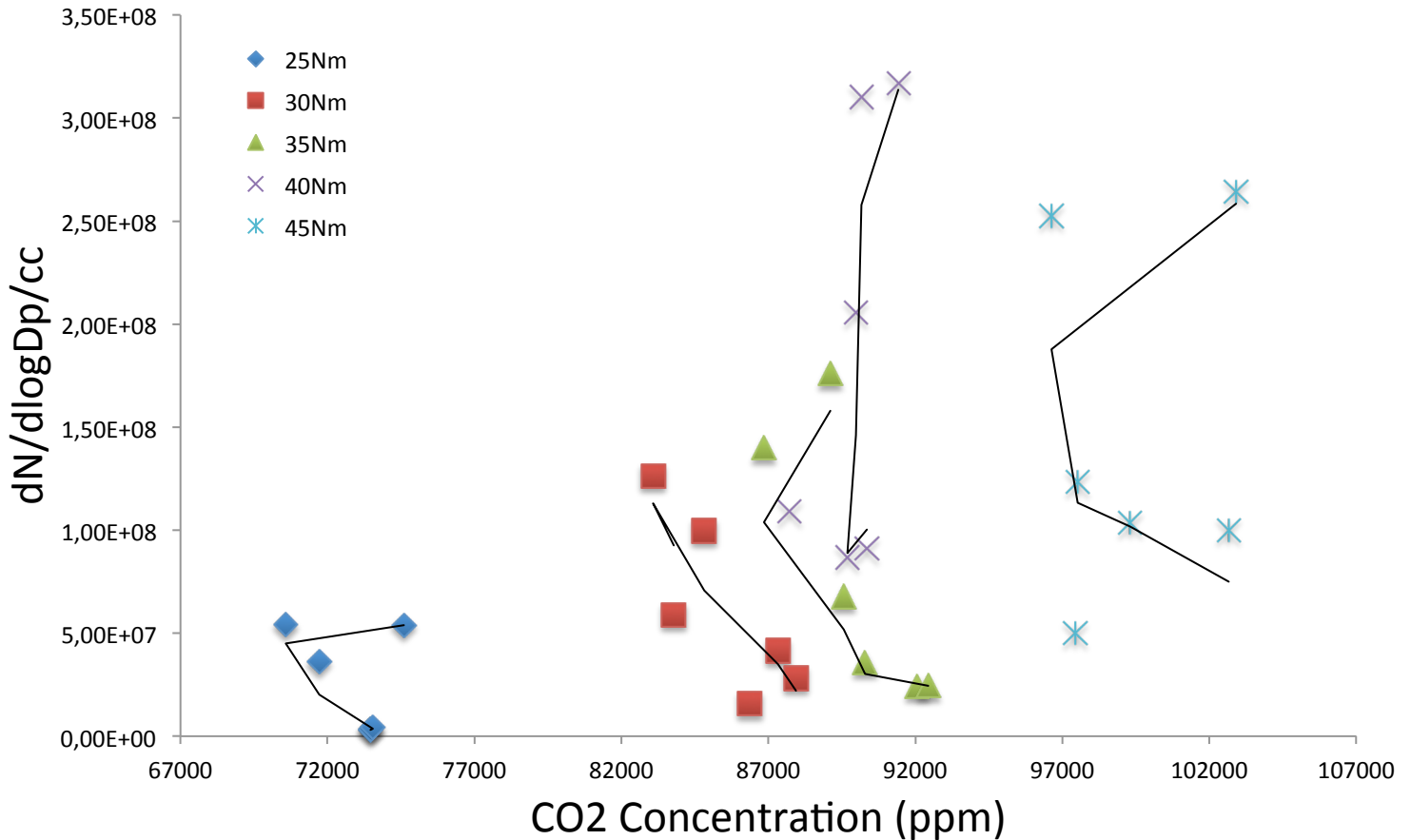
12.2.3.2. Carbon Dioxide and Particulates

Figure 54: Maximum Concentration of DME Particulates vs. CO2 Concentration

Figure 54, illustrates the lack of relationship between carbon dioxide and particulates with dimethyl ether fuelling. As the plots are arranged in a somewhat vertical stack for each series it indicates that there is little connection between the output of particulates and carbon dioxide. Therefore is can be said that the formation of particulates and carbon dioxide are two unrelated processes.

The effect of engine speed and load, however, can still be observed from figure 54. As mentioned the dependent axis is indicative of engine speed. Thus is can be said that engine speed plays little role in the formation of carbon dioxide. It can, however, be seen that engine torque does have a large effect on the engine's production of carbon dioxide. At lower engines torques the engine produces little carbon dioxide while at higher torques more is produced. What is also observed is that at lower

engine torques the vertical range is less than at higher torques. Thus where there exists a lower probability to produce carbon dioxide like at 25Nm there also exists a limit on the concentration of particulates that can be produced. This range increases with increasing torque. Therefore when higher levels of carbon dioxide are produced there exists a higher chance of a greater particulate output if the engine speed is increased.

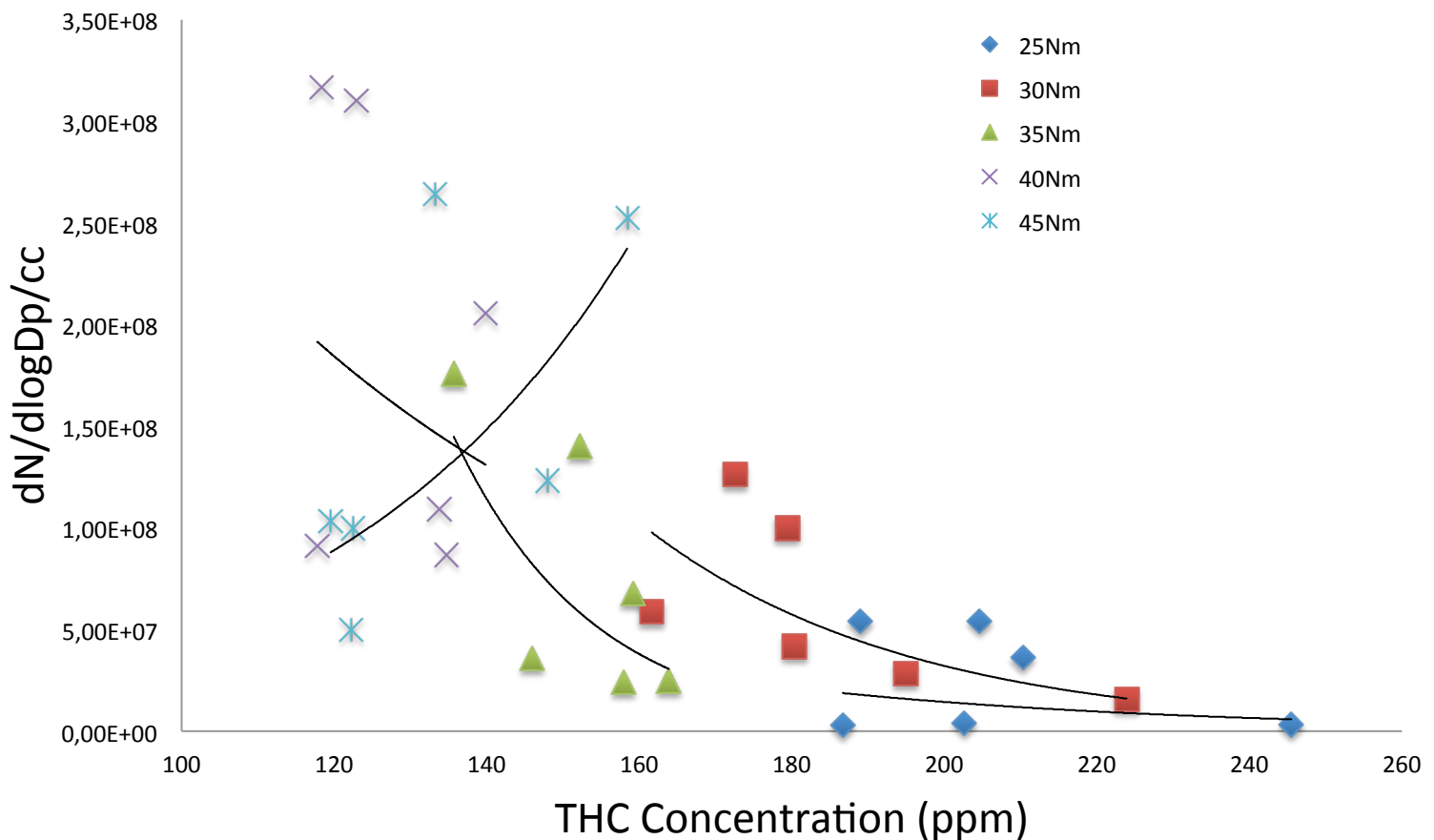### 12.2.3.3. THC and Particulates

Figure 55: Maximum Concentration of DME Particulates vs. THC Concentration

The relationship between total hydrocarbon output and particulate output when DME fuelling is used is shown in figure 55. The link between THC and particulates is seen to be strongest at lower engine loads. This link is an inversely proportional one

where increases in the THC output are met with decreases in the particulates. It must be recalled that higher particulate outputs are indicative of higher engine speeds. Thus it can also be said that increases in engine speed at lower engine loads produce a decrease in THC and an increase in particulates. However, at higher loads, like 40Nm and 45Nm, the inversely proportional relationship appears to break down as the trends observed deviate strongly from the previous ones at lower loads. But it was mentioned previously that the engine was unable to keep its set speed at high loads, and this might be a possible reason for the break down in the relationship.

It can also be observed that increasing engine load appears to decrease the THC output. This can concluded from the fact that the data sets appear to be tending towards zero as the load increases. An increase in particulate output, thus an increase in engine speed, is also met with a decrease in THC output, as explained earlier. Thus increasing engine load and speed decrease THC, in other words an increase in the engine's brake power will decrease its THC output. This could be due to the fact that, generally, at higher brake power the engine has a higher mechanical efficiency. Thus if the engine is behaving more efficiently it is more conducive to better combustion resulting in less THC. But this produces an apparent contradiction as particulates can be known as products of incomplete combustion, and they increase with increasing engine brake power. It must be recalled that dimethyl ether does not have a carbon-to-carbon bond, which is usually what is responsible for the formation of soot particles in combustion. Thus the particulates formed in a DME combustion reaction are probably products of better combustion, like water particles of some kind. It is also known that water is a product of complete combustion thus at higher brake power the DME fuel is being burnt closer to what is stoichiometrically correct, resulting in less particulates of the traditional soot type. This adds credence to DME as an improved fuel.
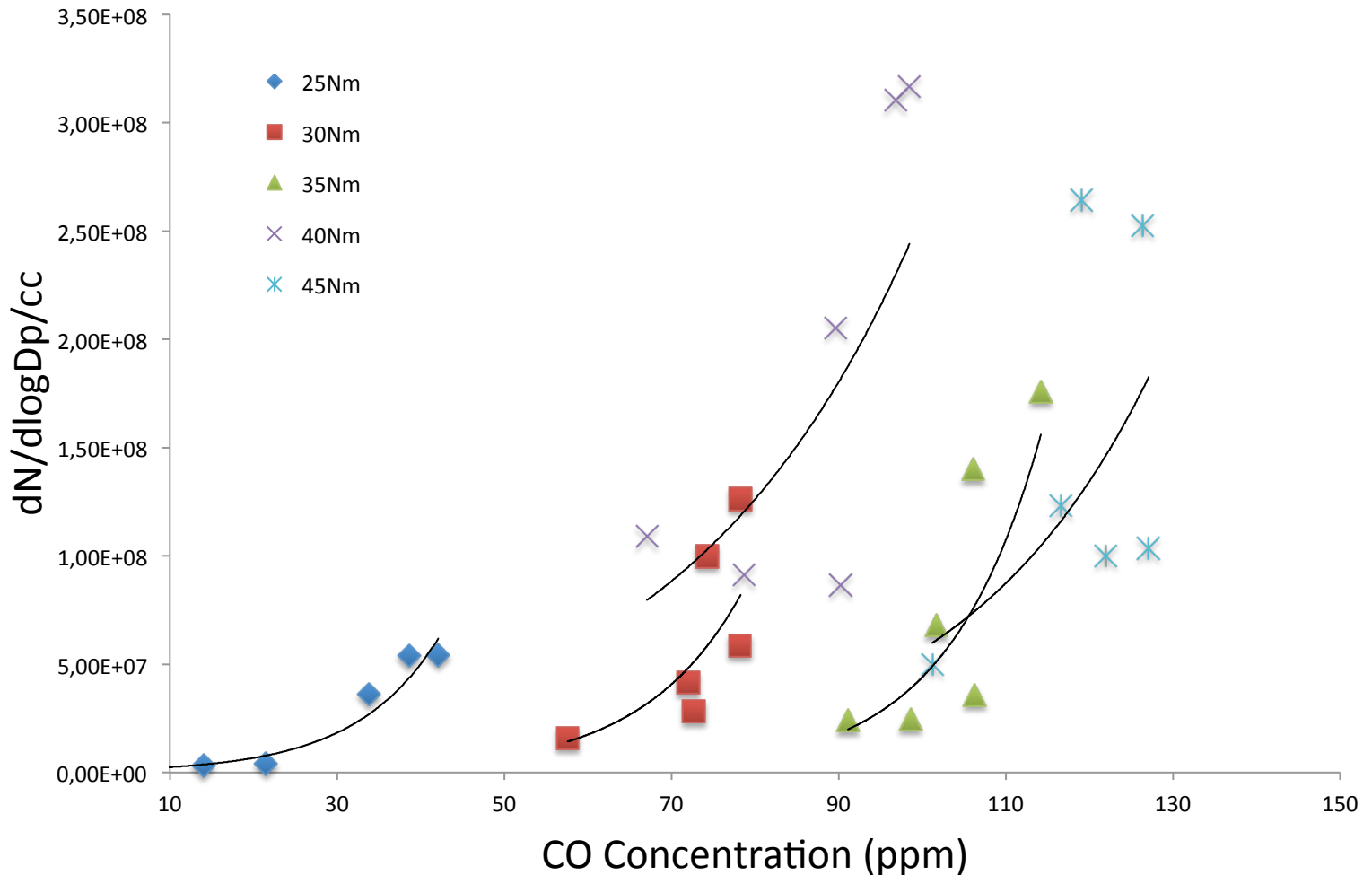
12.2.3.4. Carbon Monoxide and Particulates

Figure 56: Maximum Concentration of DME Particulates vs. CO Concentration

There appears to be a directly proportional link between carbon monoxide and particulates, as shown by figure 56. An increase in particulates is met with an increase in carbon monoxide. The link between carbon monoxide and particulates appears to remain constant with increasing engine load. This means that relative to the axis the curves remain consistent in shape. It can thus be concluded that the mechanisms that are at play to create the carbon monoxide are the same as, or in support of, the mechanisms that create particulates. It was suggested earlier that the particulates with DME fuelling are actually more likely to be particles of water resulting from more complete combustion, rather than carbon derived particles.

Carbon is needed to create carbon monoxide and the more traditional soot particulate. But if carbon was being shared it is entirely plausible, through conservation of mass that the relationship between carbon monoxide and particulates would be an inversely proportional one, which it is clearly not. Thus the previous suggestion that dimethyl ether particulates are not carbon based supports this finding.

The relationship between carbon monoxide and engine torque can also be observed from figure 56. It can be seen that there exists a general trend for carbon monoxide output to increase with increasing engine load, with all torques except 40Nm. This is indicative again of some kind of optimal operating point for the engine as far as carbon monoxide production is concerned. This optimum appears to exist somewhere between 35Nm and 45Nm. But again it must be stressed that this is unlikely to be a general optimum and is probably only linked to the very specific conditions of this experiment and engine. This does however indicate that there is room, in terms of valve design, combustion chamber design and manifold design, to optimise an engine in terms of carbon monoxide output.

It is also noted that increases in engine speed produce more carbon monoxide, thus carbon monoxide increases when engine brake power increases. This is probably due to there being more fuel present in the combustion chamber at higher brake power outputs. More fuel means that more carbon will be present for the creation of carbon monoxide. Thus the combustion of DME is more in favour of water than carbon monoxide. It could be assumed that the extra oxygen is used to create water rather that to oxidise carbon monoxide into carbon dioxide, leaving less hydrogen for THC production. Less THC at higher brake power outputs fits with the previous findings.

12.2.4. DME Particulates and Engine Performance
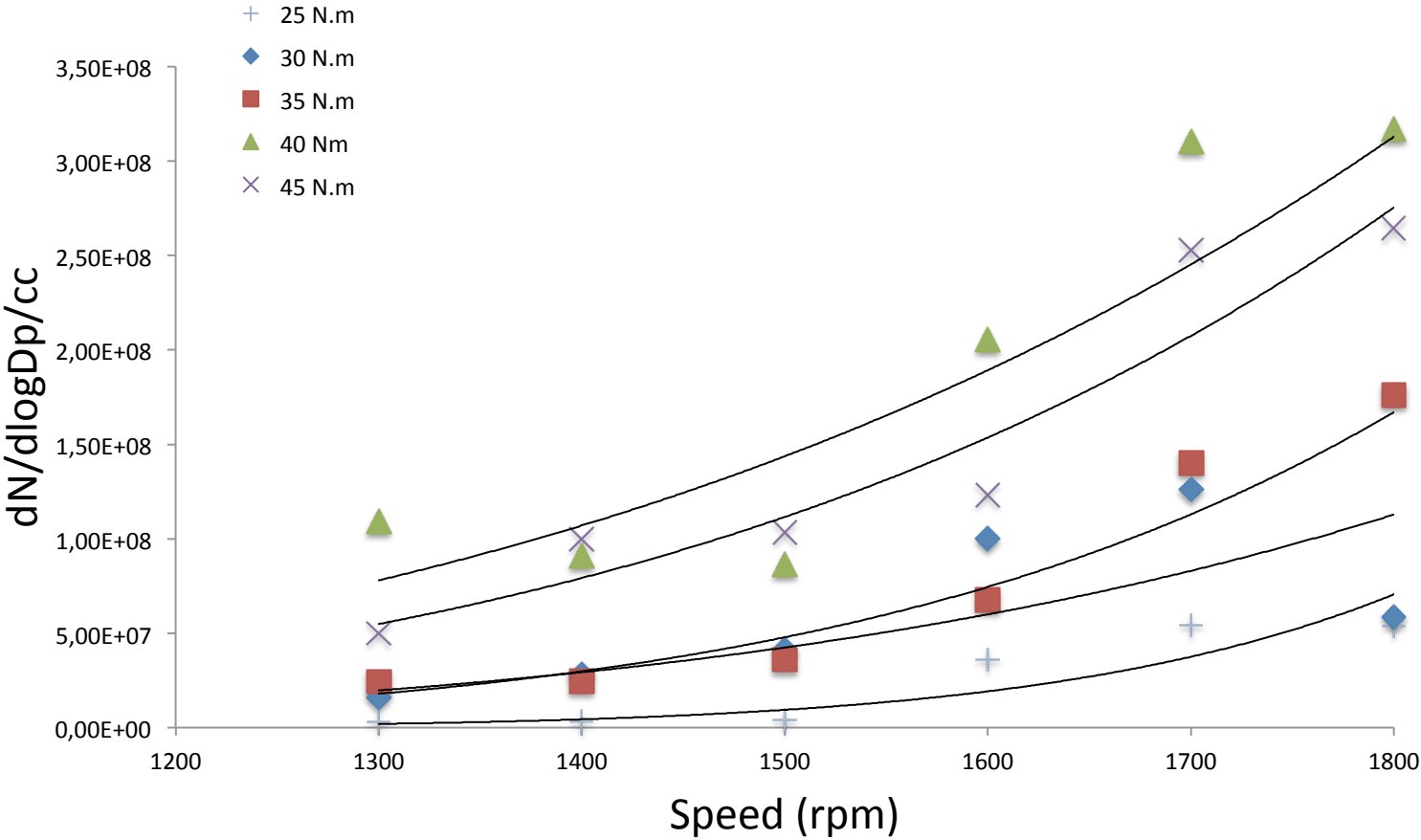
12.2.4.1. Engine Speed, Load and particulates

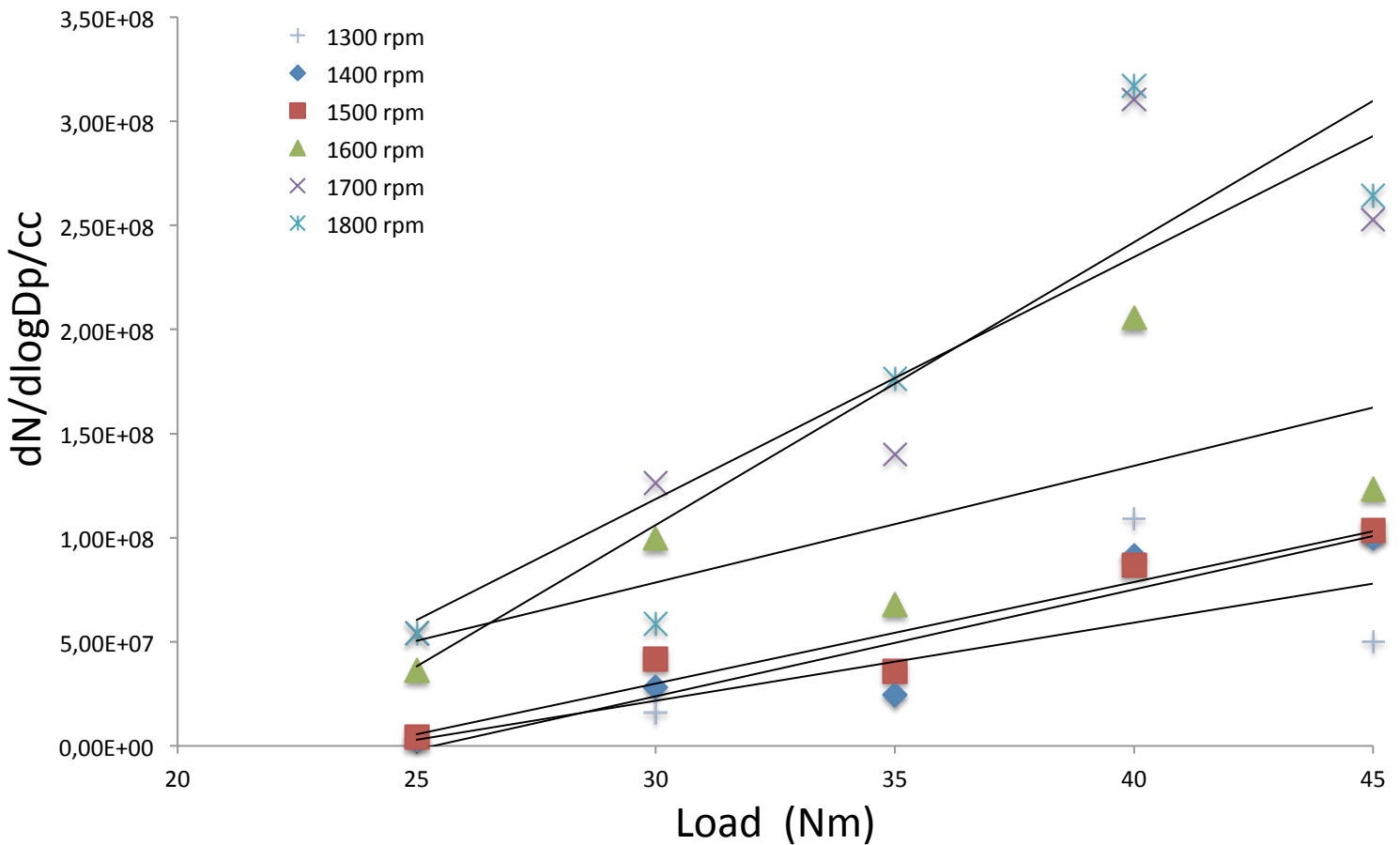Figure 57: Maximum Concentration of DME Particulates vs. Engine RPM

Figure 58: Maximum Concentration of DME Particulates vs. Engine Torque

Figure 57 is a plot of all the peaks from figures 47 to 49, versus the engine's operating speed. The various data sets are indicative of the engine load applied. The effect that speed has on the output of particulates while fuelled with dimethyl ether is clearly illustrated. Increasing speed causes an exponential increase in the output of particulates. This exponential trend appears to hold for all engine loads as all the curves correspond well with one another. The engine speed is indicative of the time that the charge spends in the cylinder. The initial thought would be to attribute a shorter time in the combustion chamber with less efficient combustion and thus more soot particles being emitted. But it was previously stated that it is believed that particulates, in the case of DME, are believed to be particles of the products of a better combustion, water being the obvious candidate. Thus it appears that at higher speeds the combustion quality is not degrading but actually remaining elevated. Thus it could be argued that the increase in particulates is merely due to there being

more fuel and thus hydrogen present and not of a less efficient and rushed, in terms of available burn time, reaction.

In figure 58 the same data is plotted except that the engine load is made the independent variable, and the data sets are arranged according to engine speed. The effect of increasing load can is seen clearly in this figure. Load, like engine speed, causes an increase in particulates. The relationship between engine torque and particulates is linear. The slope of the linear relationship appears to be flatter at low engine speeds and steeper at higher engine speeds. Thus when the engine is running at high speed a bigger change in particulate output can be expected when engine load changes. The fact that both speed and torque affect the output of particulates means that particulate output can be linked to the brake power output. The point of maximum particulates can clearly be seen to be at 40Nm and 1800rpm This is not the point of highest brake power, which is at 45Nm and 1800rpm.

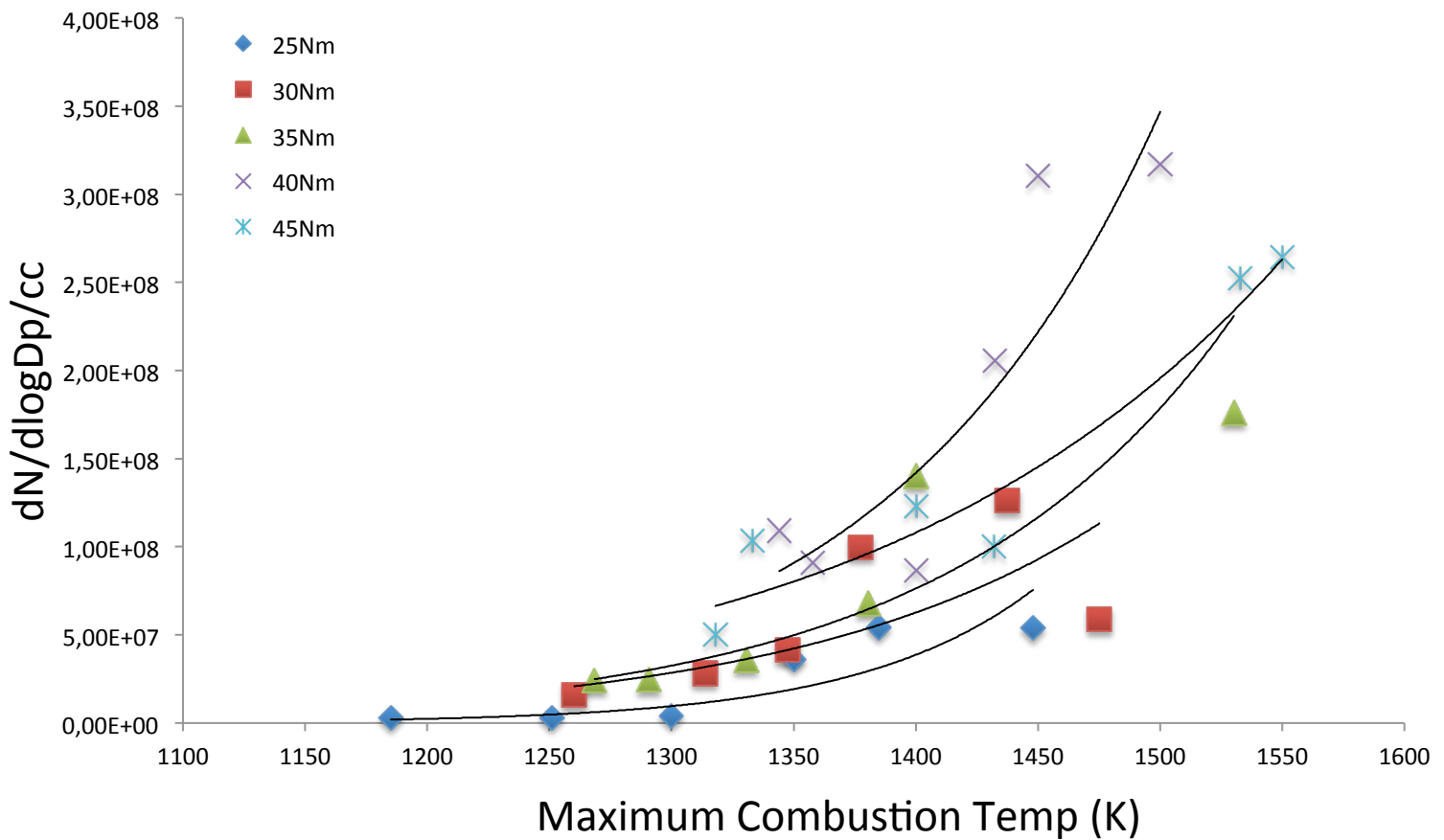## 12.2.4.2. Maximum Combustion Temperature and Particulates

Figure 59: Maximum Concentration of DME Particulates vs. Peak Combustion Temperature

Figure 59 shows that the maximum combustion temperature is related to the maximum concentration of particulates in an exponential manner. The relationship holds constant irrespective of the increase in engine load. Again however, it is seen that the maximum concentration of particulates does not occur at the highest torque of 45Nm but at the second highest torque of 40Nm.

The link between engine speed and maximum combustion temperature is noted, as it is known that the particulate concentration is indicative of engine speed. Thus increasing speed in a DME fuelled engine also increases the peak combustion temperature of the cycle, as it does in a diesel-fuelled engine. This is possibly related to the fact that the charge has less time in the cylinder, resulting in less time to transfer heat to the surrounding walls of the combustion chamber. Therefore heat

transfer is less efficient and the core of the charge gas remains hotter. It is known that an engine operating at a higher temperature will have more efficient combustion; and that the particulates in a DME engine are probably water spherules, resulting from a better combustion process. Thus a hotter combustion environment supports this notion.

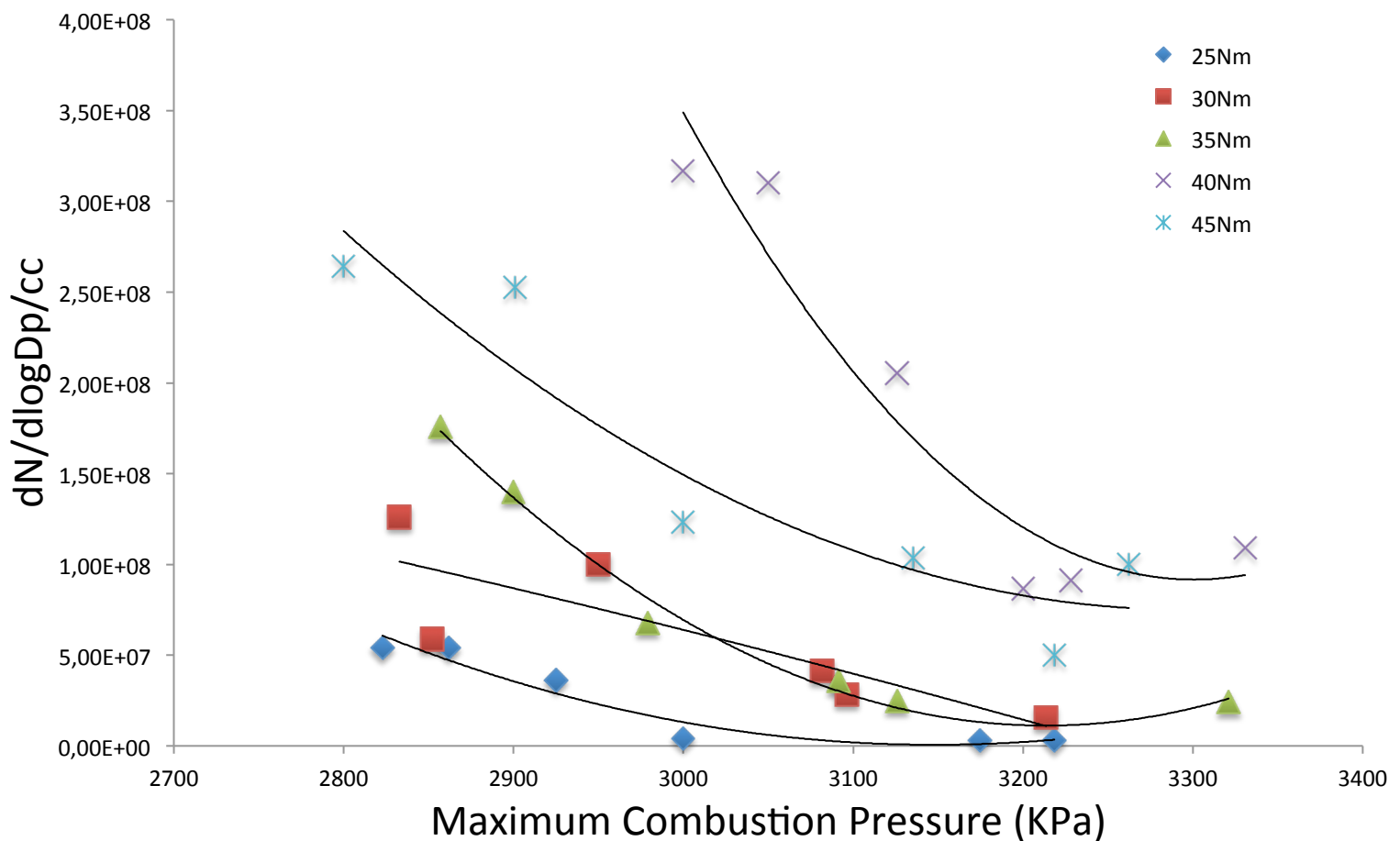## 12.2.4.3. Maximum Combustion Pressure and Particulates

Figure 60: Maximum Concentration of DME Particulates vs. Peak Combustion Pressure

The relationship between the maximum combustion pressure, engine torque and speed and particulates, is shown in figure 60. The shape of the curves suggests that an inversely proportional relationship exists between maximum combustion pressure and the concentration of particulates. Therefore as pressure is increased, at all

107

loads, less particulates are emitted. This indicates that particulates of a dimethyl ether fuelled engine, form better in a low-pressure environment. As it has already been suggested, the particulates resulting from DME combustion are probably spherules of the products of complete combustion, like water. It could be that in a high-pressure combustion chamber the water particles being formed are less likely to agglomerate and rather dissociate into single molecules, like a gaseous emission.

Figure 60 also shows that increasing torque has little effect on the trends of maximum pressure. This can be attributed to the fact that the various sets of data are seen to have similar ranges along the independent axis. However the effect of increasing torque is seen to cause an increase in the maximum particulate concentration observed at a particular pressure. It has already been established that higher maximum particulate concentrations are indicative of higher engine speeds. This demonstrates that the maximum combustion pressure is affected little by increasing engine load but rather engine speed, and an increase in engine speed is met with a decrease in maximum combustion pressure. This seems to be an odd result and could be attributed to a change in the characteristic of combustion at changing speeds when dimethyl ether fuelling is used. At higher speeds the DME, which is supplied to the fuel pumps is at 50 bar, as it is pre-pressurised to prevent it from vaporising, may be leaking out from the injector seat causing a pre-detonation of the charge and thus a less efficient burn with a consequently lower pressure. A possible explanation for the leakage of fuel from the injector seat maybe due the injector spring having insufficient time to return the needle at higher speeds, thus not effectively sealing the seat. Therefore at higher speeds, the fuel could be burning over a longer time period as some has leaked in, causing a decrease in the maximum pressure.
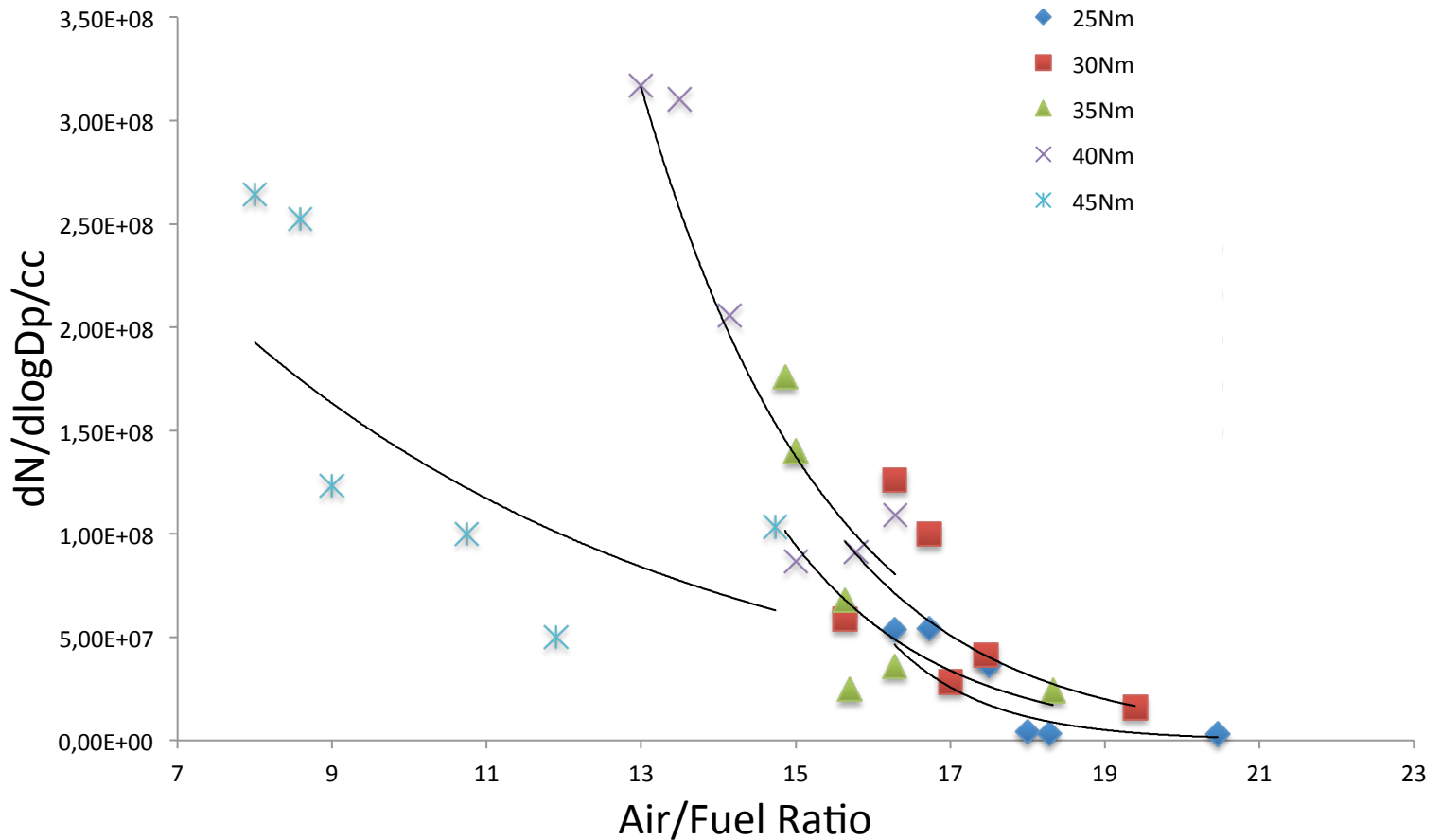
12.2.4.4. Air Fuel Ratio and Particulates

Figure 61: Maximum Concentration of DME Particulates vs. Actual Engine Air/Fuel Ratio

Figure 61 demonstrates the link between air/fuel ratio and the maximum concentration of particulates. At high air/fuel ratios, low concentrations of particulates are observed. In a compression ignition engine the amount of air admitted into the cylinder is not regulated and as the fuel flow rate is increased an increase in engine speed results. This means that if the mass of air is assumed to be constant per cycle, then the mass of fuel is what is actually determining the air/fuel ratio Thus at higher air/fuel ratios there is less fuel present. If this is the case then less fuel being burnt results in less particulates. This result is expected as the particulates themselves are composed of elements that are introduced into the combustion chamber via the fuel.

The relationship between the air/fuel ratio and the maximum concentration of particulates is seen to remain fairly constant at all torques except at the highest torque of 45Nm. But it must be remembered that the engine had trouble maintaining a constant speed at the highest load of 45Nm and the speed drifted slightly during tests. This could have produced this apparently erroneous set of data. What is seen however is that at higher loads the data sets move towards the left, therefore towards lower air/fuel ratios, translating to more fuel being used at higher loads than would be expected. The effect of engine speed on the air fuel ratio can also be deduced from figure 61. At higher maximum particulate concentrations, thus higher engine speeds, the air/fuel ratio again tends towards the left, thus an indication of more fuel being burnt at higher speeds. It can therefore be said that the air/fuel ratio is inversely proportional to the brake power.

Presented in Appendix 4 is a completed set of processed DME data in tabulated form.

12.3 Notable Comparisons Between DME Results and Diesel
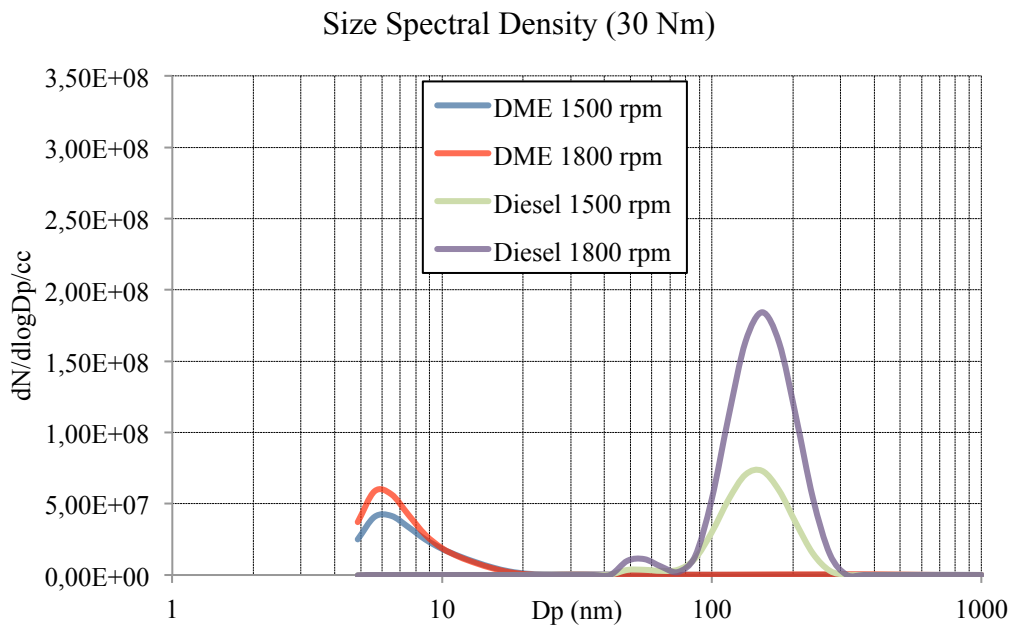
12.3.1. *Size Spectral Densities*

Size Spectral Density (30 Nm)

Figure 62: Comparison of Size Spectral Densities at 30 Nm
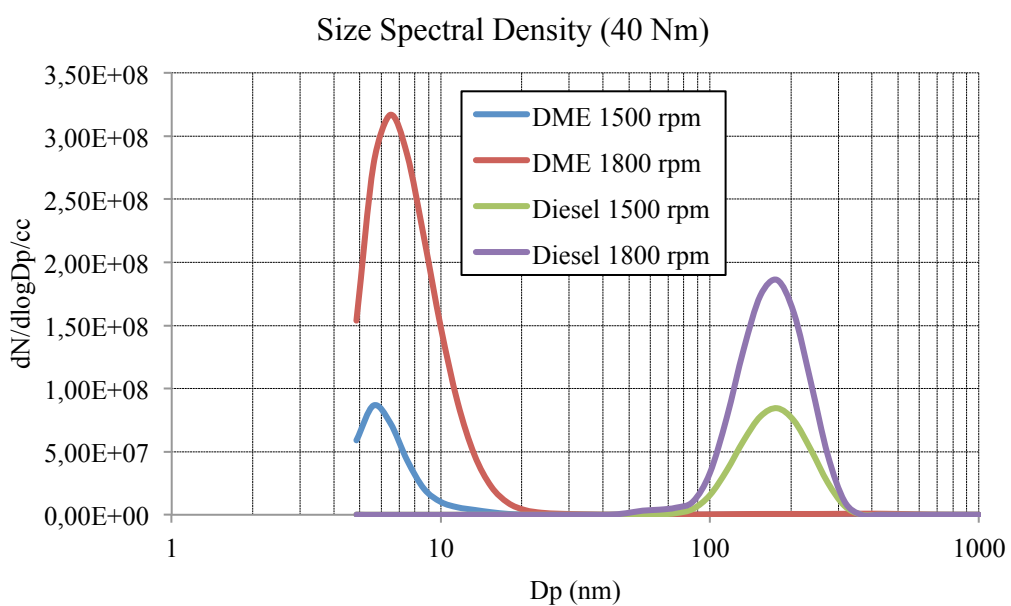
Size Spectral Density (40 Nm)

Figure 63: Comparison of Size Spectral Densities at 40Nm

The differences in the particulate spectral distributions for diesel and dimethyl ether fuelling are illustrated by figures 62 and 63. The most prominent difference is that diesel particulates are considerably larger, at about 150nm to 170nm, than those of dimethyl ether, at about 5,5nm to 6,5nm. The diesel particulates are known to be derived from soot, thus from partly oxidised fuel whereas the dimethyl ether particulates are believed to be spherules of the products of more complete combustion, thus tiny liquid drops. This is because the chemical formulae of dimethyl ether lacks a double carbon bond, thus it will produce little, if any, carbon derived soot.

Figures 62 and 63 also show that diesel particulates respond little to changes in engine torque and more so to changes in engine speed. This is deduced by comparing the peaks of the curves for each speed, at the two torques of 30Nm and 40Nm. It can be seen that the peaks increase with increasing speed but remain unchanged for each speed at different torques. By examining the dimethyl ether curves it can be said that dimethyl ether particulates are affected by both engine speed and torque. The curves are seen to increase when engine speed and load increase. It can also be observed that increasing speed, when fuelling with dimethyl ether produces slightly larger particulates, but torque changes do not affect the particulate size. However for diesel fuelling, speed changes, at a particular torque, produce no noticeable changes in the particulate sizes but increases in torque are seen to produce slightly larger particles.

From the diesel curves it can be observed that at lower torques, two peaks are present, a small one at about 50nm and a larger one at about 150nm. At higher torques, however, the small curve disappears and large one dominates. The dimethyl ether curves consistently produce one distinct peak at all loads and speeds.
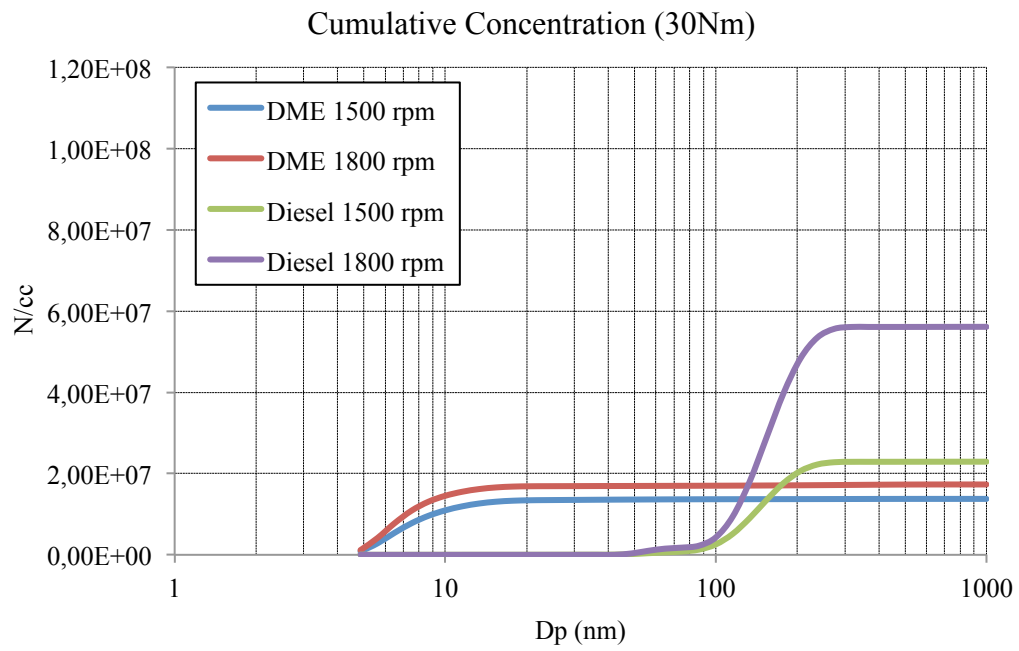
12.3.2. Cumulative Concentrations

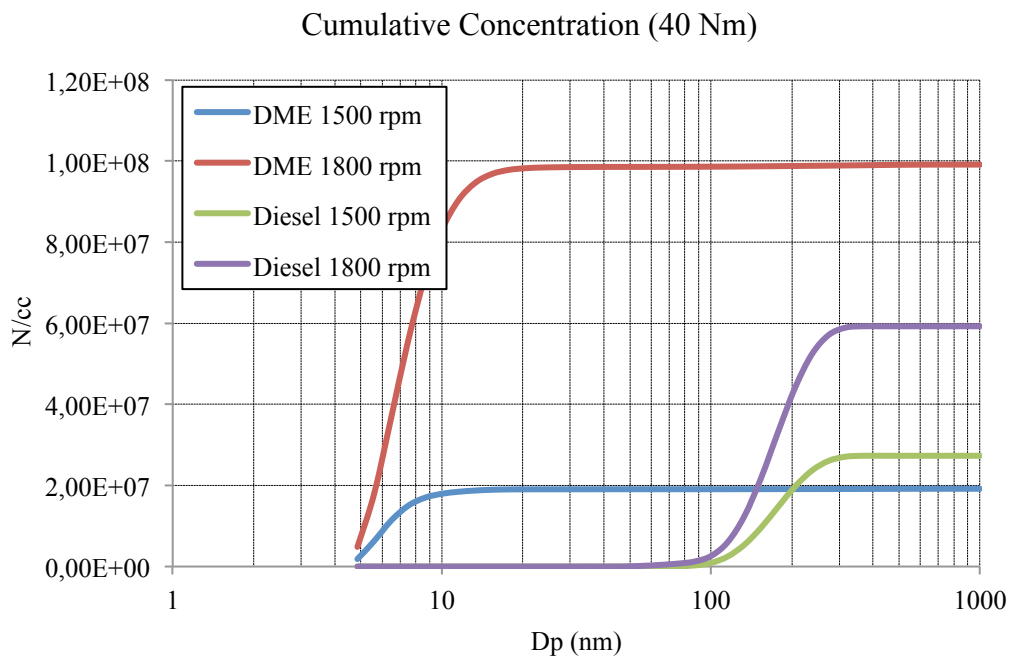Figure 64: Comparison of Cumulative Concentrations at 30Nm

Figure 65: Comparison of Cumulative Concentration at 40Nm

Figures 64 and 65 present similar information to figures 62 and 63, but in the form of an actual count of the particulates per cubic centimetre. These figures show that the concentrations of diesel particulates are in actual fact affected slightly by increases in torque. The changes, however, are very minimal when compared to those of dimethyl ether. Speed increases are still seen to be the primary contributing factor for increasing the concentration of diesel particulates. Speed and torque are the primary contributing factors for increasing dimethyl ether particulate concentration. The findings of the previous section are confirmed by the figures 64 and 65.

It is noticed that at lower speeds the concentrations of diesel particulates outweigh those of dimethyl ether, this is so across all torques. At high engine speeds and loads, the concentration of dimethyl ether particulates overtakes that of diesel. The range of particulate concentration over low to high speed for dimethyl ether, at lower engine loadings, is seen to be much less than that of diesel. At higher engine loading the range of dimethyl ether particulates exceeds that of diesel. Conversely the range of diesel particulates at all torques is seen to remain fairly constant.
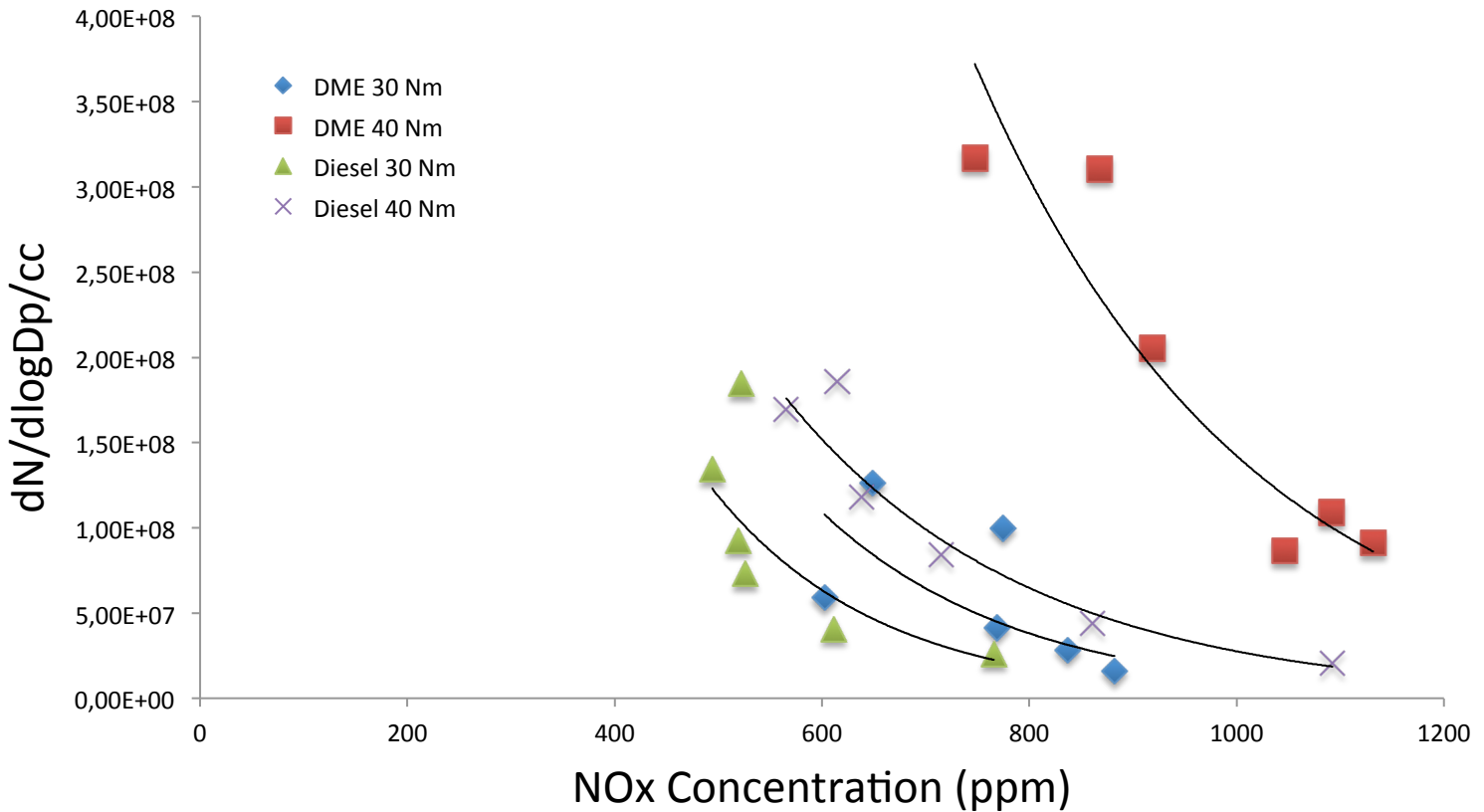
12.3.3. NOx Gases and Particulates

Figure 66: Comparison of NOx and Particulate Emissions for DME and Diesel

Comparisons between NOx and particulate outputs, when fuelled with diesel and dimethyl ether can be made from figure 66. It is noticed that the concentration of NOx gases are greater under dimethyl ether fuelling. The well-established trade-off between particulates and NOx emissions is seen to exist for both diesel and dimethyl ether. This inversely proportional trend appears to remain constant for changing engine loads under diesel fuelling, but for dimethyl ether fuelling it seems to increase in slope with greater engine load. Thus when the engine is fuelled with dimethyl ether the trade-off between NOx emissions and particulates is seen to be stronger at higher torques. Recalling that it has previously been established that higher particulate concentrations are indicative of higher engine speeds, speed increases are seen to decrease NOx emissions for both fuels, while torque increases are seen to increase NOx emissions.
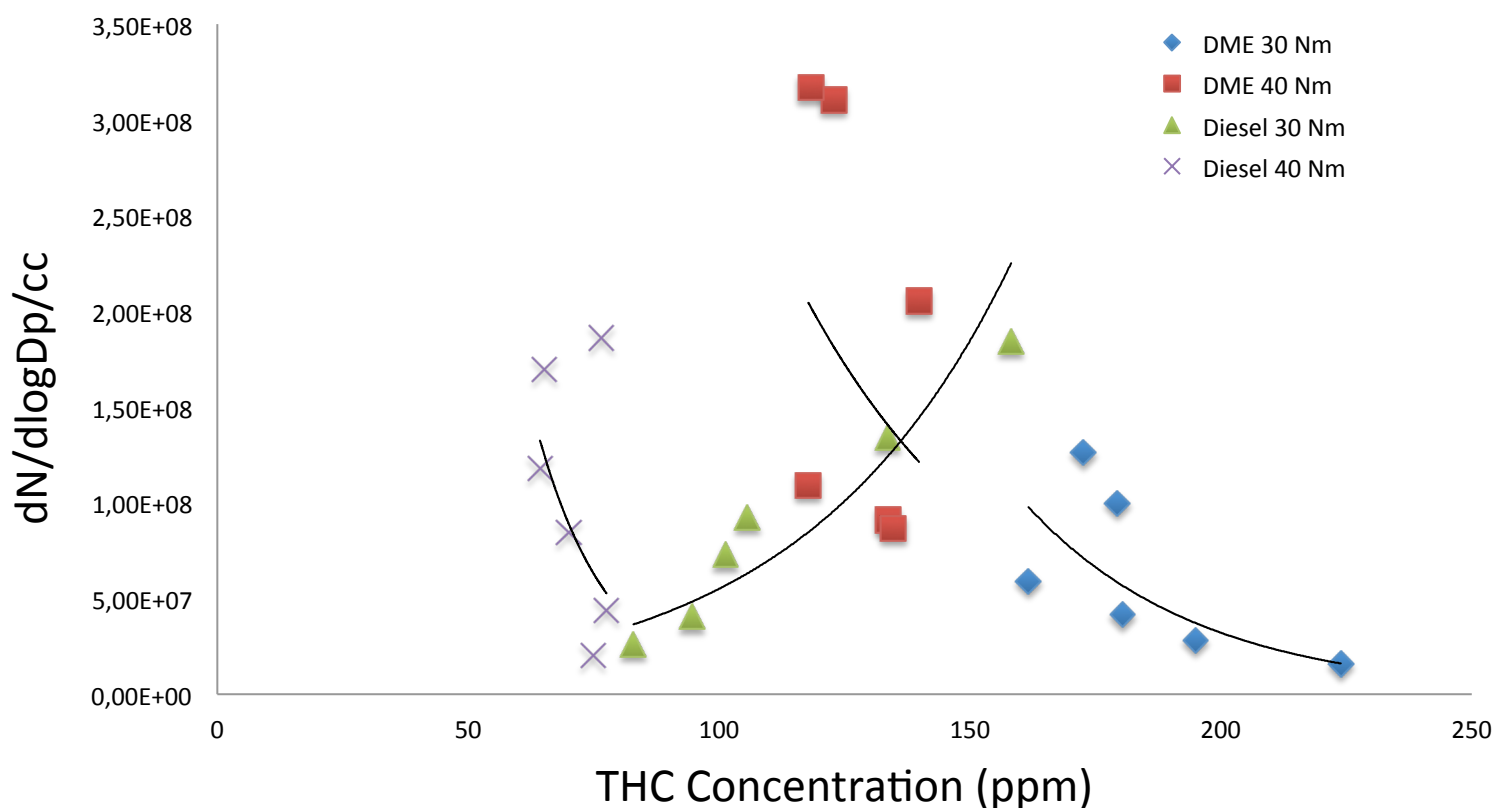
12.3.4. THC and Particulates

Figure 67: Comparison of THC and Particulate Emissions for DME and Diesel

Figure 67 shows comparative plots for THC emissions and particulates for diesel and dimethyl ether fuelling. From the figure it is seen that the relationship between THC and particulates under dimethyl ether fuelling is an inversely proportional one that remains so with changing engine load. Although the curves do tend to become steeper with increasing load, at higher loads there exists less of a link between THC and particulates. For diesel fuelling it is only inversely proportional at higher torques and becomes directly proportional at lower torques. A consequence of this is that at lower torques the effect of increasing engine speed is to increase the output of THC while at higher loads increasing engine speed causes a decrease in THC. With dimethyl ether fuelling, increasing the engine speed consistently causes a decrease in the output of THC. In all cases increasing engine load moves the data sets towards the origin. Therefore increasing engine load causes THC to decrease.
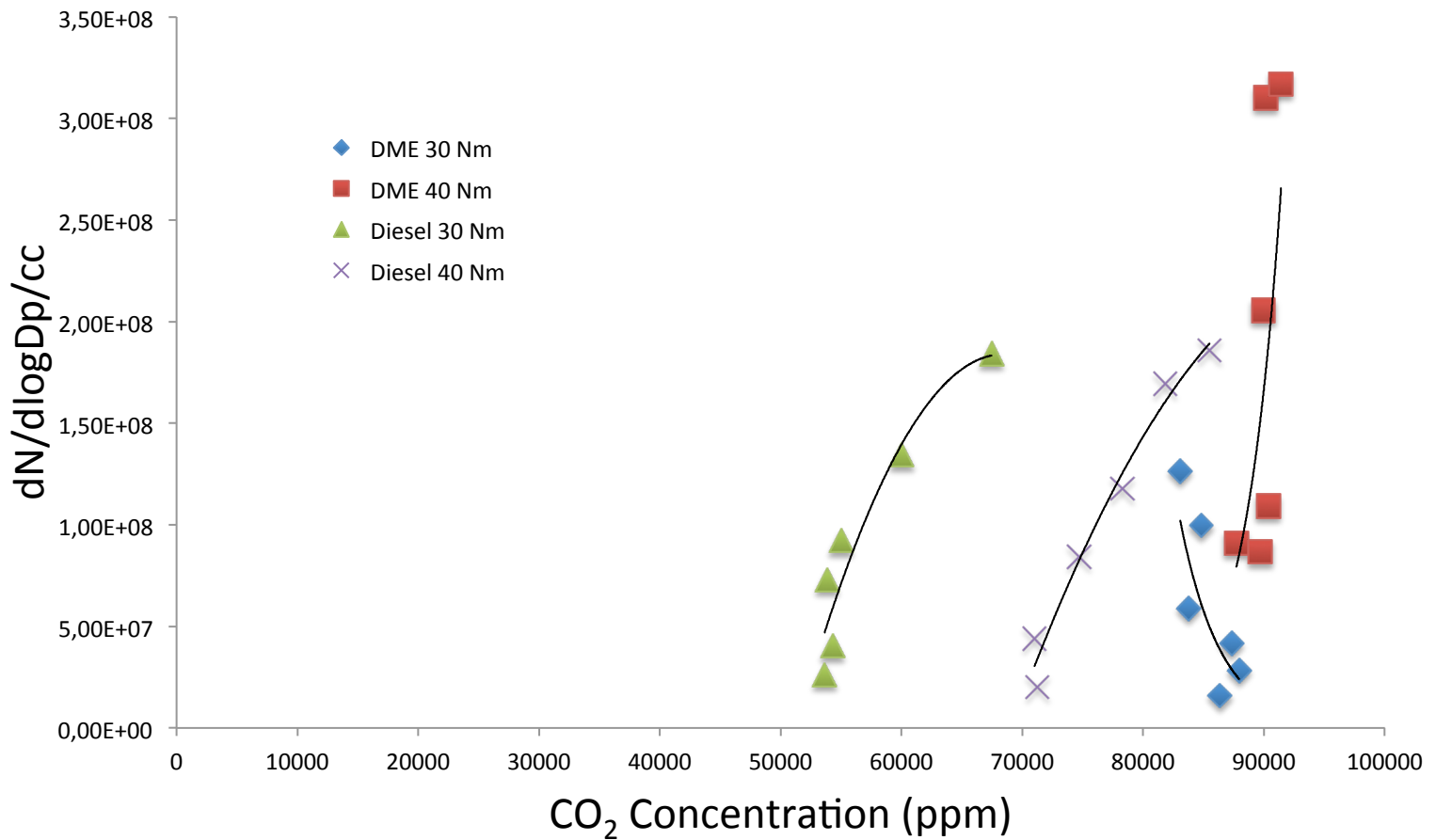
12.3.5. CO2 and Particulates

Figure 68: Comparison of CO_2 and Particulate Emissions for DME and Diesel

From figure 68 it is noted that the relationship between carbon dioxide emissions and particulates, is more prominent with diesel fuelling. This is because the curves for dimethyl ether fuelling are closer to being vertical and the diesel fuelling curves are more horizontal. It is noticed that the slopes of the curves for diesel fuelling seem to become closer to vertical when the load is increased. Therefore the relationship between carbon dioxide and particulates for diesel fuelling becomes less significant at high engine loads. It is also noticed that carbon dioxide output is higher with dimethyl ether fuelling. For both fuels it can be seen that increasing the engine load causes an increase in carbon dioxide output and speed changes do not affect carbon dioxide output.
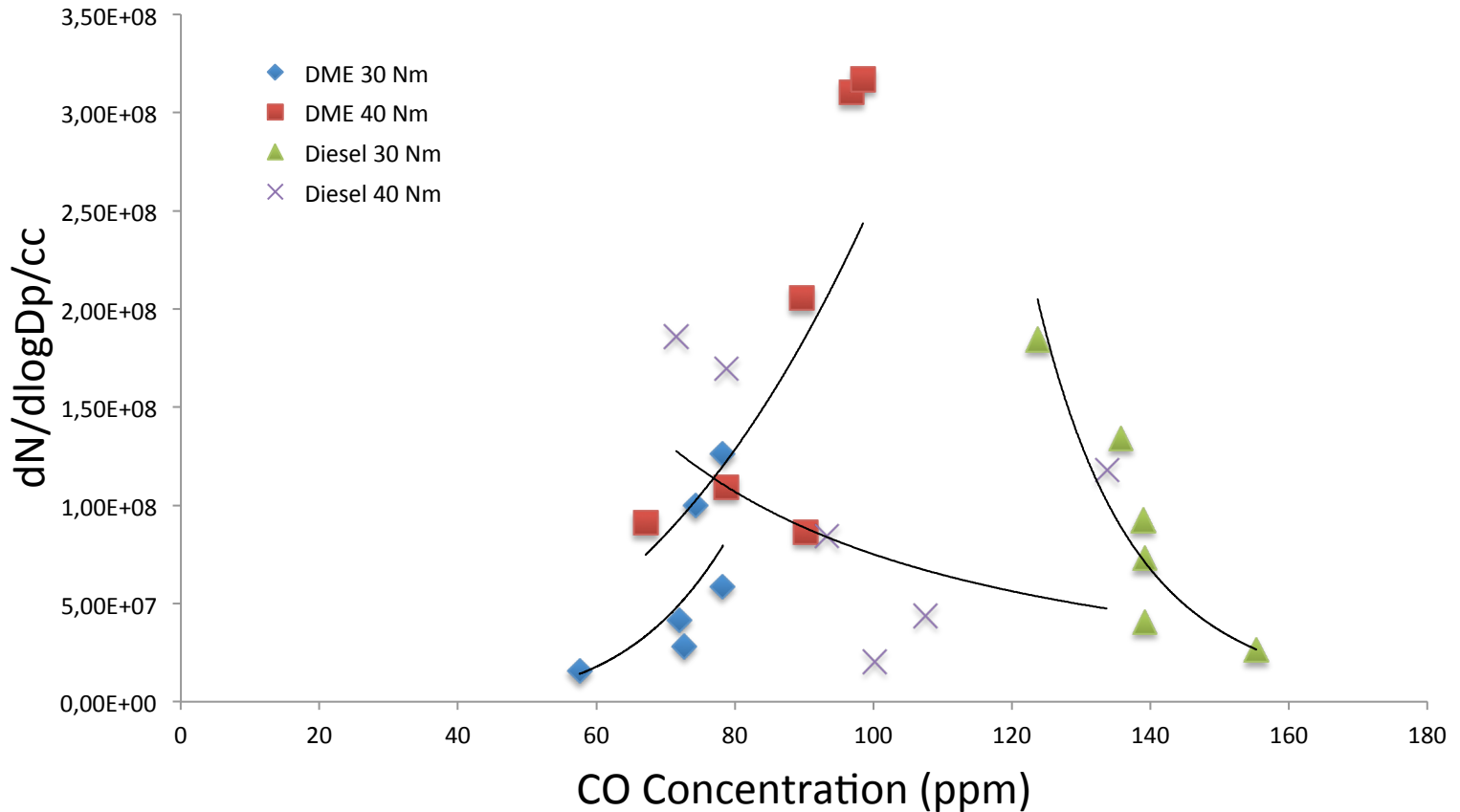
12.3.6. CO and Particulates

Figure 69: Comparison of CO and Particulate Emissions for DME and Diesel

Figure 69 characterises that the most prominent difference between carbon monoxide and particulate emission for diesel and dimethyl ether fuelling is the type of relationship that links the two. When diesel fuel is used an inversely proportional relationship exists whereas with dimethyl ether fuel it is directly proportional. Thus increasing speed causes an increase in carbon monoxide when dimethyl ether fuel is used. While when diesel fuel is used increasing speed causes a decrease in carbon monoxide. Torque changes invoke the same response as speed changes with both fuels. It is also noticed that when torque is altered, with dimethyl ether fuelling, the slope of the curves remains unchanged. With diesel fuelling increasing torque causes the curves to flatten out, thus at higher loads small changes in particulate output are characterised by large decreases in carbon monoxide output.

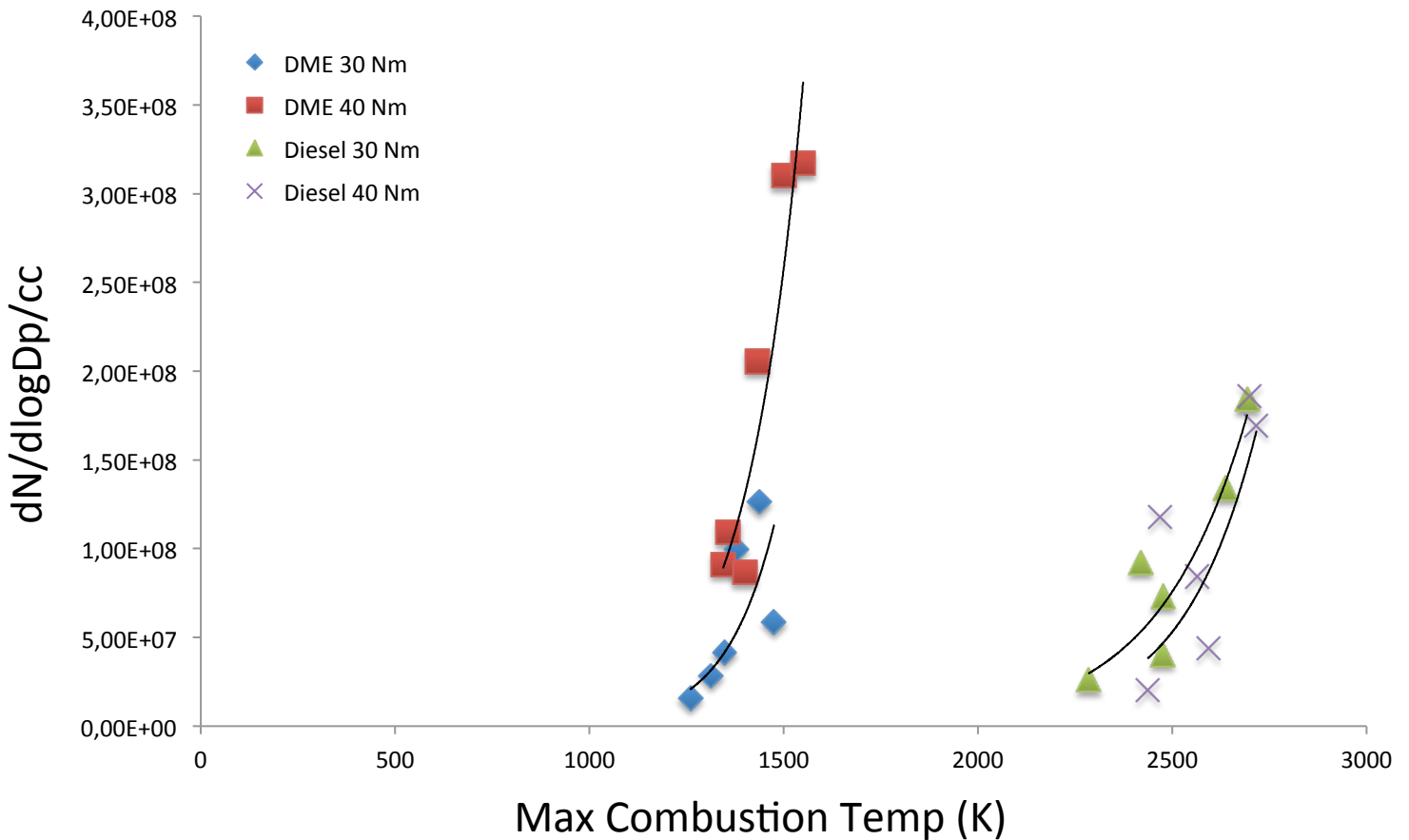## 12.3.7. Particulates and Maximum Combustion Temperature

Figure 70: Comparison of Max Combustion Temp and Particulate Emissions for DME and Diesel

It is evidenced by figure 70 that the maximum combustion temperature of the engine under diesel fuelling is considerably higher than it is with dimethyl ether fuelling. In the latter case, increasing the engine load will decrease the maximum combustion temperature, while the former will increase with increasing engine load. In all cases the maximum combustion temperature is linked to particulate output in an exponential and directly proportional manner. This implies that increasing engine speed in all cases increases the engine's maximum combustion temperature. It can also be seen that the slope of the curves for diesel fuelling are less vertical than those for dimethyl ether fuelling, thus a stronger link between particulates and maximum combustion temperature exists under diesel fuelling.
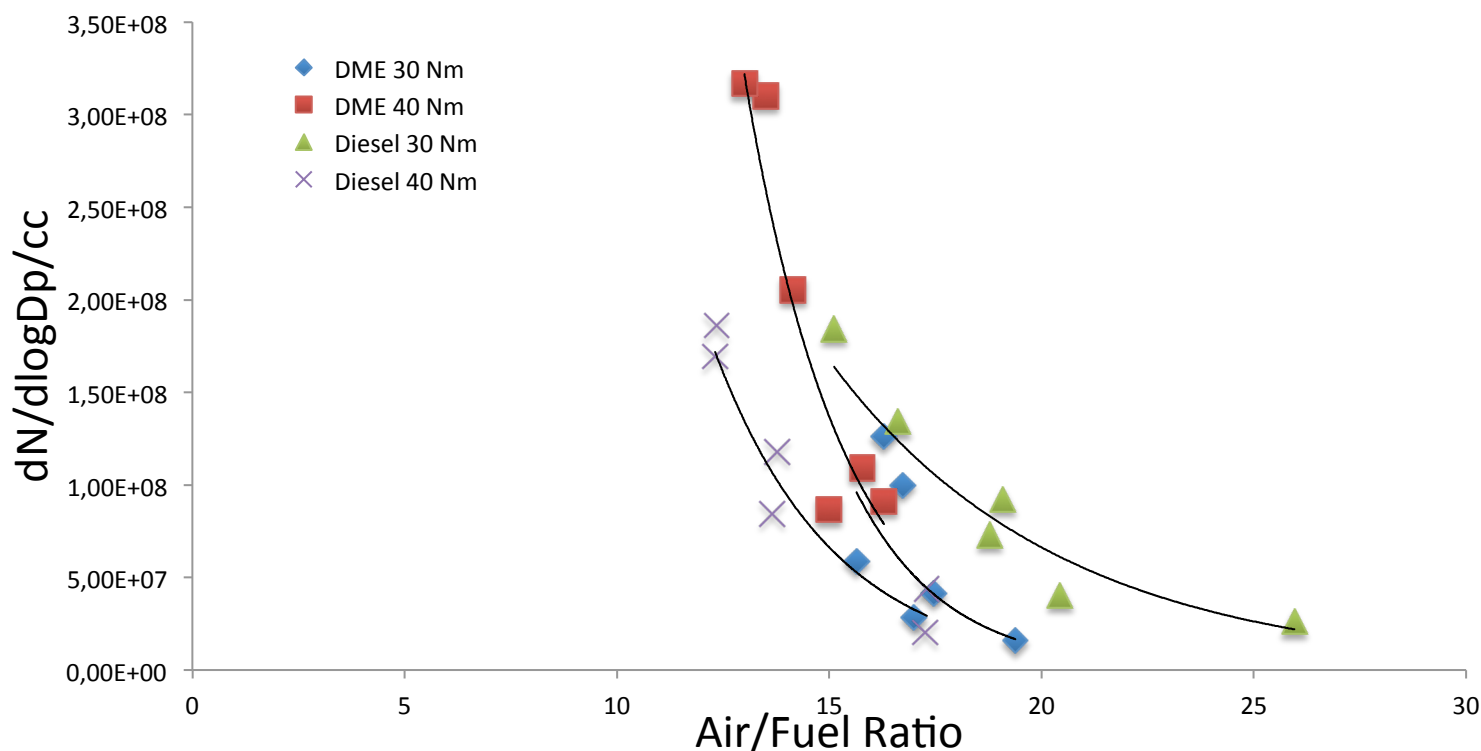
12.3.8. Air/Fuel Ratio and Particulates

Figure 71: Comparison of Actual Air/Fuel Ratio and Particulate Emissions for DME and Diesel

Figure 71 shows that increasing torque causes a decrease in the air/fuel ratio, thus the engine will always consume more fuel when operating at high load. The range of air/fuel ratios is greater under diesel fuelling, for a 10Nm load increase. At high loads the engine will use more fuel, on a mass flow basis, when diesel fuelling is used. It must be noted that the calorific value of dimethyl ether is lower than that of diesel. This means that more dimethyl ether should be consumed. A possible reason for this could be that the dimethyl ether burns very much more efficiently than diesel, thus the net effect is that less is used. The air/fuel ratio appears to be linked to the engine's particulate output in a directly proportional manner in all cases, although the curves for diesel are flatter than those for dimethyl ether. This indicates that a stronger link can be drawn between fuel consumption and particulate output when diesel fuel is used. This also implies that when more fuel is used there will be more particulates and increasing speed results in more fuel being burnt in all cases.

13. Conclusions

13.1. Diesel Fuelled Tests

1. It was observed that the general trend for particulate spectral density maxima and cumulative concentrations increased with increasing speed at fixed torque.

2. The size of particulates varied from about 150nm at 25Nm to about 190nm at 45Nm.

3. The effect of changing torque at fixed speed did not create any substantial changes in the maximum particulate output.

4. An optimal engine operating point, for minimum particulates and maximum brake power, was observed to occur at low speed and high torque.

5. The relationship between NOx gas formation and particulates is an inversely proportional one.

6. The relationship between CO_2 and the maximum particulate concentration is nearly non-existent.

7. The relationship between THC production and the maximum particulate concentration was observed to be different for different engine loads. At low loads the relationship was seen to be directly proportional, whereas at high loads it became inversely proportional.

8. Increasing maximum combustion temperature causes a consequent increase in the maximum particulate concentration.

9. An inversely proportional relationship exists between maximum particulate concentration and fuel conversion efficiency. This relationship is seen to be independent of engine torque.

10. An inversely proportional relationship exists between maximum particulate concentration and mechanical efficiency. This relationship is seen to be dependent on engine torque, as at higher torques the slope was steeper than at lower ones.

11. A directly proportional link between engine exhaust gas temperatures and the maximum particulate concentrations can be drawn. Changing engine torque

does not seem to alter this relationship but it does cause an increase in exhaust gas temperature for a given maximum particulate concentration.

13.2. Dimethyl Ether Fuelled Test

1. The spectral density maxima and the cumulative concentration maxima were seen to increase with both increasing engine speed and load.
2. The size of particulates encountered ranged from about 5,5nm at 1300rpm to about 7,5 nm at 1800rpm for all loads.
3. A trade-off was observed between particulates and NOx. This relationship becomes more pronounced at higher engine loads.
4. Little link exists between CO_2 particulates, but increases in engine torque are responsible for increases in CO_2 output.
5. There appears to be an inversely proportional relationship between particulates and THC at low to medium engine loads, but not at higher engine loads.
6. Carbon Monoxide and the maximum particulate concentration are directly proportional to one another as well as being slightly exponential in nature. This relationship is unaffected by engine load but increasing load does cause an increase in the output of carbon monoxide.
7. The maximum concentration of particulates increases with increasing maximum combustion temperature, which is also seen to increase while increasing engine load and speed.
8. The maximum combustion pressure is linked to the maximum particulate concentration in an inversely proportional way, and is affected more by engine speed than load.
9. The air/fuel ratio in the combustion chamber reveals that more fuel results in more particulates being produced, thus air/fuel ratio and particulates are linked in an inversely proportional manner.

13.3. Notable Comparisons Drawn From the Above Conclusions

1. The sizes of diesel particulates are about 150nm to 170nm and are unaffected by changes in engine speed, but are affected by engine load. Dimethyl ether particulates are about 5,5nm to 7nm and engine speed affects the particulate size but engine load does not.

2. At low engine loads the concentration of diesel particulates are higher than those of dimethyl ether, whereas at high speed and load the concentrations of dimethyl ether particulates are higher.

3. The range which particulate concentrations increase at high engine loads with dimethyl ether fuelling, is greater than with diesel fuelling. At lower loads the range of dimethyl ether particulate concentrations is less than diesel particulates. Diesel particulate concentrations have a uniform range across the torque band.

4. For both fuels NOx emissions and particulates are linked in an inversely proportional manner. NOx emissions with dimethyl ether fuelling are higher than those of diesel fuelling. In all cases increasing engine load increases NOx emissions and increasing speed decreases NOx emissions.

5. THC emissions and particulates with dimethyl ether fuelling are always inversely proportional, and increases in load and speed cause a decrease in THC. Under diesel fuelling the relationship is directly proportional at low engine loads but becomes inversely proportional at high loads.

6. In all cases increasing torque increases the output of carbon dioxide. Carbon dioxide emissions are also lower with diesel fuelling, and little link between carbon dioxide and particulates exists in all cases.

7. Carbon monoxide emissions under dimethyl ether fuelling are directly proportional to particulate emissions, and increasing engine load and speed increases the output of carbon monoxide. When diesel fuel is used the converse is true, however, diesel fuelling produces more carbon monoxide emissions.

8. In all cases maximum combustion temperature is linked to particulate emissions in an exponential manner. The maximum combustion temperatures experienced when dimethyl ether fuelling is used are considerably lower than those with diesel fuelling.

9. The air/fuel ratio decreases when particulate emissions increase. Thus if more particulates are produced then more fuel will be consumed. From the air/fuel ratio it can also be concluded that at low engine loads the fuel consumption for diesel fuelling is lower than for dimethyl ether fuelling, while at high engine loads the consumption with diesel fuelling is higher.

14. Future Recommendations

1. It is recommended that transient particulate sampling be done for both dimethyl ether and diesel. This would involve retrofitting the engine with an electronic throttle control mechanism to allow a ramped response of speed to be achieved or a constant speed be maintained with a ramped torque response.

2. The data acquisition systems, although reliable in operation, runs on out-dated computer operating systems and transferring results to newer systems is troublesome. These computers should be updated to modern standards with up-to-date data transfer options available.

3. The dimethyl ether pump currently relies on a dry ice bath to remove excess heat in the return line. Although this system works very well a new method should be investigated which would eliminate the operator needing to monitor and keep the dry ice bath full. This would make dimethyl ether fuelling more practical. This new method could still incorporate dry ice but an automated management system of the dry ice bath could be investigated.

4. The method used to acquire the flow rates of dimethyl ether during the tests is troublesome as the fluctuations on the rotameters allow for an interpretive error to be translated. An investigation into a more robust automated system should be done if at all possible.

5. A modern common rail engine, with electronically controlled fuel injection, should be considered as a replacement for the Lister Petter. This would allow the research to be directly related to modern standards which exist for newer more advanced common rail injection diesel engines.

References

1. http://www.dieselnet.com/standards/, date last accessed 2/2/2012

2. E.F. Obert, *Internal Combustion Engines and Air Pollution,* 1973, Harper & Row Publishers Inc

3. A.J. Martyr & M.A. Plint, *Engine Testing*, 3rd edition, 2007, Elsevier Ltd

4. K. Komiyana & J.B. Heywood, *Predicting NOx Emissions and Effects of Exhaust Gas Recirculation in Spark Ignition Engines,* SAE paper 730475, SAE transcript, Volume 82, 1973

5. Y. Sakai, H. Miyazaki & K. Mukai, *The Effect of Combustion Chamber Shape on Nitrogen Oxides,* SAE paper 730154, 1973

6. C.T. Bowman, *Kinetics of Pollutant Formation and Destruction in Combustion,* Program Energy Combustion Science, Volume 1, pages 33 – 45, 1975

7. G.A. Lavoie, J.B. Heywood, J.C. Keck, *Experimentation and Theoretical Investigation of Nitric Oxide Formation in Internal Combustion Engines,* Combustion Science & Technology, Volume 1, page 313 – 326, 1970

8. John B Heywood, *Internal Combustion Engine Fundamentals*, 1988, McGraw Hill Inc.

9. I.A. Vioculescu & G.L. Borman, *An Experimental Study of Diesel Engine Cylinder-Averaged NOx Histories,* SAE paper 780228, SAE transcript, Volume 87, 1978

10. R.C. Yu & S.M. Shahed, *Effects of Injection Timing and Exhaust Gas Recirculation on Emissions from a DI Diesel Engine,* SAE paper 811234, SAE transcript, Volume 90, 1981

11. J.A. Harrington & R.C. Shishu, *A Single-Cylinder Engine Study of the Effects of Fuel Type, Fuel Stoichiometry and Hydrogen-to-Carbon Ratio and CO, NO, and HC Exhaust Emissions,* SAE paper 730476, 1973

12. W.A. Daniel, *Flame Quenching at the Walls of an Internal Combustion Engine,* in Proceedings of the Sixth International Symposium on Combustion, page 886, Reinhold, New York, 1957

13. J.A. LoRusso, G.A. Lavoie & E.W. Kaiser, *An Electrohydraulic Gas Sampling Valve with Application to Hydrocarbon Emission Studies,* SAE Paper 800045, SAE transcript, Volume 89, 1980

14. M. Namazian, J.B. Heywood, *Flow in the Piston-Cylinder-Ring Crevices of a Spark-Ignition Engine: Effects on Hydrocarbon Emissions, Efficiency and Power,* SAE paper 820088, SAE transcript, Volume 91, 1982

15. W.W. Haskel & C.E. Legate, *Exhaust Hydrocarbon Emissions from Gasoline Engines – Surface Phenomena,* SAE paper 720255, 1972

16. J.T. Wentworth, *Piston and Ring Variables Affect Exhaust Hydrocarbon Emissions,* SAE paper 680109, SAE transcript, Volume 77, 1968

17. G. Greeves, I.M. Khan, C.H.T. Wang & I. Fenne, *Origins of Hydrocarbon Emissions from Diesel Engines,* SAE paper 770259, SAE transcript, Volume 86, 1977

18. James N Mattavi & Charles A Amann, *Proceedings of the Symposium of Combustion Modelling in Reciprocating Engines*, 1978, Plenum Press, (Paper: H K Newhall, *Modelling of Engine Exhaust Emissions – An Introductory Overview)*

19. OECD, *Strategies to Reduce Greenhouse Gas Emissions From Road Transport: Analytical Methods,* 2002, OECD Publishing

20. Asif Faiz, Kumeras Sinha, Michael Walsh & Amiy Varma, *Automotive Air Pollution: Issues and Options For Developing Countries,* 1990, PRE Dissemination Centre

21. Charles A Amann & Donald C Siegla, *Diesel Particulates – What They Are and Why,* Aerosol Science and Technology 1:73 – 101, 1982, Elsevier Science Publishing

22. S.H. Cadle, G.J. Nebel & R.L. Williams, *Measurements of Unregulated Emissions from General Motors' Light-Duty Vehicles,* SAE paper 790694, SAE transcript, Volume 88, 1979

23. C.A. Amann, D.L. Stivender, S.L. Plee & J.S. MacDonald, *Some Rudiments of Diesel Particulate Emissions,* SAE paper 800251, SAE transcript, Volume 89, 1980

24. S LI XinLing, Huang Zhen, Wang JiaSong & Wu JunHua, *Characteristics of Ultrafine Particles Emitted from a Dimethyl Ether (DME) Engine*, Chinese Science Bulletin, January 2008, Volume 53, No 2, page 304-312, Science in China Press, Springer

25. Oguma Mitsuharu, Tsujimura Taku, Goto Shin'I'Chi, Nikolic Danilo, *Analysis of Particulate Matter (PM) Emitted from DME Powered DI Diesel Engine –*

Measurement of PM Size Distribution -, Proceedings JSAE Annual Congress, 2006, Volume 52, No 6, page 5-8, Japan

26. Myung Yoon Kim, Seung Hyun Yoon, Bong Woo Ryu, Chang Sik Lee, *Combustion and emission characteristics of DME as an alternative fuel fro compression ignition engines with a high pressure injection system,* Fuel 87 (2008) 2779-2786, Elsevier Scientific Publishing

27. Sorensen SC, Glensvig M, Abata DL, *Dimethyl Ether in Diesel Fuel Injection Systems,* 1998, SAE International Congress and Exposition SAE 981159.

Appendix 1 – Diesel Fuelled Results

Presented in Appendix 1 is a complete set of diesel particulate results in terms of spectral densities and cumulative concentrations.

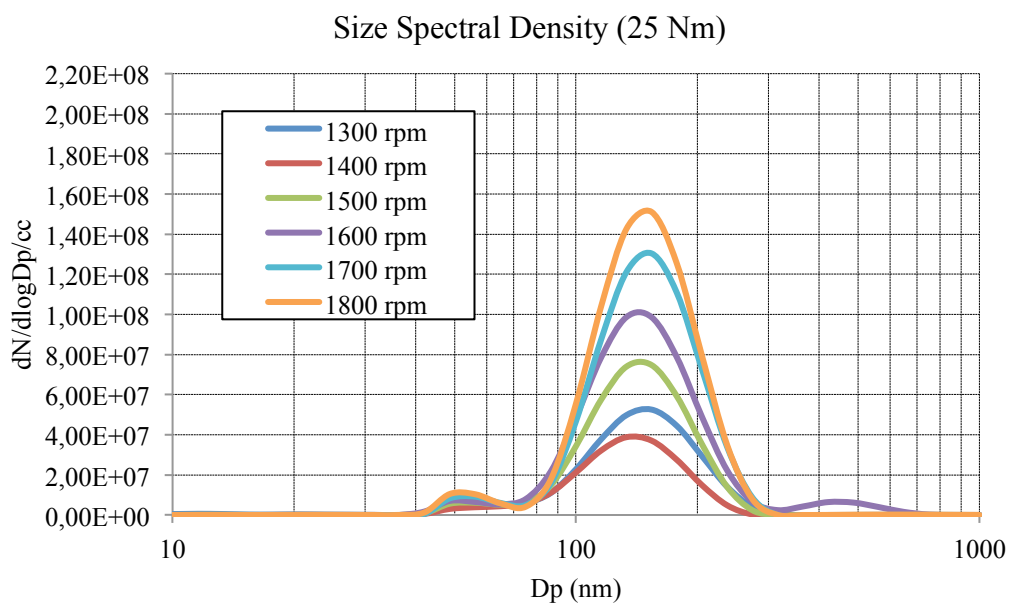## Diesel Particulate Size Spectral Distributions

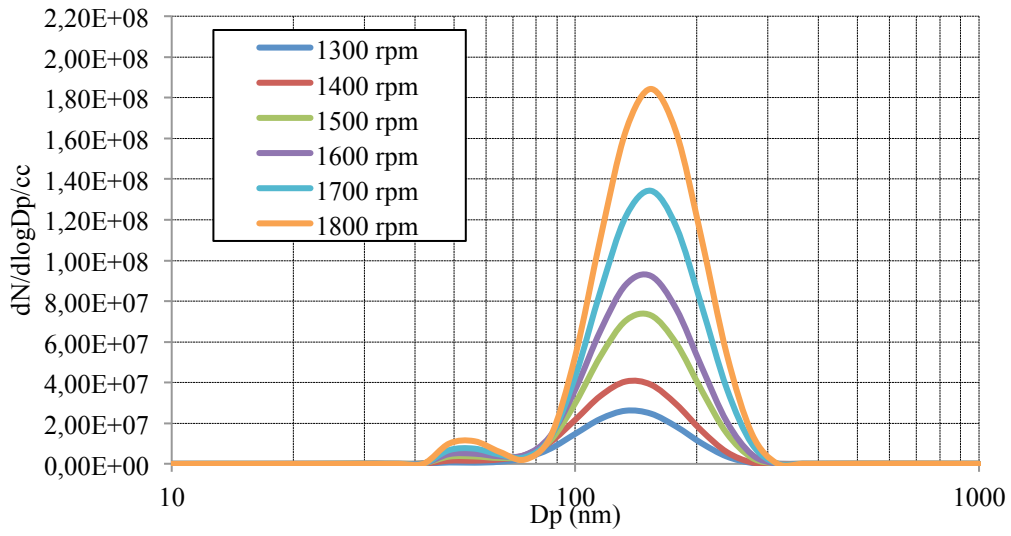Figure 72: Diesel Particulates Size Spectral Density at 25Nm

Figure 73: Diesel Particulates Size Spectral Density at 30Nm

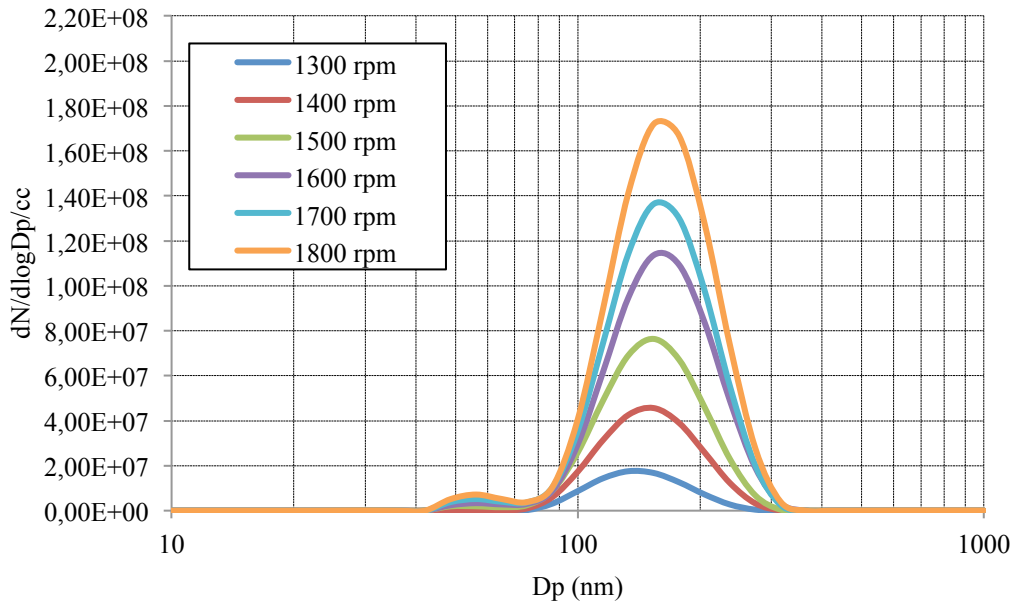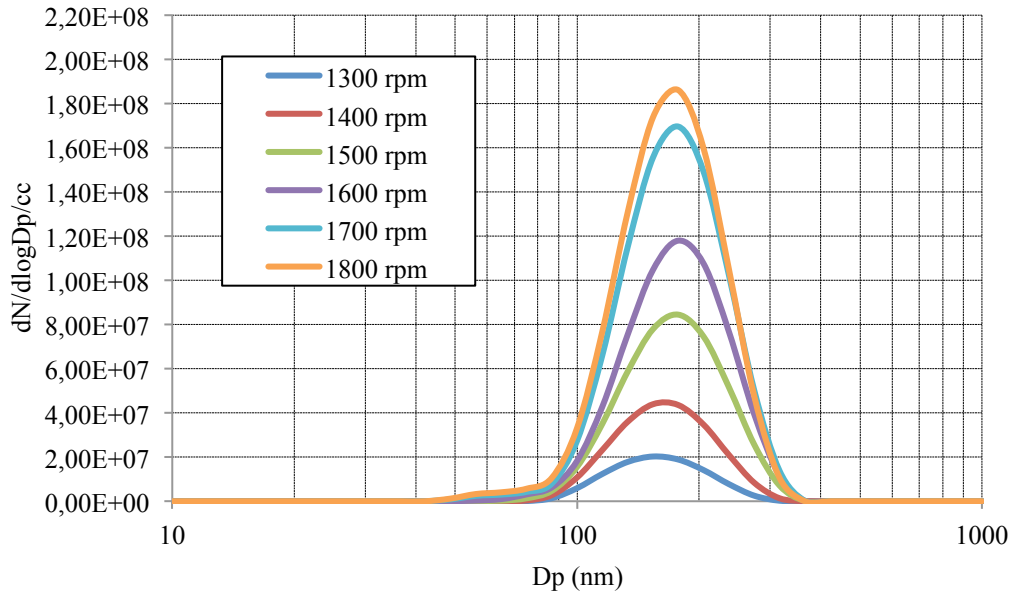

Figure 74: Diesel Particulates Size Spectral Density at 35Nm

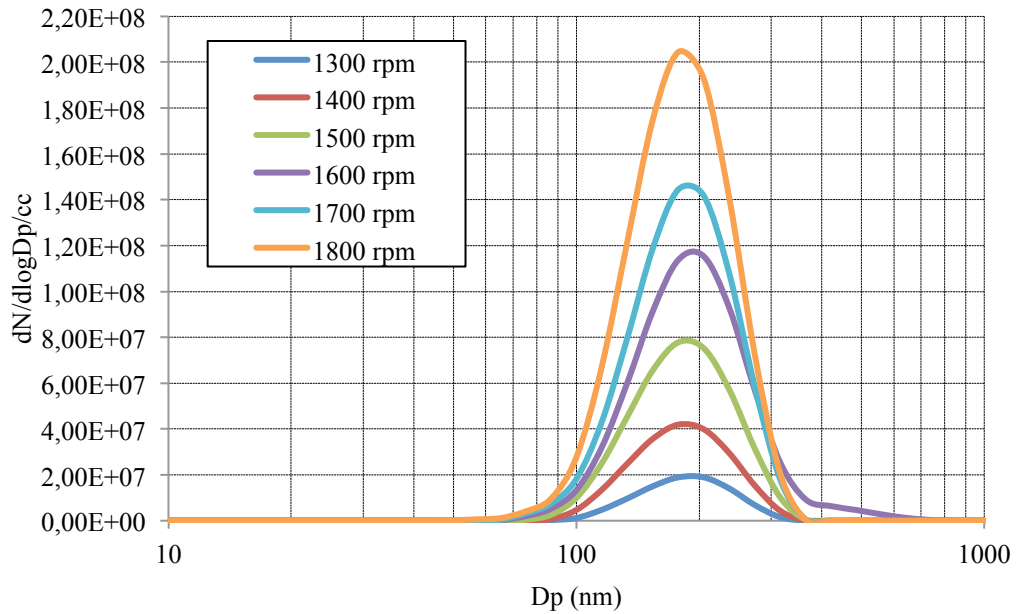Figure 75: Diesel Particulates Size Spectral Density at 40Nm

Figure 76: Diesel Particulates Size Spectral Density at 45Nm

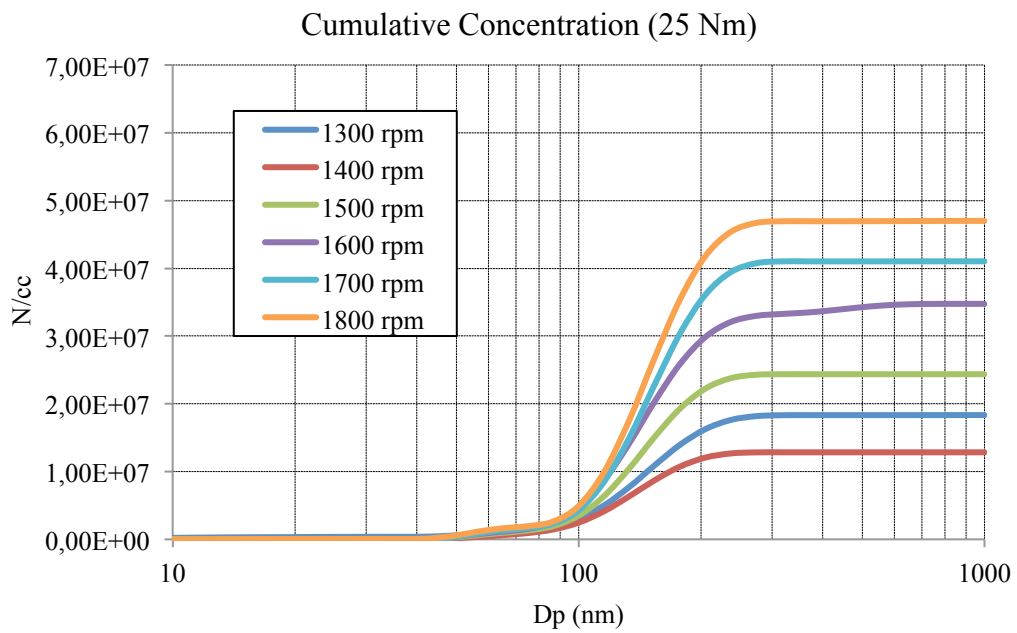# Diesel Particulate Cumulative Concentrations

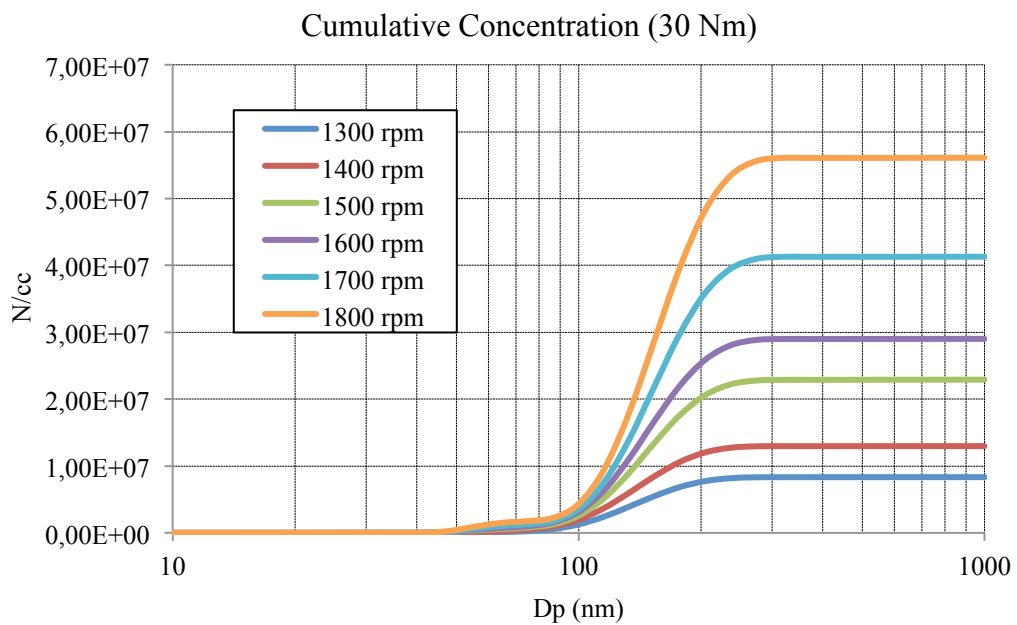Figure 77: Diesel Particulates Cumulative Concentration at 25Nm

Figure 78: Diesel Particulates Cumulative Concentration at 30Nm

Figure 79: Diesel Particulates Cumulative Concentration at 35Nm

Figure 80: Diesel Particulates Cumulative Concentration at 40Nm

Figure 81: Diesel Particulates Cumulative Concentration at 45Nm

Appendix 2: Dimethyl Ether Fuelled Results

Presented in Appendix 2 is a complete set of DME particulate results in terms of spectral densities and cumulative concentrations.

DME Particulate Size Spectral Distributions
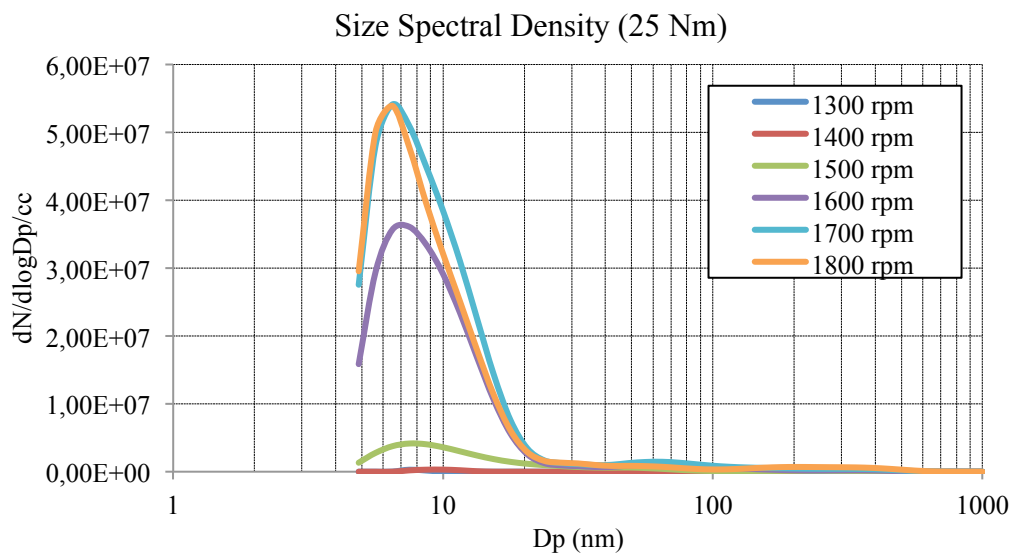
Figure 82: DME Particulates Size Spectral Density at 25Nm
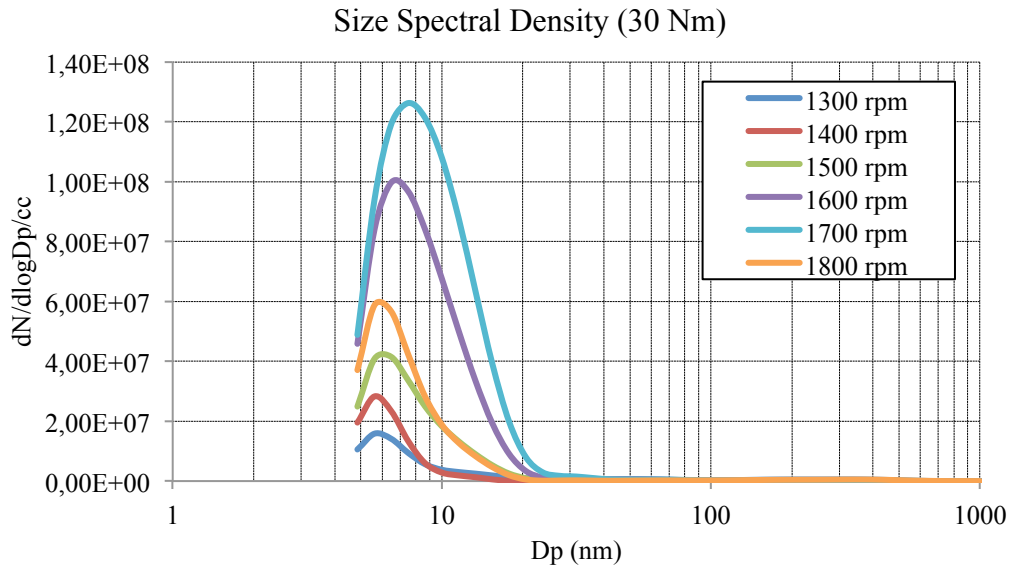
Figure 83: DME Particulates Size Spectral Density at 30Nm
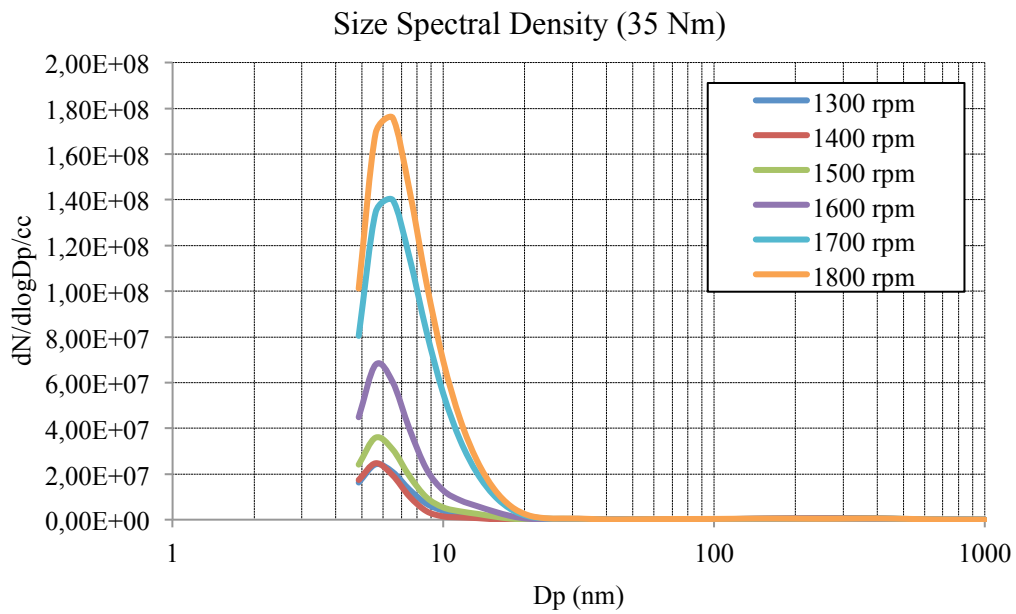
Figure 84: DME Particulates Size Spectral Density at 35Nm
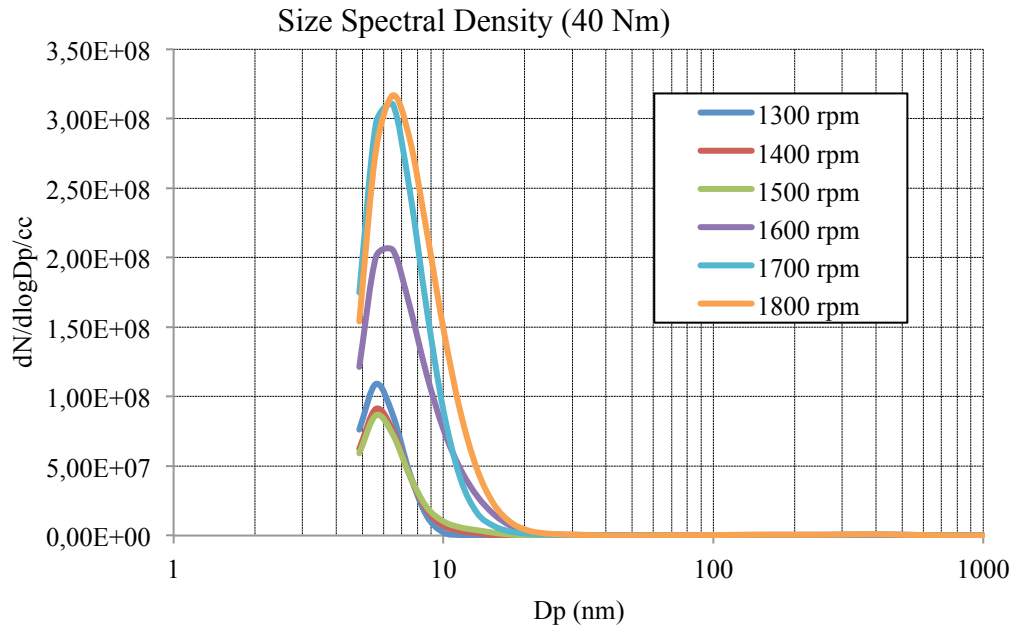
Figure 85: DME Particulates Size Spectral Density at 40Nm
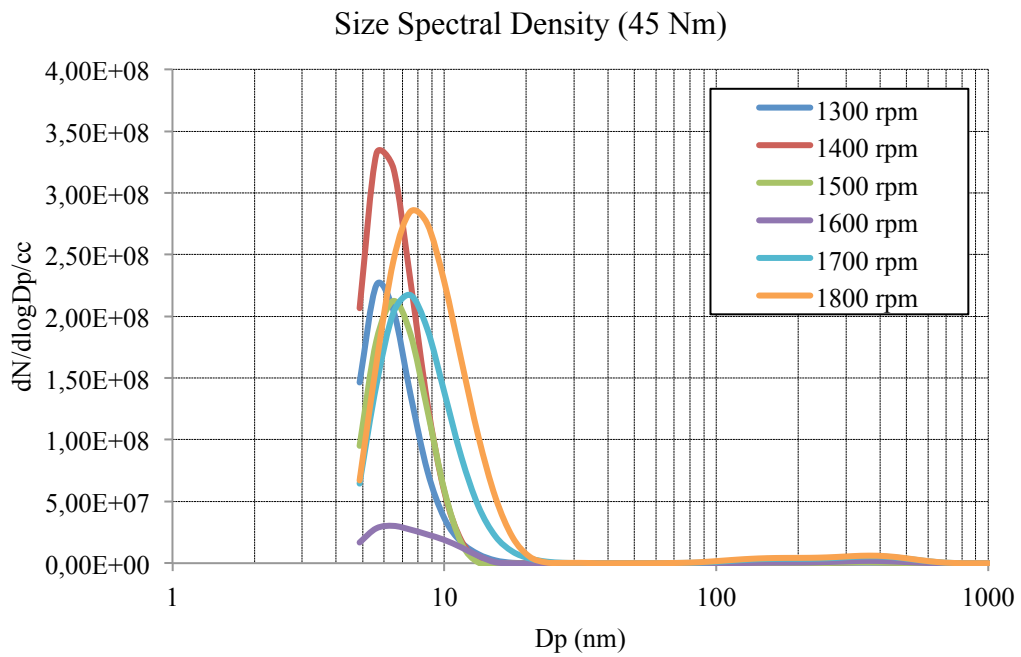
Figure 86: DME Particulates Size Spectral Density at 45Nm

DME Particulate Cumulative Concentrations

Cumulative Concentration (25 Nm)

Figure 87: DME Particulates Cumulative Concentration at 25Nm
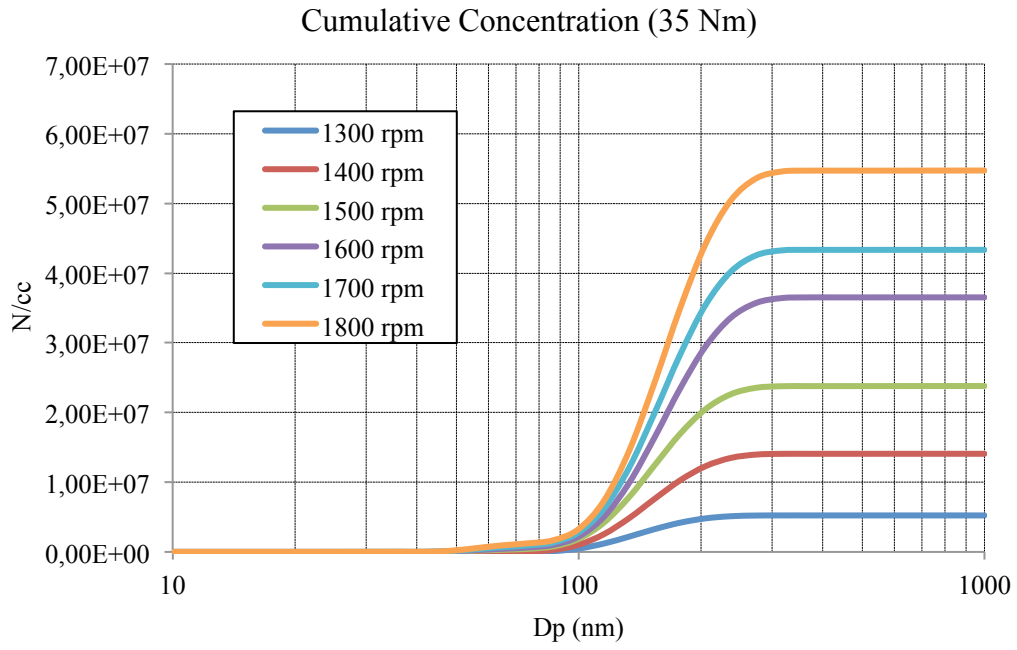
Cumulative Concentration (30 Nm)

Figure 88: DME Particulates Cumulative Concentration at 30Nm

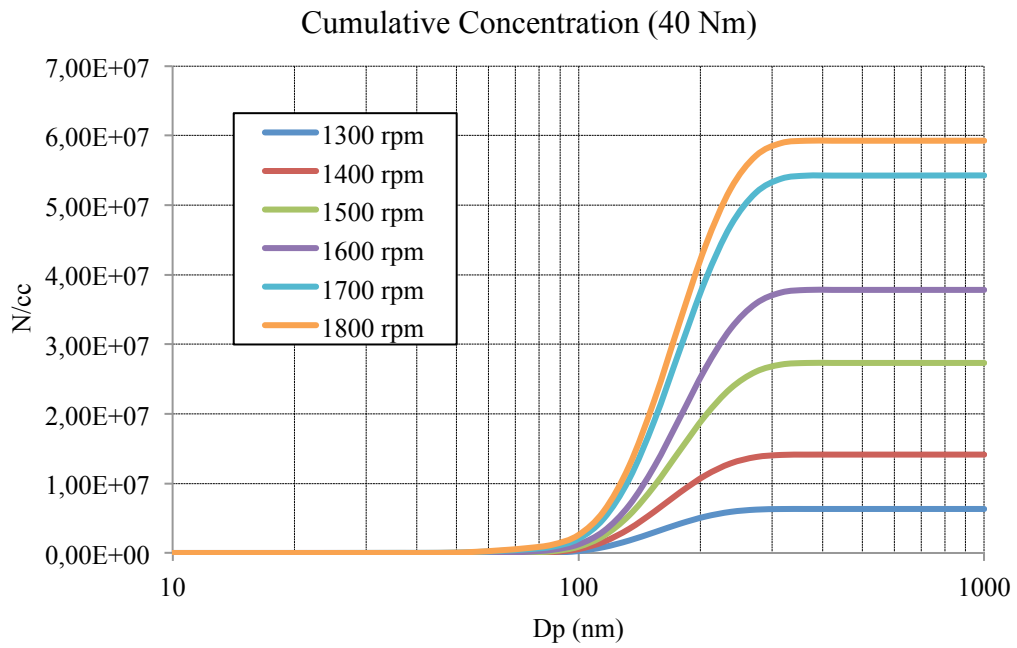Figure 89: DME Particulates Cumulative Concentration at 35Nm
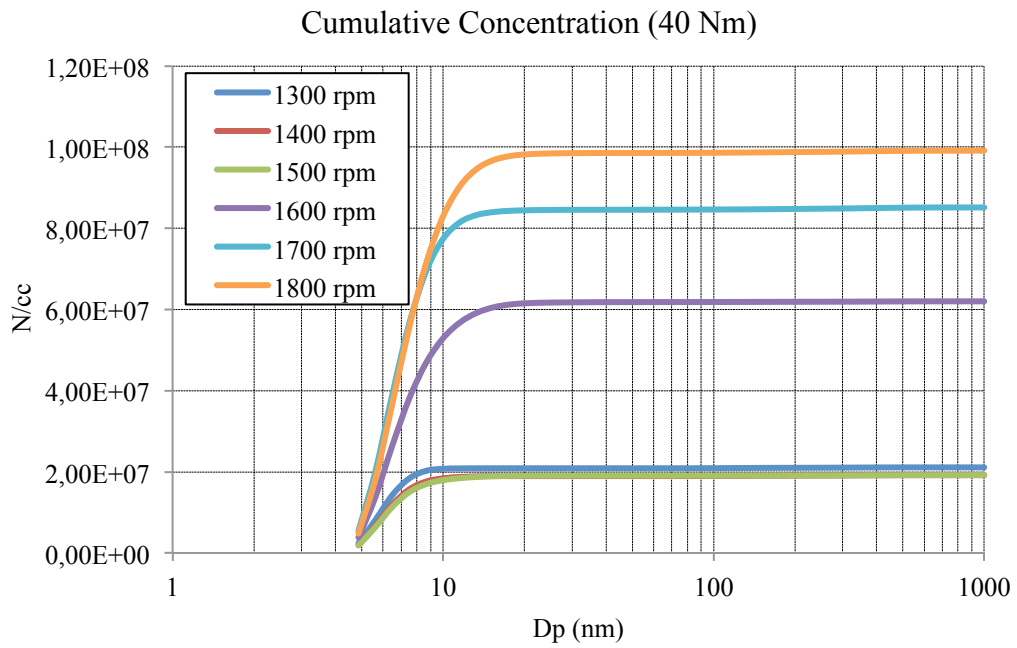
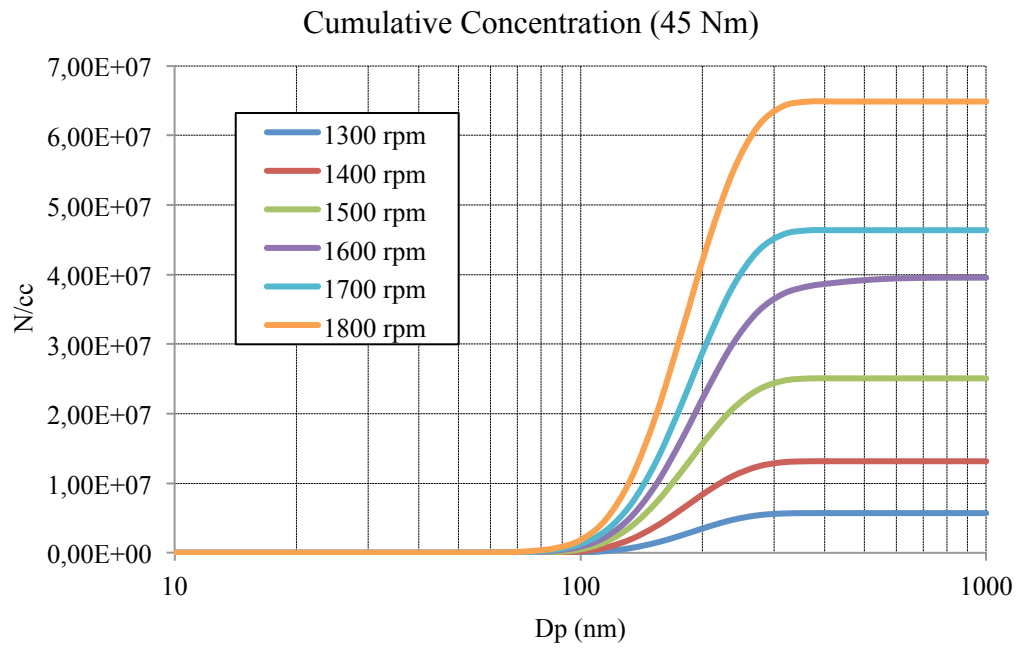Figure 90: DME Particulates Cumulative Concentration at 40Nm

139
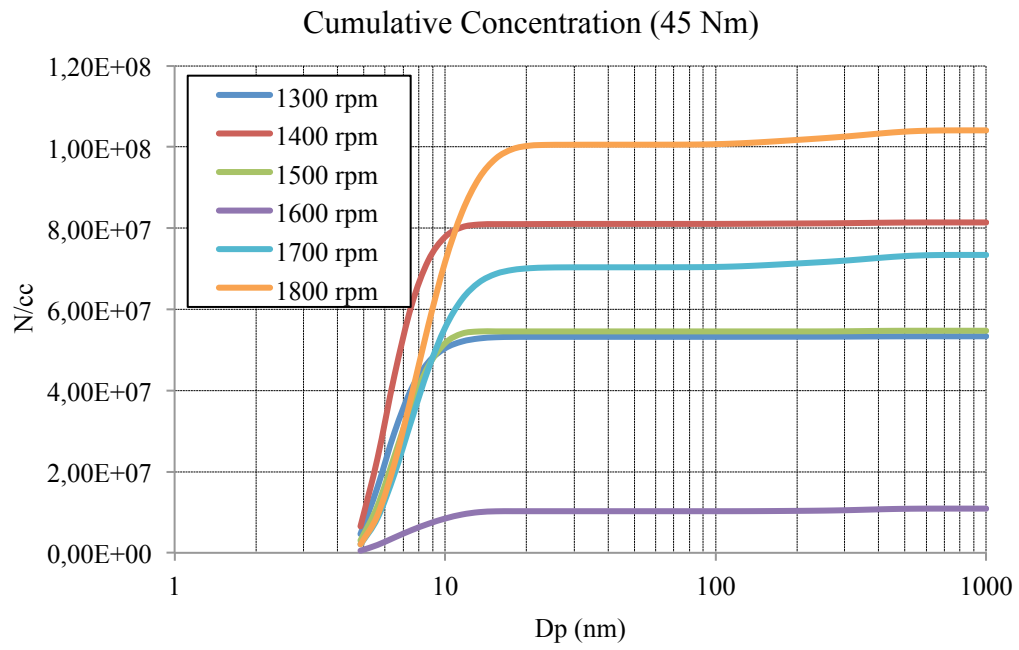
Figure 91: DME Particulates Cumulative Concentration at 45Nm

Appendix 3: Tabulated Diesel Results

Presented below is a table that illustrates the complete set of diesel data that was acquired during this investigation.

Table 9: Complete Diesel Processed Data

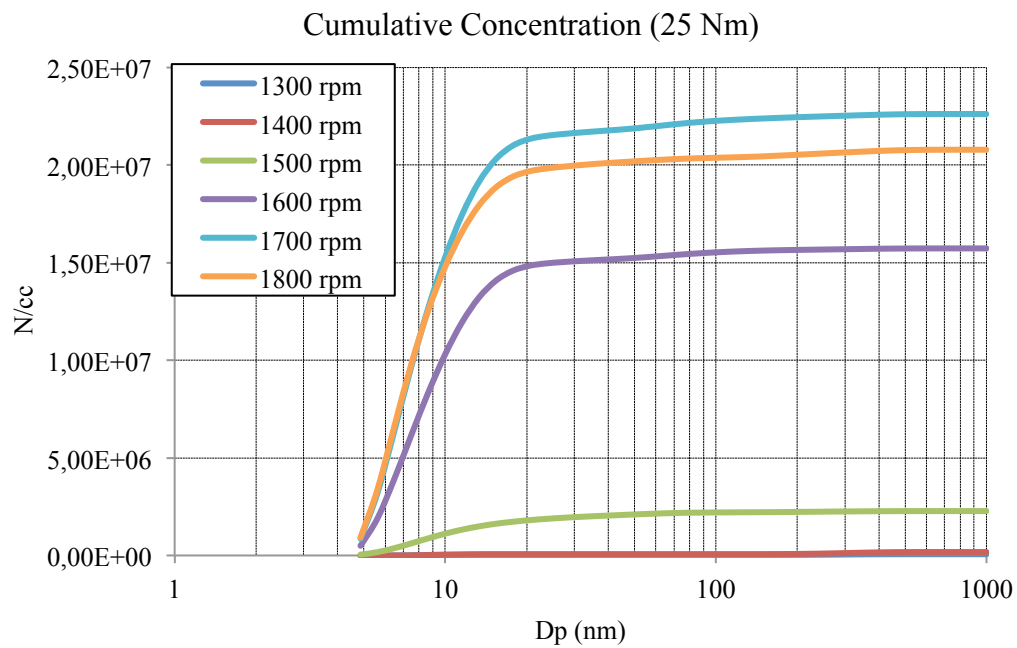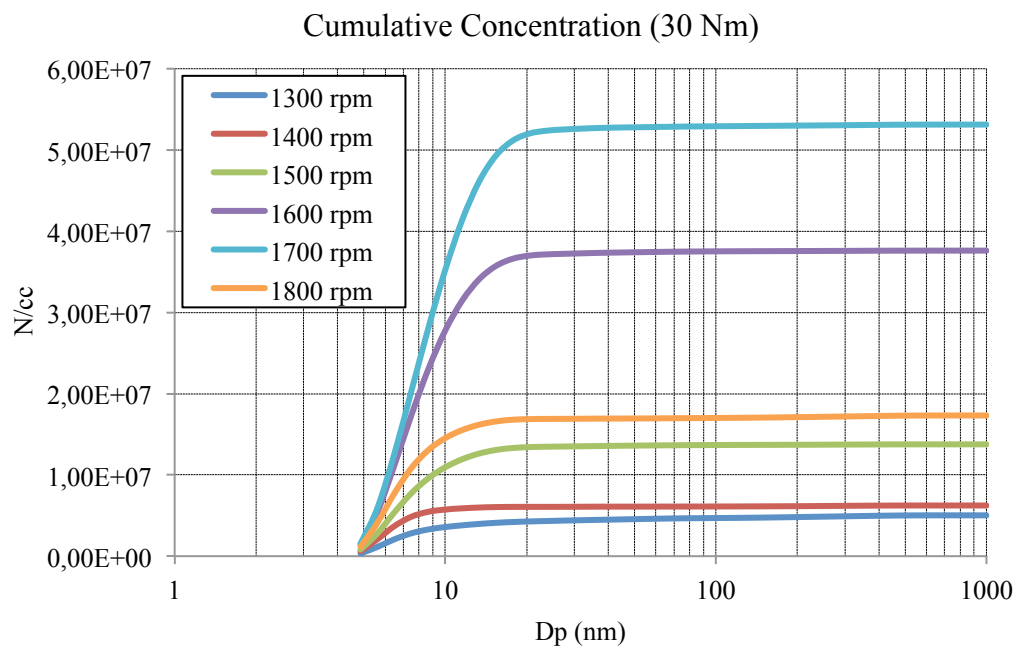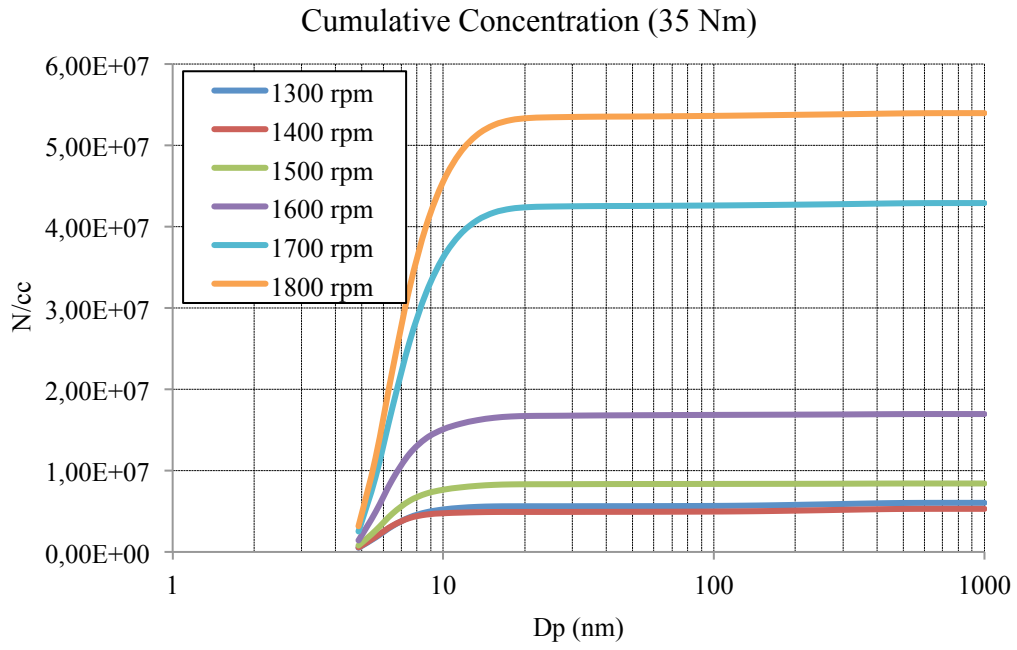| Engine Load	Engine Speed	Mechanical Efficiency	Fuel Conversion Efficiency	Maximum Cylinder Temperature	Maximum Cylinder Pressure	Exhaust Temperature	Ignition Delay	Air/Fuel Ratio	Maximum Particulate Concentration	av Nox	av THC	av CO	av CO2
N.m.	rpm	%	%	degrees celsius	Kpa	degrees celsius	degress crank angle		dN/dlogDp/cc	ppm	ppm	ppm	ppm
25	1300	55,25	26,15	2298,64	5015,15	406,5	7,3	26,285	5,25E+07	513,19	170,2	141,64	48200,7
25	1400	51,55	23,95	2475,65	5085,7	429,6	7,3	22,475	3,88E+07	485,68	119,326	135,2	45183,5
25	1500	49,8	21,15	2471,2	5117,45	445,95	5,5	20,415	7,47E+07	433,49	112,852	130,84	45753,1
25	1600	45,5	19,7	2354,35	5308,85	422,45	6,9	20,8	9,86E+07	433,78	127,297	160,76	47569,3
25	1700	43,8	19,1	2615,35	5113,5	455,85	5,7	18,235	1,30E+08	441,52	153,072	147	51751,7
25	1800	44,2	18,7	2654,75	5002,4	477,7	4,6	16,65	1,51E+08	493,73	182,531	124,26	56737
30	1300	66,4	31,9	2284,6	4675,8	440,4	6,2	25,955	2,62E+07	765,74	82,919	155,3	53637
30	1400	61,3	25,9	2474,8	5014,65	456,3	5,2	20,445	4,05E+07	611,65	94,669	139,19	54311
30	1500	58,6	23,4	2476,35	5073,25	468,35	5,3	18,785	7,30E+07	526,44	101,286	139,2	53841
30	1600	56,2	22,75	2418,2	5171,15	482,05	5,2	19,095	9,24E+07	519,36	105,602	138,96	54984
30	1700	54,2	21,6	2637,15	5084,95	491,4	5,3	16,63	1,34E+08	494,01	133,608	135,79	60020

30	1800	56	20,15	2692,75	5050,75	502,5	5	15,11	1,84E+08	522,78	158,216	123,71	67454
35	1300	76,1	32,75	2349,6	4775,15	469,55	4,7	22,295	1,76E+07	909,32	80,406	118,68	61108
35	1400	65,95	29,65	2547,8	5016,35	476,3	5,6	19,885	4,56E+07	720,14	87,805	116,97	61788
35	1500	68,85	25,5	2493,7	5072,75	485,65	4,7	17,49	7,64E+07	610,25	89,213	121,15	60358
35	1600	65,1	22,7	2531,3	5065,9	492,1	4,4	15,33	1,14E+08	586,93	86,829	116,8	64623
35	1700	62,7	22,85	2629,6	5077,15	501,55	4,6	15,055	1,36E+08	551,02	90,134	112,08	69730
35	1800	60,95	22,05	2696,25	5003,9	511,15	4,4	14,17	1,72E+08	545,89	108,973	102,09	76015
40	1300	80,25	29,15	2437,95	4974,6	496	4	17,26	2,02E+07	1092,62	74,848	100,22	71247
40	1400	76,9	30,05	2591,75	5106,2	500,05	6	17,3	4,39E+07	860,76	77,554	107,54	71015
40	1500	74,3	23,6	2564,75	5093,75	505,85	5,2	13,655	8,44E+07	714,68	70,041	93,27	74695
40	1600	72,7	22,2	2468,15	5142,35	511,6	5,5	13,77	1,18E+08	638,32	64,323	133,68	78269
40	1700	69,1	21,8	2716,4	5049,55	518,35	4,7	12,31	1,70E+08	565,51	65,204	78,79	81830
40	1800	71,15	22,25	2698,75	4944,35	525,85	4,7	12,34	1,86E+08	615	76,514	71,54	85493
45	1300	85,4	28,9	2474,65	5056,65	480,1	5,3	15,675	1,89E+07	1054,96	53,153	77,33	74525
45	1400	81,45	28,2	2578,7	5088,35	507,05	3,2	14,47	4,19E+07	870,88	60,294	140,57	77120
45	1500	78,65	23,2	2619,65	5198,25	511,65	5,5	12,025	7,78E+07	709,99	48,156	101,96	80087
45	1600	80,9	22,15	2466,05	5198	520,05	5,8	12,225	1,15E+08	858,08	40,8059	133,48	85322
45	1700	80,65	22,45	2685,35	5039,3	538,05	4,7	11,155	1,44E+08	754,96	42,8321	123,27	86169
45	1800	81,2	23	2690,55	4927,05	553,25	4,3	11,225	2,04E+08	685,71	50,772	255,55	90991

Appendix 4: Tabulated DME Results

Presented below is a table that illustrates the complete set of dimethyl ether data that was acquired during this investigation.

Table 10: Complete DME Processed Data

Engine Load	Engine Speed	Mechanical Efficiency	Fuel Conversion Efficiency	Maximum Cylinder Temperature	Maximum Particulate Concentration	av Nox	av THC	av CO	av CO2
N.m.	rpm	%	%	degrees celsius	dN/dlogDp/cc	ppm	ppm	ppm	ppm
25	1300	67,2	20,1	1185,2	2,94E+06	780	186,71	7,7	73460
25	1400	65,4	19,3	1250,8	3,18E+06	728,3	245,5	14	73460
25	1500	68	20	1300	4,15E+06	646,6	202,65	21,5	73550
25	1600	69	20,5	1350	3,61E+07	568,3	210,27	33,8	71720
25	1700	67,1	20,3	1384,8	5,41E+07	546,7	204,62	42,1	70590
25	1800	70,4	21,6	1448	5,39E+07	551,2	189,04	38,6	74600
30	1300	76,1	24,1	1260,3	1,58E+07	882,2	223,9	57,6	86370
30	1400	76,9	23,1	1313,6	2,83E+07	837	194,97	72,7	87940
30	1500	73,4	23,5	1347,5	4,15E+07	769	180,36	72	87320
30	1600	74,8	23,7	1377,5	9,98E+07	774,4	179,38	74,3	84810
30	1700	73,5	24	1437,5	1,26E+08	648,8	172,62	78,3	83070
30	1800	75	23,7	1475,1	5,88E+07	602,3	161,65	78,2	83790

35	1300	82,4	26,1	1268,5	2,42E+07	1026,5	157,92	91,1	92080
35	1400	82,3	22,6	1290,6	2,47E+07	992	163,89	98,6	92440
35	1500	82,9	24,7	1330,4	3,59E+07	910,6	145,95	106,3	90280
35	1600	81	24,5	1380,4	6,78E+07	852,9	159,17	101,7	89570
35	1700	81,5	25	1450	1,40E+08	830,8	152,22	106,1	86850
35	1800	81,6	26,6	1530,2	1,76E+08	684,8	135,68	114,2	89110
40	1300	84,3	27	1344,2	1,09E+08	1131,7	133,76	67,1	87720
40	1400	88	27,1	1358	9,12E+07	1092	117,8	78,7	90350
40	1500	87	26	1400	8,66E+07	1046,1	134,75	90,2	89690
40	1600	86,8	25,8	1432,4	2,05E+08	918,8	139,88	89,7	89970
40	1700	87	26	1500	3,10E+08	868,3	122,91	96,8	90160
40	1800	89	27	1550	3,17E+08	747,4	118,31	98,5	91420
45	1300	94,5	22	1318	5,00E+07	1158,7	122,28	101,2	97440
45	1400	87,1	21	1431,9	1,00E+08	969,2	122,47	122	102660
45	1500	88,6	25,1	1333,1	1,03E+08	936,6	119,5	127,1	99300
45	1600	90	23	1400	1,23E+08	877,1	147,93	116,6	97530
45	1700	92,1	19	1532,6	2,53E+08	761,1	158,42	126,4	96640
45	1800	92	20	1600	2,64E+08	668,1	133,23	119,1	102920